University of Alberta

TECHNICAL ASPECTS OF STUDIES IN PROTEIN TRAFFICKING IN NEURONS: THE NIEMANN-PICK TYPE C1 PROTEIN

by

Grenvil Fran Gracias

A thesis submitted to the Faculty of Graduate Studies and Research in partial fulfillment of the requirements for the degree of Master of Science In Experimental Medicine

Department of Medicine

Edmonton, Alberta

Fall 2008

Your file Votre référence
ISBN: 978-0-494-47255-2
Our file Notre référence
ISBN: 978-0-494-47255-2

Abstract

Niemann-Pick Type C (NPC) disease is an inherited, fatal, autosomal recessive neurological disorder characterized by, among other features, an abnormal accumulation of cholesterol in cell bodies of sympathetic neurons as a result of deficiency of the Niemann-Pick Type C1 protein, caused by a defect in the *NPC1* gene.

Previously in our lab, we used an adenoviral vector expressing a NPC1-eGFP fusion protein to infect Npc1-deficient mouse sympathetic neurons *in vitro*, and observed bi-directional movement of this fluorescent chimeric protein between axons and cell bodies of these neurons. Furthermore, expression of this protein abolished the abnormal cholesterol accumulation in the cell bodies of these neurons. To date, there have been very few studies performed on assessing the transport of the NPC1 protein and its various mutant forms in neurons. Therefore, our aim in the current studies was to further study the trafficking of the NPC1 protein in neurons using adenoviral constructs encoding wild-type and mutant NPC1 cDNAs tagged to eGFP, to further determine the role of NPC1 in neurons. However, a number of technical issues presented themselves when carrying out these studies.

First, we discovered that the original adenovirus NPC1-eGFP we had obtained had lost titer and infective capability. Then, after constructing a new adenovirus encoding NPC1-eGFP cDNA, we found that it did not express the fusion protein. Furthermore, transfection of PC-12 cells with plasmids encoding our fusion protein, using different commercially-available transfection reagents, was very inefficient. Also, we show that boiling a protein sample before immunoblotting decreases NPC1 detection. Moreover, analysis of the GFP sequence in the NPC1-eGFP fusion gene

revealed that it did not contain eGFP, but a variant intermediate between GFP and eGFP. Finally, transfection of COS-7 cells with NPC1-GFP plasmids and subsequent immunoblotting experiments indicated that the NPC1-GFP fusion protein is likely degraded to free GFP within the cell. RT-PCR analysis showed that the NPC1-GFP mRNA is expressed. Thus, we conclude that the degradation occurs post-transcriptionally.

Acknowledgements

First and foremost, I graciously thank my supervisor, Dr. Jean Vance, for all her support and guidance throughout this difficult project. She was always extremely encouraging and positive, and was there to provide me with help and valuable suggestions.

I extend abundant thanks to Randy Nelson, for his tremendous support and help with every aspect of this project, and for being an excellent mentor and teaching me everything I know about molecular biology.

I am very grateful to all the current and past members of the JV lab for all their help and advice along the way, for their great friendship, and for making my lab experience an especially enjoyable one: Russell Watts, Barbara Karten, Kyle Peake, Hideki Hayashi, Laurent Demizieux, Agnes Kulinski, Devi Arikketh, and Guergana Tassava.

I thank all the members of the MCBL group who have provided me with constructive criticisms and suggestions for troubleshooting during my research.

I would like to acknowledge my committee members, Dr. Richard Lehner and Dr. Bob Campenot, for their helpful suggestions and insight with regards to my research project, and for offering their expertise in their respective fields.

I also thank Russell Watts, Priscilla Gao, and Laura Hargreaves for their technical support and for performing mice surgeries.

I am also very thankful to Dr. Jean Vance for revising my thesis and for her criticisms and insightful comments.

Last, but not least, I would like to thank my parents and my sister for their constant support in my academic career and with this Master's thesis.

Dedications

I dedicate this thesis to my parents and my sister

Table of Contents

List of Figures

List of Tables

Abbreviations

3'UTR	3' untranslated region
aa	amino acid(s)
Ad	adenovirus
AdV	adenoviral vector
ACAT	acyl-coenzyme A: cholesterol acyltransferase
apo	apolipoprotein
ARAC	cytosine arabinoside
ARE	adenylate-uridylate rich element
AUF1	AU-rich RNA binding factor 1
BBB	blood-brain barrier
CAR	Coxsackie and Adenovirus Receptor
cDNA	complementary DNA
CHO	Chinese hamster ovary
CMV	cytomegalovirus
CNS	central nervous system
COS	CV-1 origin SV40 transformed monkey kidney cell line
DMEM	Dulbecco's modified Eagle's medium
EDTA	ethylenediaminetetraacetate
eGFP	enhanced green fluorescent protein
ER	endoplasmic reticulum

F12K	Kaighn's modification of Ham's F12 medium
FBS	fetal bovine serum
GFP	green fluorescent protein
HEK	human embryonic kidney cell line
HMG-R	3-hydroxy-3-methylglutaryl-Co-A reducatase
HRP	horseradish peroxidase
HS	horse serum
KSRP	K homology splicing regulatory protein
LAMP1	lysosomal-associated membrane protein 1
LAMP2	lysosomal-associated membrane protein 2
LB	Luria-Bertani
LDL	low-density lipoprotein
LE/Lys	late endosome(s)/lysosome(s)
M-6-PR	mannose-6-phosphate receptor
MEM	minimum essential medium
M.O.I.	multiplicity of infection
NeuroA2	murine blastoma cell line
NGF	nerve growth factor
NPC	Niemann-Pick Type C
PBS	phosphate buffered saline
PC-12	rat pheochromocytoma cell line
PCR	polymerase chain reaction

PL	phospholipid
PM	plasma membrane
RND	resistance-nodulation-division
RT-PCR	reverse-transcriptase PCR
SDS	sodium dodecyl sulfate
SNARE	soluble N-ethylmaleimide sensitive fusion protein attachment receptor
SNP	single nucleotide polymorphism
SSD	sterol-sensing domain
TTBS	Tween tris-buffered saline
VAMP2	vesicle-associated membrane protein 2

CHAPTER 1 – INTRODUCTION

1.1 Introduction

Niemann-Pick Type C (NPC) disease is an inherited, fatal, autosomal recessive neurovisceral disorder characterized by progressive neurodegeneration and hepatosplenomegaly (enlargement of the liver and spleen) (1). The first Niemann-Pick patient was described by German pediatrician Albert Niemann in 1914, who related similarities of the disease to Gaucher's disease (2). It was not until 1927 when Ludwig Pick determined that it was in fact distinct from Gaucher's, that it was given the name Niemann-Pick disease, which was then grouped into 3 distinct types: Niemann-Pick A (NPA), Niemann-Pick B (NPB), and Niemann-Pick C (NPC) (2). NPC disease is distinct from Niemann-Pick Type A and B, which both have defects in lysosomal sphingomyelinease activity (3). NPC is a relatively rare disease, with an estimated prevalence of 1:150,000 individuals in the general population (4), although in certain populations, such as a group in Nova Scotia, the prevalence is more frequent (~1%) (5). The main gene responsible for NPC disease (in 95% of cases), the *NPC1* gene, was localized to chromosome 18 using linkage analysis, and identified in 1997 using positional and molecular cloning techniques (6, 7). The other 5% of cases are due to a defect in the *NPC2* gene (also called *HE1*) (8), but mutations in both genes produce the same biochemical and clinical phenotype.

Biochemically, NPC disease is characterized by an intracellular accumulation of low-density lipoprotein (LDL)-derived unesterified cholesterol and glycosphingolipids

within the late endosomal/lysosomal (LE/Lys) compartments of both neuronal and non-neuronal cells (9). In the liver and spleen, accumulation of sphingomyelin, cholesterol, lysobisphosphatidic acid (LBPA), neutral and acidic glycosphingolipids, and phospholipids (PLs) are seen; however, the lipid storage pattern in the brain is much different, where glycolipids, especially certain gangliosides, are the main storage material (4, 10). Following the discovery of the *npc*^{nih} mouse, the most widely used murine model of NPC disease which completely lacks NPC1 protein (130), extensive biochemical studies on NPC1 function have been performed on human fibroblasts, as well as on Chinese hamster ovary (CHO) cell mutants (131).

Clinical manifestations of NPC disease include cerebellar ataxia, supranuclear gaze palsy, cataplexy, dystonia, epilepsy, seizures, cognitive loss, and other neurological impairments, which usually become evident in early childhood, with death typically occurring in the teenage years; however, the timing of onset can range from perinatal to adulthood (12). NPC disease shares many histopathological similarities to other neurodegenerative diseases such as Alzheimer's. One of the major hallmarks of NPC disease is the progressive loss and death of neurons in the brain, especially in the thalamus and the Purkinje cell layer of the cerebellum (132). Other neuropathological features include the presence of inclusion bodies, axonal spheroids, meganeurites, and ectopic dendrites in neurons and glia throughout the brain (133-135). **Figure 1.1** depicts the timeline and progression of NPC disease in both mice and humans. Currently, there is no cure or effective treatment available for this disease. The current chapter will summarize the theories proposed and the studies performed in the field of

NPC research over the years, with a focus on studies attempting to elucidate the function of the NPC1 protein in neurons.

1.2 Structure and Topology of NPC1 and NPC2

The *Npc1* gene, located on chromosome 18q11-12 (13), spans approximately 47 kilobases (kb) and has 25 exons of varying size (14). It encodes a 4.9-kb messenger RNA (mRNA) that produces a 1278-amino-acid (aa) polytopic membrane glycoprotein, consisting of 13 membrane-spanning helices, 3 large luminal loops, and 6 smaller cytosolic loops (13), as depicted in **Figure 1.2**. The estimated size of the protein is 142 kDa, but upon immunoblotting the apparent size is 170-190 kDa because of its N-glycosylation. NPC1 protein is ubiquitously expressed in all tissues and cell types, but its level of expression is highest in the liver (15). It is primarily localized to late endosomes and lysosomes, as evident by its association and co-localization with the late endosomal/lysosomal marker protein lysosomal-associated membrane protein-2 (LAMP2) as well as late endosomal markers Rab 7 and 9, although it also transiently associates with the Golgi apparatus (16).

There are several functionally important regions of NPC1 which are crucial for its function: an amino-terminal leucine-zipper motif, designated the "NPC1 domain" (aa 73-94), a hydrophobic putative sterol-sensing domain (SSD) occurring between transmembrane domains 3-7 (aa 615-797), a cysteine-rich luminal domain in the third luminal loop, which contains a ring-finger motif (aa 855-1098) and has zinc-binding

activity, and a cytosolic C-terminal segment that includes a di-leucine sequence, which targets the protein to the lysosomal membrane (14, 17). All three of the luminal loops are heavily glycosylated, most likely in order to protect them from proteolytic degradation by endosomal and lysosomal proteases (13). The existence of a leucine-zipper as well as a ring-finger motif suggests that NPC1 interacts with other proteins (16). An important feature of the five transmembrane domains that comprise the putative sterol sensing domain is that this motif has been identified in other proteins which are involved in cholesterol homeostasis (16). The SSD of NPC1 shares approximately 30% identity with the SSDs of 3-hydroxy-3-methylglutaryl-Co-A reductase (HMG-R) - the rate-limiting enzyme in endogenous cholesterol synthesis, sterol regulatory element binding protein cleavage-activating protein (SCAP), NPC1-like 1 (NPC1-L1), and the morphogen receptor Patched (18). It is interesting to note however, that contrary to previous notions, it has now been shown that this putative SSD in NPC1 may, in fact, not have any binding affinity for cholesterol or oxysterols. In breakthrough studies, Infante et al. (2008) very recently purified the NPC1 protein and showed high-affinity binding of cholesterol and 25-hydroxycholesterol to the first luminal loop of NPC1 (a 240-aa domain with 18 cysteines), and their results suggest that this loop contains the majority, if not all, of the cholesterol and oxysterol-binding activity of NPC1 (17, 19). Furthermore, 25-hydroxycholesterol had a stronger binding affinity to NPC1 than did cholesterol (19). There was no former evidence to indicate that NPC1 bound oxysterols.

In addition, contained within the NPC1 protein sequence are sites which are found in prokaryotic permeases of the resistance-nodulation-division (RND) family

(20). NPC1 and members of the RND family share the same RND signature which is repeated twice: six transmembrane domains separated by a large hydrophilic loop between transmembrane domains 1 and 2 (21). It is interesting to note that members of the RND family are also membrane transporter proteins with a range of substrates which include fatty acids and lipids (13). Although they are yet precisely unknown, possible roles proposed for NPC1 include: a cholesterol "flippase", a fatty acid permease, a ganglioside transporter, a cholesterol sensor, and a member of a multi-protein complex which facilitates cholesterol movement out of late endosomal/lysosomal membranes (21-24).

The *Npc2* gene, on the other hand, contains only 5 exons encompassing 13.5 kb, and is situated on chromosome 14q24.3 (14). It encodes a 151 aa soluble lysosomal protein, that can be secreted by cells (17). The crystal structure of NPC2 protein has been solved (**Figure 1.3**), and it has been shown to bind cholesterol and other sterols with high affinity (17). NPC2 has generally been studied to a much lesser extent than NPC1, and the exact functions of both these proteins still remain elusive. It has been proposed that the two proteins act in concert, and function in transport of cholesterol and other lipids out of late endosomes/lysosomes (14); however, the precise mechanism by which this occurs is yet to be identified. Recently, work by Cheruku et al. (2006) has shown that NPC2 can transport cholesterol to phospholipid vesicles via a collisional mechanism which involves a direct interaction with the acceptor membrane, and this suggests that NPC2 may function directly as a cholesterol transport protein (25).

1.3 NPC and cholesterol metabolism in peripheral tissues

The link between NPC and cholesterol was first made in 1985 by Pentchev et al. (136), and since then, most of the characterization of NPC defects were carried out in human patient fibroblasts and in Chinese hamster ovary (CHO) cells (137,138). Mammalian cells tightly regulate their cholesterol content and its intracellular distribution (26). Cellular cholesterol can be obtained from two sources: endogenously, by *de novo* synthesis in the endoplasmic reticulum (ER), or exogenously, by endocytosis of LDL-derived cholesterol via uptake of plasma lipoprotein particles (27). Under normal circumstances in both cases, this cholesterol redistributes within the cell to enrich cholesterol pools in membranes, primarily the plasma membrane (PM) (27). The plasma membrane contains 50-90% of the total cellular cholesterol content, with much lower concentrations in the membranes of lysosomes, Golgi, and ER, respectively (28). Re-distribution of *de novo* synthesized cholesterol to the PM and ER is ATP-dependent, vesicular, and not Golgi-mediated (29-31), whereas exogenous cholesterol re-distribution is mediated by the Golgi (32). Support for the latter observation came from studies in which normal cells were treated with brefeldin A (BFA), a compound which disrupts the function of the Golgi apparatus (33). In these cells, all of the lysosomal cholesterol re-distributes to the ER, but not to the PM. In normal cells with an intact Golgi, however, two-thirds of lysosomal cholesterol goes to the PM first before reaching the ER (33). Therefore, these results suggested that the transport of exogenous cholesterol from the lysosome to the plasma membrane is Golgi-dependent (33).

In normal fibroblasts and other cells of the periphery, such as in the liver, most of the cholesterol is obtained exogenously. As shown in **Figure 1.4**, plasma LDLs are endocytosed by LDL receptors, which are clustered in clathrin-coated pits on the cell surface, via clathrin-mediated endocytosis (16). The cholesteryl esters in LDLs are then hydrolyzed to unesterified cholesterol and free fatty acids within the late endosomes/lysosomes (16). This unesterified cholesterol is then distributed primarily to the PM, via an unknown mechanism which involves NPC1 and NPC2 (16). Some of the free cholesterol is also shuttled to the ER, where an increased cholesterol content results in several homeostatic responses by the cell: an inhibition of *de novo* cholesterol synthesis via inhibition of HMG-R, a decreased uptake of exogenous LDLs via decreased LDL-receptor synthesis, and an increase in cholesterol esterification via increased expression of the cholesterol esterifying enzyme acyl-coenzyme A: cholesterol acyltransferase (ACAT) (16). In NPC-deficient cells, however, unesterified cholesterol becomes sequestered in late endosomes/lysosomes, leading to a marked decrease in cholesterol content of the PM (16). Moreover, although there is an overall increase in cholesterol accumulation in the cell, none of it reaches the ER; therefore, instead of sensing the increased cellular cholesterol, the ER inaccurately senses a depletion in cholesterol content, and homeostatic mechanisms to increase cholesterol synthesis and uptake continue unabated, leading to a compounding increase and overload of cholesterol in the cell (16). The synthesis of cholesterol and LDL receptors continues, and cholesterol esterification is inappropriately decreased [Reviewed in Ref. (16)].

1.4 NPC and cholesterol metabolism in the central nervous system (CNS)

The brain is the most cholesterol-rich organ in the body, and contains five to ten times more cholesterol than any other organ (35). Although the brain only comprises approximately 5% of body mass, it contains 25% of the body's cholesterol (16). Cholesterol metabolism in the CNS differs from that in the periphery in that all of the cholesterol in the CNS is synthesized endogenously in situ (36-38). This is because plasma lipoprotein particles are unable to cross the blood-brain barrier (BBB), and therefore the brain cannot acquire exogenous LDL-derived cholesterol from the plasma. The majority of cholesterol in the adult brain (~70-80%) resides in myelin, although neurons and glial cells also contain cholesterol (11). The rate of cholesterol synthesis in the CNS is highest in young animals, when the process of myelination is highest, and decreases in the adult animal once myelination is complete (39). The low level of cholesterol synthesis that does occur in the mature animal brain primarily reflects that in neurons and astrocytes (16). Since ~90% of the cells in the brain are glial cells, neurons contribute only a small fraction of total brain cholesterol (40). The half-life of cholesterol in the brain is 4-6 months (16). Since cholesterol synthesis is ongoing, cholesterol homeostasis must be maintained by removing excess cholesterol from the brain. This is thought to happen primarily by the action of the enzyme cholesterol 24-hydroxylase, which is expressed in only a subset of neurons but not in astrocytes or oligodendrocytes, and converts cholesterol into 24-hydroxycholesterol (41, 42). This soluble compound, which can cross the BBB, enters the plasma and is delivered to the liver for excretion into bile (41, 42). Interestingly, in NPC disease, cholesterol

accumulates in all tissues except the brain. In fact, there is actually a marked decrease in cholesterol content in NPC-deficient brains with increasing age (43). This is because extensive demyelination occurs in NPC disease, and since the vast majority of cholesterol is contained in myelin, the progressive loss of myelin masks any age-related increase in the cholesterol content of neurons and astrocytes (44).

1.4.1 NPC1 and glial cells

All 3 of the major types of glial cells in the brain (astrocytes, oligodendrocytes, and microglia) are affected in NPC disease (10). Microglial activation is one of the earliest abnormalities in brains of NPC mice, and as early as 2 weeks after birth, there is an increased number of microglia as well as altered morphology in several brain regions (45, 46). Activation of astrocytes occurs at later stages of the disease (46).

Glial cells play a major role in cholesterol transport in the CNS. In fact, it has been proposed that in adult animals, neurons synthesize only small amounts of cholesterol and obtain the majority of cholesterol by uptake of cholesterol-containing lipoproteins secreted by glial cells (47). These glia-derived lipoproteins contain apolipoprotein E (apoE), the most abundant apolipoprotein (apo) in the CNS, which is synthesized primarily by astrocytes, although a small amount may be made by neurons under certain conditions (48, 49). ApoE-containing lipoproteins bind to, and are taken up by, lipoprotein receptors in neurons (50).

One important question regarding the cause of NPC disease pathology is: Are the neurological deficits a result of dysfunctional processes in glial cells or in the

neurons? Previous studies from our lab have demonstrated that the composition of apoE-containing lipoproteins generated by *Npc1*$^{-/-}$ glia are normal, and therefore does not significantly contribute to the neurological deficits in NPC disease (51). Other studies also indicate that the neurological problems seen in NPC disease are more likely attributable to neuronal defects rather than defects in glial lipoproteins (52).

1.4.2 NPC1 and cholesterol trafficking in neurons

Although the NPC1 protein is ubiquitously expressed in all tissues and cell types examined to date, it is striking that the most profound effects of its deficiency affect primarily the CNS and, in particular, neurons. Neurons seem to be especially sensitive and vulnerable to loss of functional NPC1. A defect in NPC1 leads to degeneration of axons and dendrites, and ultimately neuronal death, especially in cerebellar Purkinje fibers and cells of the thalamus (53, 54). To date, there have only been a few studies on the function of NPC1 at the molecular and cellular level in neurons (51). Sympathetic, cerebellar, and cortical neurons all have a significantly altered distribution of intracellular cholesterol in the absence of normal NPC1 activity (8, 55, 56). Until about six years ago, it was unclear whether or not NPC1-deficient neurons accumulate cholesterol. Studies from our lab involving staining with filipin, which stains for unesterified cholesterol, revealed a characteristic punctate intracellular staining pattern in cultured NPC1-deficient neurons that was markedly different from the staining seen in wild-type neurons (8, 55). Although the total cholesterol content of *Npc1*$^{+/+}$ and *Npc1*$^{-/-}$ neurons as a whole was the same, the cholesterol content of distal axons was

decreased, and the mass of cholesterol in cell bodies was increased, in *Npc1*$^{-/-}$ compared to *Npc1*$^{+/+}$ neurons (8). Since cholesterol, unlike phospholipids, is synthesized only in the cell body of neurons but not in distal axons, this accumulation of cholesterol in cell bodies suggested that the transport of cholesterol from cell bodies into distal axons is impaired in NPC1-deficient neurons (8). Further studies from our lab showed that the amount of exogenous LDL-derived cholesterol that reaches the distal axons is the same in both wild-type and knockout neurons; however, the transport of endogenously synthesized cholesterol is impaired (55). Indeed, these observations correlated with a reduced rate of anterograde transport of endogenous cholesterol from cell bodies into distal axons (55). A similar re-distribution of cholesterol was seen when mouse sympathetic neurons were incubated with the amphiphilic drug U18666A, a compound that has been widely used to mimic the NPC-like phenotype, since it leads to cholesterol accumulation in late endosomes (57). Treatment of hippocampal neurons with U18666A also reduced the cholesterol content in axonal plasma membranes (58). However, this drug also inhibits cholesterol biosynthesis and decreases the anterograde transport of cholesterol in sympathetic neurons to a far greater extent than does the loss of NPC1 (55). Also, LDL-derived cholesterol did not support normal axonal growth of *Npc1*$^{-/-}$ neurons when endogenous cholesterol synthesis was inhibited (55, 59). An important question which still remains unanswered is whether it is the lack of cholesterol in the distal axons, or its accumulation in the cell bodies, that is ultimately responsible for the neurodegeneration seen in NPC disease.

1.5 Possible roles for NPC1 in endosomal vesicular transport, synaptic vesicle recycling, and synaptic transmission

It is now becoming clear that loss of NPC1 function seems to have significant effects on multiple vesicle transport processes (60), that go beyond the formation of lipid-laden endosomes. In addition to LAMP2, Rab proteins, which are small molecular weight GTPases, are also marker proteins for late endosomes (61, 62), and play important roles in many aspects of membrane trafficking. Of particular importance in endosomal trafficking are Rab7, a regulator of vesicular endosomal traffic to lysosomes (63), and Rab9, a regulator of endosomal traffic to the *trans*-Golgi network (64). NPC1 has been shown to co-localize with both Rab7 and Rab9, indicating that it too may be involved in endosomal vesicular trafficking. NPC1-deficient fibroblasts display a reduced motility of endosomal tubulovesicular structures (65). It is interesting to note that in these fibroblasts, overexpression of Rab7 and Rab9 has been shown to normalize cholesterol and glycosphingolipid trafficking out of late endosomes/lysosomes, thereby reducing the cholesterol accumulation in these compartments (64,65). The trafficking of mannose-6-phosphate receptors (M-6-PR) out of late endosomes, which is Rab9-dependent, is also impaired in NPC1-deficient cells, suggesting that mistargeting of some proteins may occur, since M-6-PRs mediate trafficking of late endosomal/lysosomal proteins (60). Furthermore, NPC1 deficiency led to an increase in Rab9 protein by reducing Rab9 degradation (68). Therefore, an increased expression of Rab7/9 seems to partially bypass some of the trafficking defects seen with deficiency

of NPC1 (16). The role of Rab proteins in NPC disease may prove to be crucial, but still remains to be determined.

Several lines of evidence support a role for NPC1 in cholesterol modulated late endocytic vesicular transport. In studies by Neufeld et al. (1999), assessment of vesicular transport in NPC fibroblasts suggested that intracellular trafficking of cholesterol is mediated by vesicular transport (69). This group also demonstrated that NPC1-deficiency results in defective trafficking of a late endocytic compartment, and since late endocytic vesicle trafficking in both normal and mutant cells is inhibited by cholesterol overload, cholesterol modulates late endocytic trafficking in fibroblasts (69). Cholesterol loading increases the association of the NPC1 protein with membrane rafts in late endosomes, and has been proposed to disrupt sterol trafficking by promoting raft overcrowding in these endosomes, which are usually not rich in rafts (70).

Further evidence also suggests that NPC1 facilitates cholesterol delivery to the ER via a vesicular transport pathway. For example, chemical agents that disrupt the cytoskeleton and acidic compartments inhibit LDL cholesterol esterification (71). Furthermore, cells expressing NPC1-GFP show that NPC1 trafficks from an endosomal compartment via rapidly moving tubular extensions, reminiscent of microtubules, and subsequent budding of NPC1-containing vesicles (65, 72).

A similar trafficking of NPC1-containing late endosomes/lysosomes along axonal microtubules may also occur in neurons. Neurons are known to be highly dependent upon microtubules for axonal transport (65). Within axons, three types of transport exist: fast anterograde transport, which occurs at a rate of approximately 400mm/day, slow anterograde transport, occurring at an estimated rate of 2mm/day, and

retrograde transport, which occurs at an approximate rate of 200mm/day (73-76). Fast anterograde axonal transport is thought to be responsible for the transport of secreted proteins as well as membrane-associated proteins and lipids, via vesicles that are carried along axonal microtubules (77). Most of the proteins in neurons, including those which make up the cytoskeleton, such as microtubules, neurofilaments, and actin filaments, as well as cytosolic proteins, are transported via slow anterograde axonal transport (73, 75). Retrograde axonal transport is responsible for the transport of aging mitochondria and endocytic vesicles from axons back to the cell body (77). Recent findings from our lab using immunofluorescence and confocal microscopy have shown bi-directional movement of NPC1 protein-containing vesicles between cell bodies and distal axons of *Npc1*$^{-/-}$ mouse sympathetic neurons, when they are infected with an adenovirus expressing a cDNA encoding NPC1 tagged with green fluorescent protein (GFP) (9). Furthermore, adenoviral expression of NPC1-GFP eliminated cholesterol accumulation in cell bodies of these neurons (9). This strongly supports a potential role for NPC1 in trafficking of late endosomes along axonal mictrotubules in neurons.

Using a variety of techniques, our lab has shown that NPC1 and NPC2 proteins are expressed not only in cell bodies and proximal axons, but also in distal axons of mouse sympathetic neurons (55). Since these proteins are localized to late endosomes/lysosomes, and lysosomal degradation is presumed to occur only in cell bodies of neurons (78, 79), this was indeed a surprising finding. These discoveries suggested that NPC1 and NPC2 may have a neuron-specific role in axons.

Several findings have indicated that NPC1 is involved in synaptic vesicle recycling and may also affect synaptic transmission. **Figure 1.5** summarizes the

possible role of NPC1 in presynaptic terminals. Synaptic vesicle recycling and neurotransmitter release are two important processes that occur at the synaptosomes, or nerve terminals, of presynaptic neurons (80). Previous studies have established that the membranes of synaptic vesicles contain a higher cholesterol content than those of other organelles, suggesting that large amounts of cholesterol may be necessary for vesicle biogenesis (81-85). In addition, cholesterol levels in the cell determine the complexation of two synaptic vesicle proteins, synaptophysin and synaptobrevin, and formation of this complex determines synaptic efficacy (86). Furthermore, two studies have shown that SNARE-dependent exocytosis in a neuronal cell line occurs at cholesterol-rich domains in the plasma membrane (87, 88). SNARE is a protein complex that mediates fusion of presynaptic vesicles with the presynaptic membrane for exocytosis of neurotransmitters. Taken together, these studies indicated that cholesterol may be necessary for assembly of the vesicle exocytosis apparatus in the presynaptic plasma membrane (35). Therefore, since NPC1-deficiency decreases cholesterol content in distal axons and synaptic terminals, it is indeed feasible that this deficiency may affect the fusion of vesicles to the presynaptic plasma membrane, the formation of the exocytosis apparatus and, in turn, neurotransmitter release and synaptic transmission.

Our lab has demonstrated that NPC1 is present in recycling endosomes in presynaptic nerve terminals, and extensively co-localizes with the synaptic vesicle marker synaptophysin, which binds cholesterol (80, 89). NPC1 and synaptophysin partially co-localized to the same population of vesicles, but purified synaptic vesicles from synaptosomes did not contain NPC1 (80). However, NPC1 in nerve terminals co-

localized with the endosomal/lysosomal marker lysosome-associated membrane protein-1 (LAMP1), which indicated that NPC1 is present in endosomes, which are likely the recycling endosomes involved in synaptic vesicle recycling (80). Although the cholesterol content of synaptic vesicles from *Npc1*$^{+/+}$ and *Npc1*$^{-/-}$ synaptosomes was not different, their protein content was altered (80). First, the relative amounts of synaptophysin and synaptobrevin were altered in NPC1-deficient synaptic vesicles (80). Second, the ratio of vesicle-associated membrane protein 2 (VAMP2) to synaptophysin was lower in NPC1-deficient synaptic vesicles (80). The formation of the VAMP2/synaptophysin/synaptobrevin complex is a key event in tethering of synaptic vesicles to the presynaptic plasma membrane, as well as in synaptic vesicle recycling (90). Interestingly, in *Npc1*$^{-/-}$ mice brains, formation of this complex is reduced compared to *Npc1*$^{+/+}$ brains (139). Furthermore, electron microscopy studies of cerebellar synaptosomes showed that NPC1-deficient synaptosomes contained a population of aberrantly large synaptic vesicles of altered morphology that were not present in *Npc1*$^{+/+}$ synaptosomes (80). Taken together, all of these findings strongly suggest a neuron-specific role for NPC1 in the synaptic vesicle recycling pathway and synaptic transmission. A possible model is one in which impaired cholesterol transport from cell bodies to distal axons in neurons and loss of functional NPC1 in recycling endosomes that are involved in synaptic vesicle recycling ultimately leads to defective synaptic transmission, and may contribute to the neurological defects in NPC disease (11).

1.6 Mutations in domains of NPC1

To date, there are approximately 230 mutations in NPC1, of which only 3 are frequent (91), and these are scattered over the entire gene coding sequence. Of these mutations, around 70% are missense mutations, with more than one-third of them being located in the cysteine-rich luminal loop of NPC1 (92). The remaining 30% are nonsense mutations which lead to expression of a truncated, non-functional NPC1 protein (13). More than 50 single nucleotide polymorphisms (SNPs) have been identified in NPC1 (93). Interestingly, the combination of alleles and/or SNPs can induce a disease phenotype not seen in a patient homozygous for either allele or SNP alone (91). For example, an I1061T/P1007A heterozygote displayed an earlier onset of symptoms and slower disease progression than an I1061T homozygote (94). Therefore, the molecular diagnosis of NPC disease is complicated by the vast number of genetic variants in *NPC1* and the combination of different mutations in compound heterozygotes (14), making it relatively difficult to establish meaningful genotype-phenotype correlations.

The order of functional and/or structural significance of the various NPC1 domains seems to be luminal loop 1 (cysteine-rich region)>transmembrane domains (SSD)>luminal loop 3>luminal loop 2 (13). **Table 1** lists some known NPC1 disease-causing point mutations and their locations within NPC1. I1061T (3182T>C in exon 21) is the most prevalent *NPC1* mutation and accounts for approximately 20% of mutations in Western Europeans (95). It involves a substitution of thymine with cytosine at nucleotide 3182, leading to an aa change of isoleucine to threonine. Two

other frequent mutations include P1007A and G992W in patients of European descent and from an isolated population in Nova Scotia, respectively (94, 96). The most commonly studied specific NPC1 mutations have been I1061T and P691S (P692S in the mouse ortholog – a mutation in the SSD of NPC1). In both cases, mutation leads to the NPC phenotype, with an accumulation of cholesterol in late endosomes/lysosomes, although both mutant proteins still are transported and localize to late endosomal/lysosomal membranes. In addition, mutations in the leucine zipper motif at the N-terminal (L73P/L80P) showed the same effects (97). Since leucine zippers are involved in protein folding and protein-protein interactions, it has been proposed that a misfolded N-terminal domain might prevent movement of the NPC1 protein to a possible site of action within the lysosomal core (98). Furthermore, the correct formation of intra- or interchain disulfide bonds may be vital for the accurate assembly of NPC1 proteins, which consequently could affect maintenance of an active conformation (99). Deletion of the C-terminal di-leucine lysosomal targeting motif also led to an NPC1 protein that was unable to correct the cholesterol trafficking defect, but that accumulated in the ER, and not in late endosomes/lysosomes (98). This shows that the di-leucine motif is crucial in targeting NPC1 to late endosomes/lysosomes. In contrast, an N70Q mutant, bearing a mutation in the N-terminal glycosylated loop 1, did not cause cholesterol accumulation and was correctly targeted to the lysosomal/late endosomal membrane (45). Another mutation at this site, Q79A, abolished binding of radiolabeled cholesterol and 25-hydroxycholesterol to NPC1, showing that glutamine 79 in luminal loop 1 of NPC1 is important for sterol binding (17). Interestingly, this mutant restored cholesterol transport to NPC1-deficient CHO cells (17), indicating that

the sterol-binding site on luminal loop 1 is not essential for NPC1 function in cultured fibroblasts *in vitro*, although it may function in other cells where deficiency of NPC1 causes more severe abnormalities (17). The exact consequences and effects of the described NPC1 mutations still remain elusive, especially in neurons, and is an area of particular interest in our lab.

1.7 Models for studying the transport of NPC1 protein in murine sympathetic neurons *in vitro*

Because of the highly elongated shape of neurons, it is challenging to study protein transport and lipid metabolism in primary cultures of neurons (100). However, although they are difficult to work with, neurons provide excellent models for studying compartmentalization of lipid metabolic processes and axonal lipid and protein transport (100). The following section describes several models and methods that can be used to study the transport of proteins in murine sympathetic neurons, and particularly focuses on the methods used in the present studies for studying the transport of the NPC1 protein in these neurons.

1.7.1 Compartmented cultures of murine sympathetic neurons

There is a long spatial separation between the cell bodies and axons of many neurons in the body, and the two compartments are often exposed to different cellular and fluid environments (100, 101). In order to overcome this issue, Campenot, in 1977,

developed a method for the compartmented culture of neurons, in which cell bodies and proximal axons reside in a compartment separate from distal axons, and the two compartments can be exposed to different fluid environments, closely simulating the situation *in vivo* [Reviewed in Refs. (102, 103)]. Since its initial development, this method has been used widely and has proven to be highly effective for numerous applications such as immunoblotting experiments, lipid analyses, radiolabeling experiments, and enzymatic assays, which can be performed on isolated pure axons as well as cell bodies/proximal axons (100). The compartmented culture method for mice neurons presents several advantages over other neuronal cell culture systems commonly used. First, the neurons are pure, primary, and post-mitotic, and are largely free from contamination by other cells types (100). Furthermore, distal axons and cell bodies/proximal axons can be subjected to different treatments independently, and cellular material can be isolated and harvested separately for biochemical analyses (100). Although the compartment culture system was first developed for rats, our lab has established an efficient method for mice using similar methodology (104). Although this system is most commonly used for sympathetic neurons, it could be used theoretically for any type of neuron that extends axons of several millimeters in length (100). **Figure 1.6** shows a schematic of a compartmented neuron culture, which summarizes how the system works.

Although it offers many advantages, one drawback of using the compartmented culture system is that the number of neurons able to be plated in the culture dish is relatively small (approximately 2000 cells per dish), and therefore the amount of cellular material available for use is also limited (100). Thus, these cultures may not be

sufficient for use for some biochemical studies which require large amounts of cellular material (100). This problem may be partially solved by pooling together the cellular material of multiple dishes so that enough can be acquired; however, one small limitation is that the experiments are time consuming and it requires a considerable amount of skill to construct the compartmented cultures (100). Regardless, for many types of experiment, this method is the only available and best suitable option (100). For example, the compartmented neuron culture model is ideal for investigating the mechanisms of intraneuronal transport of proteins and lipids.

1.7.2 Primary neuronal cells and neuronal cell lines

Both primary sympathetic neuronal cultures and cultures of neuron-like cell lines can be used to study neuronal protein transport, and each of these models offers distinct advantages. The use of commercially available neuronal cell lines, which has become increasingly popular, has a number of advantages for performing standard biochemical studies such as immunoblotting experiments and immunofluorescence localization studies (100). These cell lines can be cultured easily and efficiently under defined conditions, and are readily open to transfection with cDNAs (100). In addition, they can be used more frequently and are more readily available and easily accessible for use than primary neuronal cultures, which require waiting for mice of the required age, gender, and genotype. Two of the neuronal cell lines most commonly used are PC-12 cells and NeuroA2 cells. PC-12 cells are rat pheocromocytoma cells that are derived from a tumor of the adrenal medulla, whereas NeuroA2 cells are murine blastoma cells

(105, 106). Although initially existing in non-neuronal phenotypic states, both these cell lines can be induced to display neuronal phenotypes under defined conditions. PC-12 cells, upon exposure to the neurotrophin nerve growth factor (NGF) and the subsequent activation of mitogen-activated protein kinase, stop dividing and rapidly adopt a neuronal phenotype within 24 hours which includes the sprouting and extension of neurites (105, 107). These cells, therefore, have certain properties which resemble features of peripheral neurons. Furthermore, when NGF is withdrawn from the culture medium, the neurites retract and the cells revert to their original, non-neuronal phenotype (101). On the other hand, NeuroA2 cells sprout neurites when exposed to retinoic acid, and in some ways resemble neurons of the CNS (106). Although these commercially available neuronal cell lines are convenient and serve as useful models, they still do differ from primary neurons (100, 101). As a result, primary cultures of neurons from mice must be used in some cases to get around some of the shortcomings of using neuron-like cell lines. However, it is important to note that primary neuronal cultures are more difficult to transfect with cDNAs, and are more susceptible to death induced by certain transfection reagents. In addition, they are more difficult to culture and may require much longer waiting periods before beginning culture studies, because mice with the desired age, genotype, and sex must first be generated. Also, one must take into account the fact that primary neuron cultures still represent an *in vitro* model, the results of which cannot be generalized to in situ or *in vivo* models of the nervous system, since neurons in the body interact closely with a variety of other cell types (100). For the present studies, we have used both murine primary neuron cultures, as well as PC-12 cells.

1.7.3 Expression of plasmid cDNAs in murine sympathetic neurons

The expression of cDNAs in primary neurons via plasmid transfection has proven to be an extremely difficult and inefficient process, despite the numerous cell transfection reagents that are available commercially. Exactly why primary neurons are much harder to transfect than many other primary cell types, remains elusive. Certain neuronal cell lines, such as PC-12 cells, show more promise when transfected with plasmid cDNAs. In particular, PC-12 cells are relatively easy to transfect in their undifferentiated non-neuronal state using a variety of methods such as calcium phosphate, lipofection, and electroporation. However, once neuronal differentiation occurs, the efficiency of transfection by all of these methods drops significantly (108). Therefore, the most ideal way to achieve a highly efficient transfection with plasmid cDNAs is to transfect the undifferentiated PC-12 cells, and subsequently induce neuronal differentiation via NGF, within a few hours. In the present studies, we have constructed plasmid cDNAs encoding wild-type and mutant (I1061T, P691S) NPC1 proteins tagged to enhanced GFP (eGFP), and used them in transfection of PC-12 cells in conjunction with a number of commercially available transfection reagents, namely, Lipofectamine 2000 (Invitrogen), Superfect (Qiagen), HD FuGENE (Roche), and Targefect (Targeting Systems). Since there have not been many studies in transfection of neurons, and neurons are difficult to transfect, we attempted to discover if any of these methods would produce high and optimal transfection efficiencies, in hopes to study the intraneural transport of the wildtype and mutant NPC1 proteins.

1.7.4 Expression of recombinant cDNAs in primary sympathetic neurons using adenoviral vectors

Post-mitotic primary neurons are impervious to standard methods of transfection and cannot be infected by commonly used retroviral constructs (109). Therefore, there has been much interest in the potential use of DNA viruses for expressing foreign genes in primary neurons. Adenovirus (Ad) is a DNA virus that naturally targets the respiratory epithelium, and was first discovered in 1953 when researchers were investigating the causative agents of the common cold (109, 110). In 1993, Le Gal La Salle et al. discovered that adenovirus was capable of infecting neurons (111). Since then, adenoviral vectors (AdV) have been used for foreign gene delivery in many different neuronal populations *in vitro* and *in vivo* (109), and today, the use of adenoviral vectors as a gene-delivery tool for gene therapy in neurons is an area of great investigation. The most commonly used adenoviral vectors for gene delivery are derived from human Ad serotypes 2 and 5 (110, 112).

Adenoviruses are non-enveloped icosahedral DNA viruses whose capsid is composed of hexons and pentons (110, 112). From each of the penton tips projects a fibrous protein with a globular tip called the knob domain, as depicted in **Figure 1.7**. The viral genome consists of a 36-kb non-segmented double stranded linear DNA, which is flanked on each end by Inverted Terminal Repeats (ITR) which act as an origin of replication (110, 112). The rest of the genome is divided into regions that are expressed at an early stage of the infection cycle, and others expressed at a later period (110). The early genes (E1a, E1b, E2, E3 and E4) encode products that are generally involved in viral gene transcription, DNA replication, host immune suppression, and

inhibition of host cell apoptosis, whereas the late genes (L1-L5) encode products that are required for virion assembly (112). The entry of Ad into target cells first involves binding of the knob domain to the Coxsackie virus and Adenovirus Receptor (CAR), followed by internalization via receptor-mediated endocytosis, which involves specific interactions between a motif on the penton base and integrins on the cell surface [Reviewed in Ref. (110)] (**Figure1.8**). Once internalized, the Ad escapes from the endosomes and translocates to the nucleus, where viral transcription and replication begin (112). Once the virus life cycle is complete, cell death and the release of progeny viruses are subsequently triggered (112).

There are many advantages of using a recombinant replication-deficient adenovirus for foreign gene expression. First, Ads can infect a broad range of mammalian cells, so they allow the expression of recombinant proteins in most mammalian tissues and cell lines (110). Second, retroviruses and certain other viruses can only infect replicative cells, whereas Ads are capable of also infecting primary non-dividing cells. Third, Ads can be replicated efficiently to high titers through propagation in human embryonic kidney (HEK) cells (110). Fourth, by deleting certain early regions of Ad, most commonly E1 and E3, additional cloning space is provided, and allows for the insertion of a single or multiple foreign genes of up to 7.5 kb into one recombinant Ad (110). Deleting these two regions also renders the viruses themselves replication-defective, and enables the Ad to express only the foreign gene(s) of interest. Finally, with a strong, constitutively active cytomegalovirus 5 (CMV5) promoter in Ads, recombinant proteins can be efficiently expressed at levels of up to 30% of total cellular proteins (110).

In addition to enjoying the aforementioned advantages, primary sympathetic neurons are also ideal targets for Ad because they express the CAR on their surface. Cells which do not express CAR, such as fibroblasts, smooth muscle cells, and macrophages, are poor targets for Ad gene transfer (113). In fact, it has been demonstrated that CAR is rate-limiting for Ad infection, and that CAR expression can increase Ad binding and gene transfer (114). Previously in our lab, we had used an adenoviral vector to express a chimeric construct consisting of the NPC1 protein fused to eGFP (Ad NPC1-eGFP), and were therefore able to observe the movement of the fluorescent NPC1 chimera bi-directionally between axons and cell bodies of murine primary sympathetic neurons *in vitro* (9). In addition, our lab found that expression of this chimeric protein abolished the abnormal accumulation of cholesterol in the cell bodies of Npc1-deficient neurons (9). These results suggested that this method could be highly promising for observing the intraneuronal transport of NPC1 and its mutants in sympathetic neuronal cultures, and for analyzing their expression, localization, movement, and functional properties *in vitro*. In the present studies, upon discovering that our original Ad NPC1-eGFP had lost the majority of its titer due to improper long-term storage, we re-constructed a new Ad encoding the NPC1-eGFP cDNA, which was obtained in plasmid form as a generous gift from Dr. Robert Maue (Dartmouth Medical School). We hoped that infection of $Npc1^{+/+}$ and $Npc1^{-/-}$ murine sympathetic neurons with this Ad would prove the Ad NPC1-eGFP to be functional, after which we would attempt to make Ads expressing mutant forms of NPC1 for further studies in the transport and function of the chimeric constructs in these neurons.

1.8 Thesis objective

To date, there have been very few studies performed on assessing the transport of the NPC1 protein and its various mutant forms in neurons. The focus of this thesis is on the technical aspects of studying the trafficking of the NPC1 protein in neurons, and it outlines why it has been extremely challenging to carry out these studies successfully. We first discovered that the Ad NPC1-eGFP we were using to infect primary sympathetic neurons had lost titer and was infective ability. After constructing a new adenovirus with a cDNA encoding the NPC1-eGFP, we found that it did not express the fusion protein. Also, using a variety of different techniques and approaches, we have accumulated data showing that neurons are very difficult to transfect with our wild-type and mutant NPC1-expressing plasmids, even with a variety of commercially-available transfection reagents [Lipofectamine 2000 (Invitrogen), HD FuGENE (Roche), Superfect (Qiagen), and Targefect-F2 plus Virofect (Targeting Systems)]. In addition, we show how boiling a cell lysate sample before immunoblotting for NPC1, which is normally a standard procedure for most proteins, drastically reduces the detection of NPC1. We also created two mutant forms of NPC1, the I1061T and P691S mutants. Sequence analysis later showed that our wild-type and mutant NPC1-eGFP fusion constructs did not contain enhanced GFP (eGFP) as we had previously assumed and expected, but rather, they contained a GFP variant which was an intermediate between GFP and eGFP. This variant form of GFP could also help explain some of our results and why fluorescence of our construct was much dimmer compared to a control eGFP construct. Finally, we obtained results which indicate that the NPC1-GFP mRNA is

expressed in infected and transfected neurons, but that the fusion protein is likely degraded to free GFP via an unknown post-transcriptional or post-translational mechanism. The contents of this thesis will be a valuable resource and knowledge base for anyone wishing to use plasmid transfections and adenoviral infections in performing studies in the transport of the NPC1 protein in neurons, and it will illustrate the potential challenges and problems encountered when undertaking these tasks.

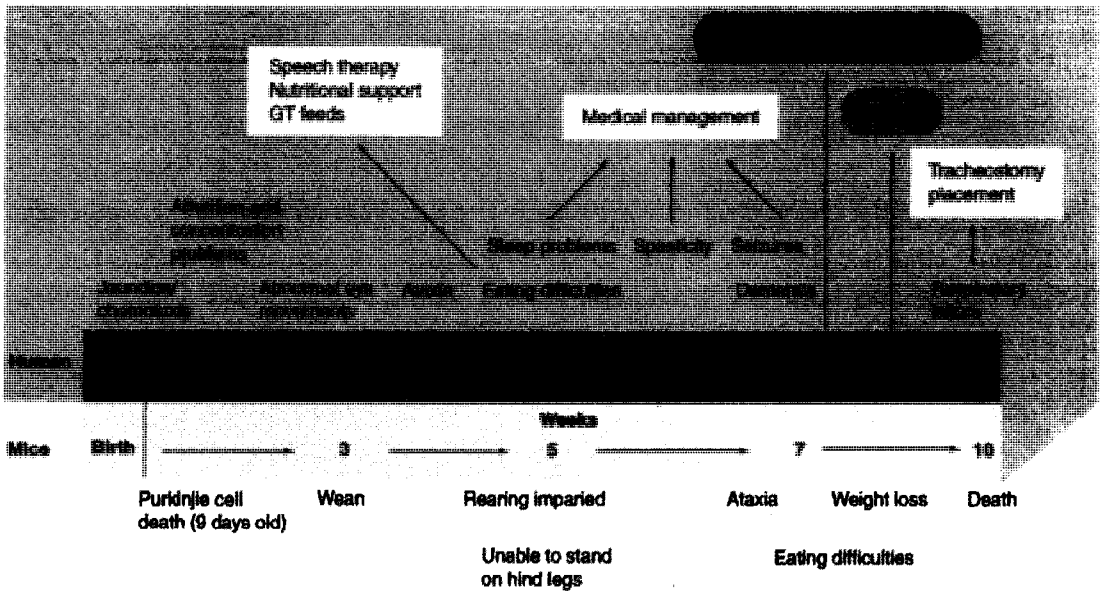

Figure 1.1 Timeline of the progression of Niemann-Pick type C disease in mice and humans. The clinical symptoms at each stage of NPC disease as it progresses are depicted in both mice and humans. In humans, the timeline is extremely variable. Bone marrow or liver transplants can be required in adulthood in humans with NPC. Miglustat is a drug which has been investigated for treating symptoms of the disease; however, results on this drug are inconclusive to date. Fig. adapted from Munkacsi *et al.*, 2007.

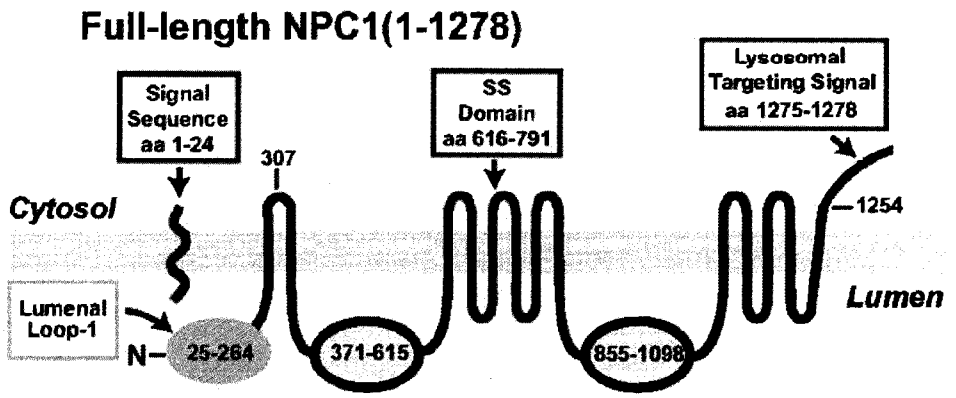

Figure 1.2 Topological structure of the NPC1 protein. NPC1 is a 1278-aa lysosomal membrane glycoprotein, consisting of 13 transmembrane domains (TMD), with the N-terminal located in the lumen of the lysosome and the C-terminal in the cytosol. TMDs 3-7 comprise the "sterol sensing" domain. The lysosomal targeting motif is located on the C-terminal end, and the N-terminal (NPC domain) contains a leucine zipper motif involved in protein-protein interactions. The cysteine-rich region is located in the third luminal loop. Fig. taken from Infante *et al.*, 2008.

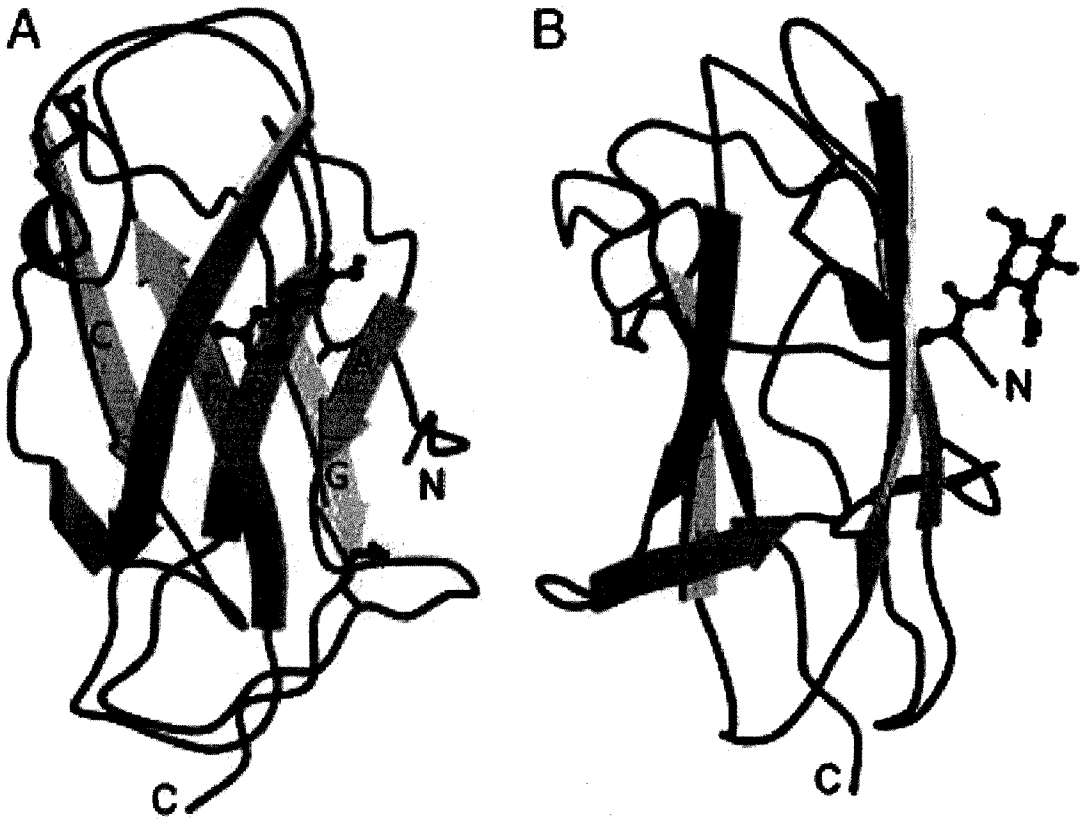

Figure 1.3 Structure of bovine NPC2. The model in B is a 90° rotated view of the model in A. One set of β sheets are depicted in green and the other in cyan. NPC2 is a 151 aa soluble lysosomal protein with the ability to bind cholesterol. NPC2 is thought to act in concert with NPC1, although the exact mechanism by which this occurs is elusive. Fig. taken from Friedland *et al.*, 2003.

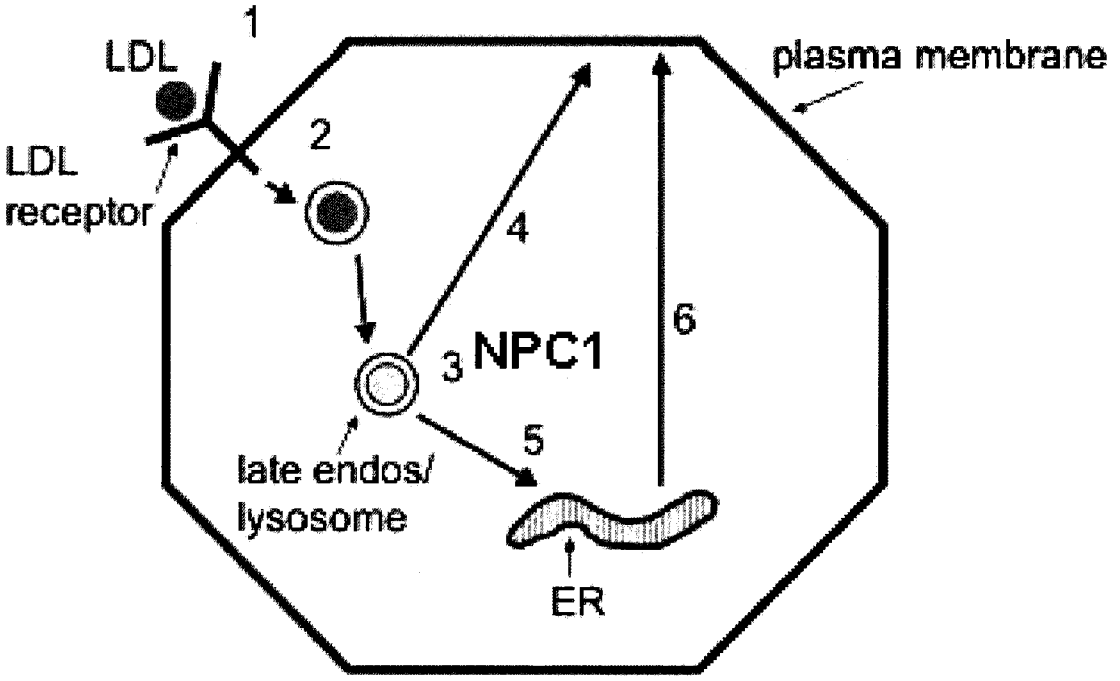

Figure 1.4 Model depicting how NPC1 is required for the removal of LDL-derived cholesterol from late endosomes/lysosomes. In normal cells, (1) LDL binds to LDL receptors on the cell surface, and is taken up by the cell via clathrin-mediated endocytosis (2). In late endosomes/lysosomes, the LDL-derived cholesteryl esters are hydrolyzed to unesterified cholesterol (3), which is then distributed throughout the cell, with the majority being delivered to the plasma membrane (4), and a small amount reaching the ER (5). Both these processes occur via an unknown mechanism that involves NPC1. The ER acts as a homeostatic cholesterol sensor, where increased cholesterol content results in a decreased synthesis of cholesterol and LDL receptors, as well as an increase in cholesterol esterification via ACAT. Cholesterol that is synthesized in the ER is also delivered to the plasma membrane (6). In NPC1-deficient cells, loss of NPC1 results in an abnormal accumulation of cholesterol in late endosomes/lysosomes, due to an inability to transport cholesterol out of these compartments. In addition, because cholesterol is unable to reach the ER, the cell senses a false deficiency of cellular cholesterol, and as a result, synthesis of cholesterol and LDL receptors continues unabated. Additionally, cholesterol synthesis via ACAT is also inappropriately decreased, resulting in a compounding further accumulation of unesterified cholesterol. Fig. adapted from Vance, 2006.

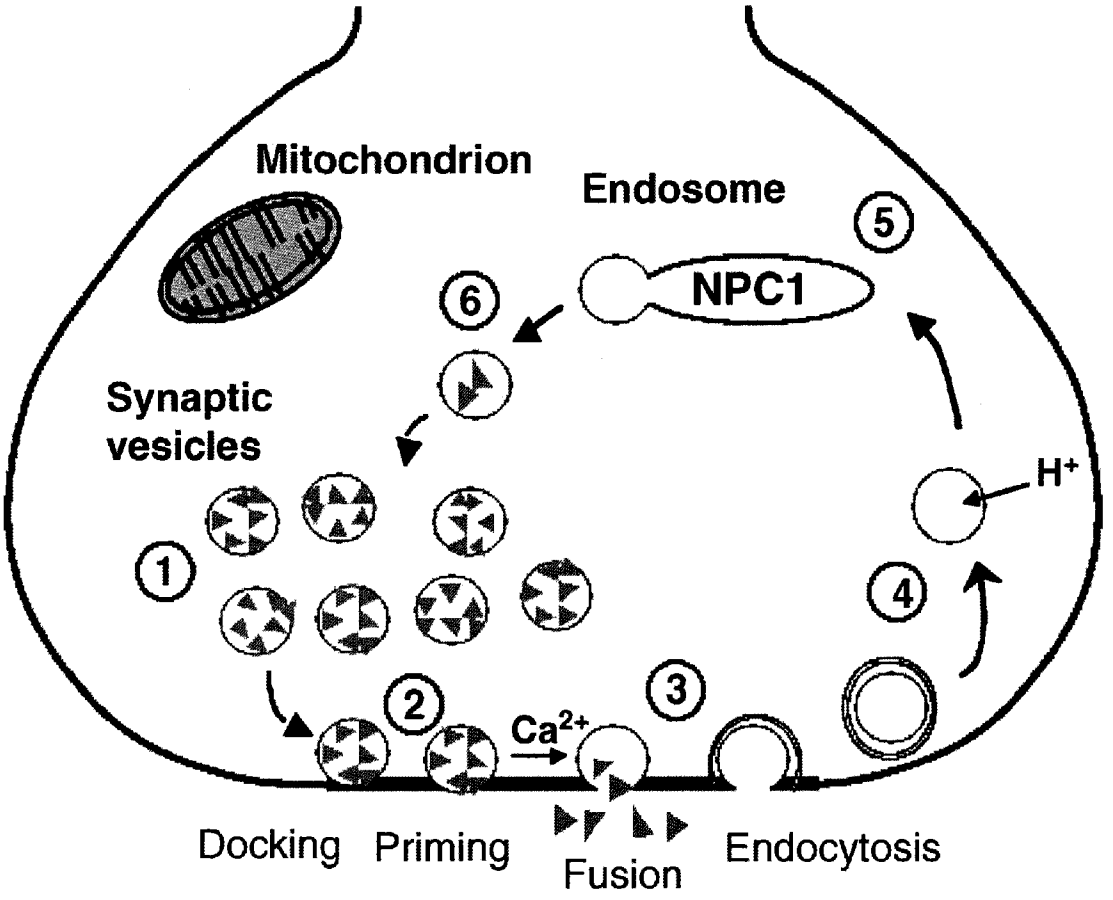

Figure 1.5 Proposed role of NPC1 in synaptic vesicle recycling in presynaptic nerve terminals. A pool of synaptic vesicles filled with neurotransmitters is present in the presynaptic nerve terminal, in close proximity to the plasma membrane (1). Nerve depolarization and influx of various ions triggers the docking and priming for fusion of these vesicles to the active zone at the presynaptic membrane (2), a process which requires the formation of a SNARE protein complex containing VAMP2, synaptophysin, and synaptobrevin, and involves calcium. Once fusion of vesicles occurs, neurotransmitters are released into the synaptic cleft (3). Synaptic vesicles are reinternalized (4) via clathrin-mediated endocytosis. These vesicles then shed their clathrin coat, undergo reacidification, and reach endosomal compartments containing NPC1 (5). Synaptic vesicles are reformed from the recycling endosome (containing NPC1), and are refilled with neurotransmitter (6). Fig taken from Karten *et al.*, 2006.

Table 1

List of some known NPC1 disease-causing point mutations

Loop 1	Loop 2	Loop 3	Loop 3 (cont.)	TM domains (3-7)	Other
C63R	V378A	D874V	R978C	M272R (1)	I642M
C74Y	L380F	P888S	G986S	M631R (3)	S652W
Q92R	A388P	V889M	G992W/R	G640R (3)	L724P
C113R	R389C	Y890C	M996R	G660S (4)	S734I
T137M	P401T	Y899D	S1004L	V664M (4)	R789C/G
P166S	R404Q/W	G910S	P1007A	C670W (4)	Y825C
C177Y/G	P433L	A927V	G1012D	G673V (4)	C1168Y
N222S	E451K	L929P	In frame del. of 1015–1032	L684F (5)	R1186H
G231V	S473P	R934Q	H1016R	P691S (5)	E1189G
In frame del. of S230, V231	P474L	S940L	V1023G	L695V (5)	
P237S	Y509S	W942C	A1035V	D700N (5)	
D242N/H	H510P	I943M	A1054T	F703S (5)	
C247Y	H512R	D944N	R1059Q	In frame del. of F740, S741 (6)	
G248V	R518W/Q	D945N	I1061T	E742K (6)	
	A521S	D948Y/N	F1087L	A745E (6)	
	P543L	V950M	Y1088C	A767V (7)	
	A605V	S954L	E1089K	Q775P (7)	
	E612D	C956Y	I1094T	S849I (8)	

Loop 1	Loop 2	Loop 3	Loop 3 (cont.)	TM domains (3-7)	Other
	R615C	R958Q/L	M1142T	Y852C (8)	
		C976R		N1137I (10)	
				G1140V (10)	
				M1142T (10)	
				N1150K (11)	
				N1156S (11)	
				V1165M (11)	
				T1205R/K (12)	
				L1213F (12)	
				G1236E (13)	
				S1249G (13)	

Table adapted from Scott and Ioannou, 2004.

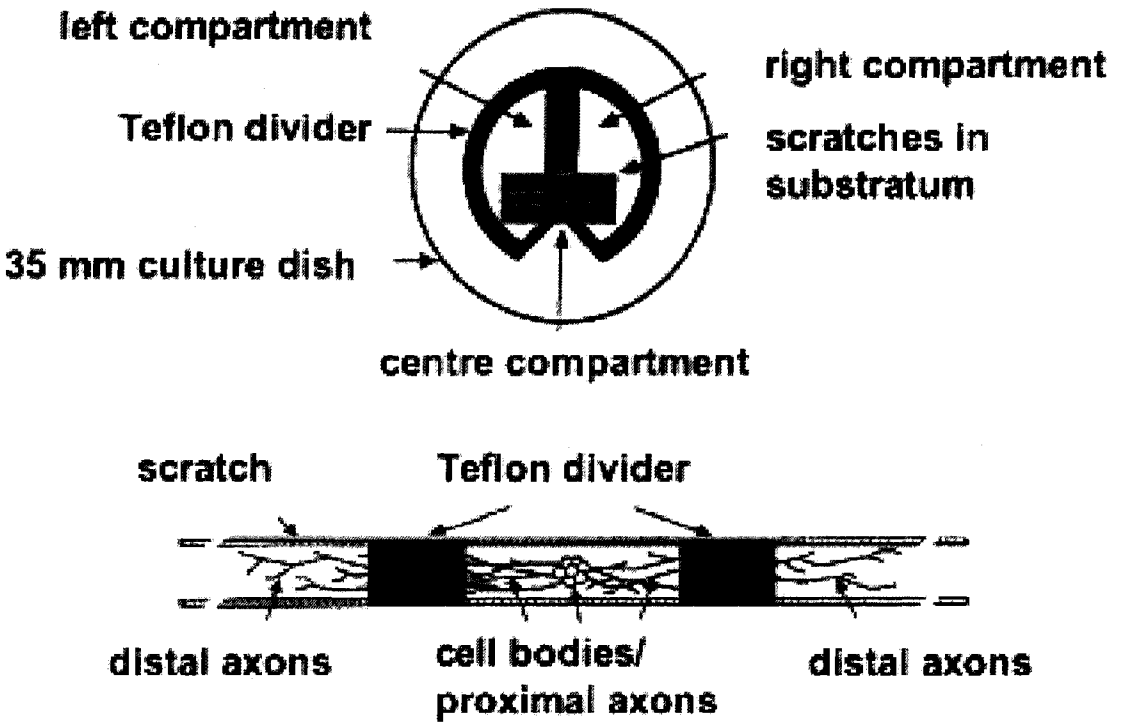

Figure 1.6 Schematic of a compartmented neuron culture. Parallel scratches are made on the surface of the collagen-covered 35mm culture dish. A Teflon divider is applied to this surface with silicone grease, and divides the dish into three compartments. Neurons are plated in the centre compartment of the dish, and axons grow and extend under the barriers, along the parallel tracks made by the scratches, into the two side compartments. The center compartment contains only cell bodies and proximal axons, whereas the two side compartments contain only distal axons. Thus, cell bodies/proximal axons can be subjected to different treatments than distal axons, and the two may be harvested separately for biochemical analyses applications. Fig. taken from Karten *et al.*, 2005.

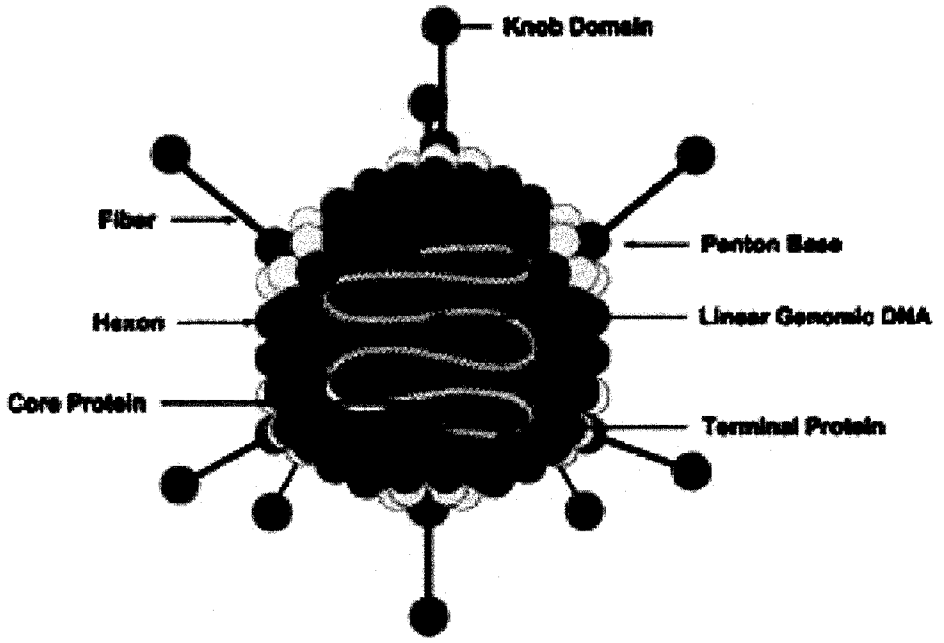

Figure 1.7 Adenovirus morphology. Adenoviruses are non-enveloped icosahedral DNA viruses, whose capsids are composed of hexons and pentons. Projecting from each penton base is a fiber protein containing a globular tip on its end called the knob domain. The diameter of the adenovirus capsid is 80-90 nm, and about 140 nm when the fibrous protein is included. Fig. taken from Adenovator Vector system applications manual Version 1.1, www.qbiogene.com.

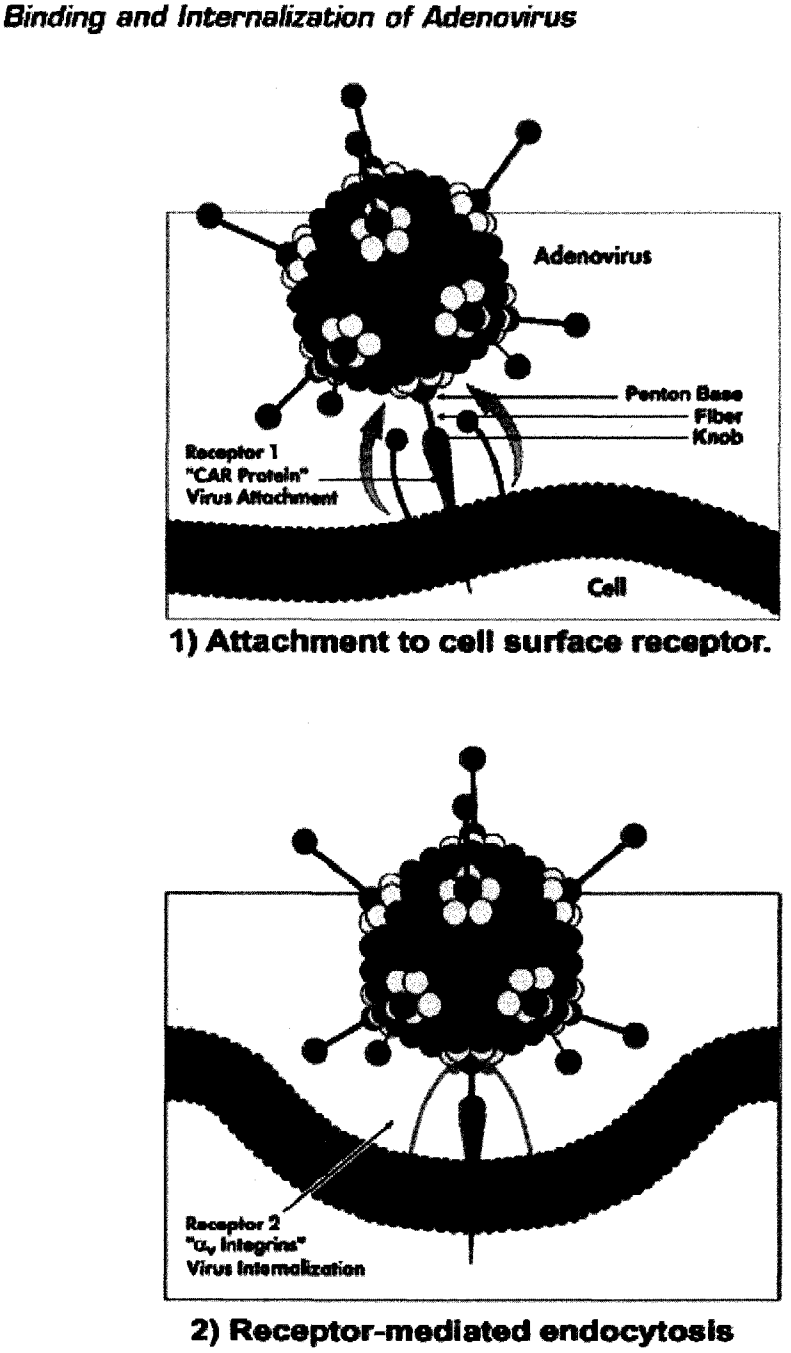

Figure 1.8 Schematic of the binding and internalization of adenovirus. First, the knob domain on the end of the adenovirus fiber binds to the Coxsackie and Adenovirus Receptor (CAR) on the cell surface. Then, the adenovirus is internalized into an endosomal membrane compartment via receptor-mediated endocytosis, a process which involved the interaction of a specific motif on the penton base with certain integrins on the cell surface. Once internalized, the adenovirus escapes from the endosome into the cytosol, and is transported into the nucleus, where transcription, replication, and viral packaging all occur. Fig. taken from Adenovator Vector system applications manual Version 1.1, www.qbiogene.com.

CHAPTER 2 – EXPERIMENTAL METHODS AND TECHNIQUES

2.1 Cell Culture

All cell cultures were maintained in a humidified 5% CO_2 environment at a temperature of 37°C.

2.1.1 Genotyping of mice and primary cultures of mouse sympathetic neurons

Superior cervical ganglia were dissected from 1-day-old mouse pups obtained from a breeding colony of Balb/cNctr-*npc*^{N}/+ mice established at the University of Alberta from original breeding pairs (Jackson Laboratories, Bar Harbour, ME). The mice were maintained under temperature-controlled conditions with a 12-h light : 12-h dark cycle. The genotypes of these pups were determined by PCR analysis of genomic DNA from tail clippings using primers as described previously (115), to determine whether they were wild type (*Npc1*$^{+/+}$), heterozygous (*Npc1*$^{+/-}$), or homozygous (*Npc1*$^{-/-}$) for the *Npc1* mutation. *Npc1*$^{+/-}$ mice were used for breeding. Once the genotypes were determined, *Npc1*$^{+/+}$ and *Npc1*$^{-/-}$ ganglia were pooled separately in sterile microfuge tubes containing L15 medium supplemented with 10% rat serum and 50 ng/mL nerve growth factor (NGF). The ganglia were kept overnight at 4°C, but for no longer than 24 h, before dissociation. The neurons were plated on 24-well plates at a density of 2 ganglions/well. They were maintained for 5-7 days in L15 medium containing 2.5% rat serum, 1mg/mL vitamin C, 2.5μg/mL cytosine arabinoside, 50ng/mL NGF, 0.4%

methylcellulose, and other additives as described previously (116), prior to the start of experiments.

2.1.2 COS-7 cells

Cells with an initial passage number of 11 were plated in Dulbecco's Modified Eagle's Medium (DMEM) (Gibco BRL, Burlington) containing 10% heat-inactivated fetal bovine serum (FBS) (Gibco BRL, Burlington). FBS was first heat-inactivated by incubation in a 56°C water bath for 30 minutes. Cells were maintained thereafter in the same medium, which was renewed every 2 days. Cells were split and passaged every 3-4 days in order to maintain appropriate confluency, and were used in experiments at passage numbers of less than 17, and at approximately 70-80% confluency.

2.1.3 PC-12 cells

Undifferentiated PC-12 cells were plated and maintained in a 75cm^2 culture flask (Falcon) in Kaighn's modification of Ham's F12 medium (F12K) with 2mM L-glutamine and 1.5g/L sodium bicarbonate (Gibco), supplemented with 15% heat-inactivated horse serum (HS) (Gibco) and 2.5% FBS. Media was renewed every 2-3 days thereafter. In some experiments, neuronal differentiation was induced prior to cell transfection, and in other experiments neuronal differentiation was induced following transfection. Prior to each experiment, PC-12 cells were plated in collagen-coated 6-well plates at a density of 200,000 cells/well. The cells were incubated overnight and

then differentiation was induced by replacing the culture media with F12K medium containing 2.5% heat-inactivated HS and 50ng/mL NGF.

2.1.4 HEK 293 cells

Human embryonic kidney (HEK) 293 cells were cultured and maintained in Minimum Essential Medium (MEM) (Gibco) containing 10% heat-inactivated FBS and the antibiotic gentamycin (Invitrogen). Cells were passaged every 4-5 days, and medium was renewed every 2 days. Cells were used at passage numbers of no more than 38, and at confluencies varying from 60-80%.

2.1.5 Primary cultures of mouse hepatocytes

Npc1$^{+/+}$ and *Npc1*$^{-/-}$ mouse livers were harvested (MCBL SOP #006 "Isolation of Hepatocytes from Rats and Mice", April 2007), and hepatocytes were plated in collagen-coated 35mm culture dishes in DMEM containing 10% FBS. Cells were plated at a density of 1 X 10^6 cells/dish. Cells were incubated for 4 hours, after which time the media was renewed with fresh media, and transfection/infection experiments were performed.

2.2 Molecular Genetics and Cloning

2.2.1 Re-cloning NPC1-eGFP into the pAdenovator vector

The cDNA sequence encoding NPC1-eGFP in the Qbiogene Ad-CMV5 NPC1-eGFP vector (obtained from Dr. R. A. Maue, Dartmouth Medical School) was sub-cloned into the commercially available vector pAdenovator (Qbiogene). The Ad-CMV5 NPC1-eGFP, which will be referred to as the "Maue" plasmid in all future references, was used as a template in a PCR using two synthesized primers (5'–AGAGAGCTCGAGAAAGGCGTCTAACCA-3'; 5'-TCTCTCGTTTAAACTTACTTGTACAGCTCGTCCAT-3'), corresponding to the 5' end of NPC1 and the 3'end of eGFP, respectively, in order to amplify the region of DNA containing the NPC1-eGFP. The forward primer consisted of the nucleotide sequences corresponding to the 5' end of NPC and included a sequence for the XhoI restriction site. The reverse primer consisted of the nucleotide sequences corresponding to the 3' end of eGFP and included a sequence for the PmeI restriction site. The PCR product was then purified on Qiaprep columns (Qiagen), and 2μg of this purified product was digested with the restriction enzymes PmeI and XhoI, in order to cut out the NPC1-eGFP insert. 2μg of the pAdenovator vector was also digested with PmeI and XhoI, and shrimp alkaline phosphatase was added to this digested vector to de-phosphorylate the ends of the vector, in order to increase ligation efficiency. The digested vector product was then subjected to gel electrophoresis on a 0.7% low-melting agarose gel, and the desired band was cut out and subsequently purified using a

gel extraction kit (Qiagen). The NPC1-eGFP insert was then ligated into the digested and de-phosphorylated pAdenovator vector, using insert:vector ratios of 3:1 and 10:1, via T4 DNA ligase (Invitrogen). The ligation reaction was left overnight at 16°C. Competent *Escherichia coli* (DH5-α) cells were then subjected to chemical transformation with the ligation products, and were plated on agar plates containing the antibiotic kanamycin, the resistance marker for the pAdenovator vector. Twenty colonies were made into miniprep DNA and five of these DNA samples showed the desired pAdenovator NPC1-eGFP product by restriction enzyme digest and PCR analyses. The correct NPC1 cDNA sequence was further verified by uni-directional sequence analysis.

2.2.2 Construction of the I1061T mutation in the cysteine-rich loop and the P691S mutation in the sterol-sensing domain of the NPC1 protein

The Quikchange II XL Site-directed mutagenesis kit (Stratagene) was used to make a point mutation at base 3182 of the NPC1 cDNA, which led to a substitution of threonine for isoleucine, resulting in the production of the I1061T mutant NPC1 construct. The wild-type pAdenovator NPC1-eGFP plasmid was used as the template for the mutation. Briefly, forward and reverse primers were designed (5'-TGCCATGAAGAAAGCTCGGCTAACAGCCAGTAACAT-3'; 5'-ATGTTACTGGCTGTTA GCCGAGCTTTCTTCATGGCA-3') around the expected mutation site, which amplified the expected mutated form of NPC1 when subjected to a PCR reaction. The amplified product was then digested with the restriction enzyme

DpnI, in order to digest the parental methylated and hemimethylated DNA. The digested product containing the mutation was then transformed into XL 10-Gold ultracompetent cells, and these cells were incubated at 37°C for 17 hours until sufficient bacterial growth was observed. Screening of a few colonies by preparing miniprep DNA samples and subjecting them to restriction enzyme digestion analysis showed that the NPC1-eGFP insert was present in the plasmid. Further verification of the I1061T mutant plasmid by sequence analysis showed only the single and correct nucleotide base change at position 3182 of NPC1. Using the same mutagenesis kit, another point mutation was made at base 2071 of the NPC1 cDNA, using forward and reverse primers around the mutation site (5'-TGCCATGAAAGCTCGGCTAACAGCCAGTAACAT-3'; 5'-ATGTTACTGGCTGTTAGCCG AGCTTTCTTCATGGCA-5') which led to a substitution of serine for proline, resulting in the production of the P691S mutant NPC1 construct. The sequence of the mutant was confirmed by sequence analysis. Expression of this mutant plasmid was also confirmed by transfecting COS-7 cells and viewing the fluorescent protein using fluorescence microscopy.

2.2.3 Re-cloning NPC1-eGFP into the pEGFP-N1 vector

To determine if a large plasmid size prevented high transfection efficiencies, the NPC1-eGFP cDNA was re-cloned into the smaller commercially available vector pEGFP-N1 (~4.7 kb). The pAdenovator NPC1-eGFP vector was used as the starting template. Forward and reverse primers (5'-AGAGAGGCTAGCGGCGACAGCATGGGTGCG-3'; 5'-GAGAGAGCGGCCGC

GATCTTTACTTGTACAGCTCGTCC-3') were synthesized around the NPC1-eGFP coding sequence of the plasmid, and this gene product was amplified via PCR using PfuTurbo DNA Polymerase (Stratagene). The forward primer, which corresponded to the 5' end of NPC1, included a sequence for the NheI restriction site, and the reverse primer, which corresponded to the 3' end of eGFP, included a sequence for the NotI restriction site. Both the PCR product and the template vector were then subjected to sequential digestion with the NheI and NotI restriction enzymes. Ligation reactions were set up overnight at 16°C, followed by chemical transformation of competent *E. coli*. Screening by restriction enzyme digestion analysis confirmed that the desired clone was produced. Note that the eGFP gene sequence from the pEGFP-N1 vector was not used, as it was removed in the digestion process, prior to ligation with the NPC1-eGFP fusion gene construct.

2.3 Production and purification of Adenovirus NPC1-eGFP

The following protocol was obtained from Amy Barr (University of Alberta), which was modified from the protocol set forth by Tong-Chuan He *et al.* (1998). The pAdenovator NPC1-eGFP vector was used as the starting template for production of Adenovirus NPC1-eGFP. 2μg of this template was linearized with the restriction enzyme FseI. The linearized vector was then purified by phenol/chloroform extraction, and precipitated with 3M sodium acetate (pH 5.2) and 95% ethanol. The recovered dry DNA was re-suspended in sterile water and quantified. Then recombinant adenoviral plasmids were generated by homologous recombination in *E. coli*. Briefly, BJ5183 –Ad

Easy 1 electroporation competent cells (Stratagene), which contained the adenoviral backbone, were electroporated with 100ng of the purified FseI-digested vector, using a pre-programmed protocol (Ec2) on a BioRad MicroPulser. 500μL of Luria-Bertani (LB) medium was added to this mixture, and 10μL, 100μL, and 200μL were plated on separate LB agar + kanamycin plates and incubated for 24h at 37°C. 12 colonies were picked and miniprep DNA was produced from these colonies. Each of the DNA samples was digested with the restriction enzyme PacI and the digested DNA was subjected to gel electrophoresis on a 1% agarose gel. The successful recombinants were then re-transformed into DH5-α cells and a maxiprep of recombinant DNA was prepared for transfection into mammalian HEK 293 cells for large-scale production of adenovirus NPC1-eGFP. The adenoviral lysate, before being purified, was used to infect mouse hepatocytes and COS-7 cells to determine whether the NPC1-eGFP lysate was functional at this point. The adenoviral lysate was then precipitated by ammonium sulfate and subsequently purified via a cesium chloride gradient. HEK 293 cells were then infected with the purified adenovirus NPC1-eGFP in serial dilutions in order to determine the infective capability and titer of the virus. The number of fluorescent cells were counted after 2-3 days (fluorescent titer method), and also the number of plaques formed were counted after approximately one week (plaque titer method). An overview of the technology used to produce an adenovirus is shown in **Figure 2.1**.

2.4 Adenoviral infection of mouse sympathetic neurons with NPC1-eGFP

Npc1$^{+/+}$ and *Npc1*$^{-/-}$ mouse sympathetic neurons were grown for 5 days under routine conditions (L15 base medium, 2.5% rat serum, 1mg/mL vitamin C, 50ng/mL NGF, 0.4% methylcellulose, glucose, fresh vitamin stock, Penicillin/Streptomycin, glutamine) on collagen-coated 6-well plates. Medium was then changed to infection medium (DMEM:Ham's F-12 1:1, + 50ng/mL NGF, B27 supplement (Gibco), glutamine, and fresh vitamin stock). The original adenovirus NPC1-eGFP viral stock, with a concentration of 5.77 X 10^{11} viral particles/mL (obtained from Dr. R. Maue) was diluted into the infection medium to a concentration of 2µL/mL. 150µL of this medium was added per well. Cells were incubated for 24h with the virus-containing medium, after which the medium was aspirated and replaced with normal L15 medium. Cells were viewed by fluorescence microscopy 3 days after the start of the infection. (Protocol adapted from Dr. Barbara Karten, "Adenovirus infection of sympathetic neurons", 2005). A control adenovirus-eGFP (obtained from Dr. Rene Jacobs, University of Alberta) was used in infections as a positive control to check for infection efficiency of Adenovirus NPC1-eGFP.

2.5 Filipin labeling of mouse sympathetic neurons

Npc1$^{+/+}$ and *Npc1*$^{-/-}$ mouse sympathetic neurons were stained with filipin (Sigma), a marker of unesterified cholesterol, to determine localization of unesterified

cholesterol in the cells. Briefly, cells were grown for 5 days, then washed twice with phosphate-buffered saline (PBS). This was followed by incubation of the neurons for 15 minutes with 4% paraformaldehyde in PBS. Following the incubation period, cells were washed twice again with PBS, and then incubated for 1h at room temperature, in the dark, in PBS containing 0.15mg/mL filipin. The cells were then washed twice more with PBS and viewed under fluorescence microscopy.

2.6 Transfection of COS-7 cells, PC-12 cells, and mouse sympathetic neurons

COS-7 cells were plated in 6-well plates at a density of 200,000 cells/well, grown for 24h, and transfected with various plasmid DNAs, as well as infected with the crude adenoviral NPC1-eGFP lysate (before purification of the adenovirus). Cells were transfected with the Maue plasmid, pAdenovator NPC1-eGFP, pEGFP-N1 NPC1-eGFP, and adenoviral NPC1-eGFP plasmid (the plasmid containing NPC1-eGFP in the adenoviral backbone, prior to production of adenovirus). 5μg of each plasmid DNA was used with the transfection reagent HD FuGENE (Roche) in a FuGENE:DNA ratio of 2:1, and transfections were carried out according to manufacturer specifications. Transfection complexes, which were formed in 250μL of Opti-MEM Reduced serum medium (Gibco), were added directly to the cell culture medium, and left on for 24h before media was renewed. Cells were also infected with 500μL of adenoviral NPC1-eGFP crude lysate as another separate treatment, and media was also renewed after 24h. Cells were viewed by fluorescence microscopy 24h, 48h, and 72h after transfection/infection.

Undifferentiated PC-12 cells were plated at a density of 200,000 cells/well in a collagen-coated 6-well plate. The medium was changed to plain serum-free F12K medium 12h after plating. Cells were transfected with the various NPC1-eGFP-containing plasmids, as described above for COS-7 cells. Cells were transfected 12h after plating, using the commercially-available transfection reagents Superfect (Qiagen), Lipofectamine 2000 (Invitrogen), HD FuGENE, and Neuronal Targefect-F2 plus Virofect enhancer (Targeting Systems), according to each of the manufacturers' protocols. Many different conditions were tested for each reagent in order to produce the optimal transfection efficiencies, including transfection of differentiated and undifferentiated cells, both in the presence and absence of serum. DNA amounts, as well as ratios of DNA:transfection reagent were manipulated. It was determined that 4μg of each plasmid DNA was optimal for the transfections. Briefly, DNA was added in a 3:1 ratio to Lipofectamine 2000, a 2:1 ratio to HD FuGENE, a 2:1 ratio to Superfect, and a 2:1 ratio to Targefect-F2, and incubated for 20 minutes at room temperature to allow formation of DNA-transfection reagent complexes, which were then applied to PC-12 cells. For undifferentiated cells, 12h after transfection, the cells were given serum-free F12K medium containing 50ng/mL NGF, to promote neuronal differentiation. All cells were viewed by fluorescence microscopy after 48h and 72h.

Npc1$^{+/+}$ and *Npc1*$^{-/-}$ mouse sympathetic neurons were also transfected with the new commercially-available transfection reagent Neuronal Targefect-F2 (Targeting Systems), using manufacturer protocols.

2.7 Immunoblotting of NPC1-eGFP fusion protein

COS-7 cells, *Npc1*$^{+/+}$ and *Npc1*$^{-/-}$ mouse hepatocytes, and PC-12 cells were scraped and harvested into ice-cold homogenization buffer consisting of a protease-inhibitor solution (Complete Mini, Roche Diagnostics, Manheim, Germany), PBS + 0.1% DOC + 0.1mg/mL EDTA. Samples were sonicated at room temperature for 3-5 seconds using a sonicator. Protein assays were performed on each sample to determine total protein concentration. 20μg of each sample (non-boiled) were used, and the proteins were resolved on 6% polyacrylamide gels containing 0.1% sodium dodecyl sulfate (SDS) by electrophoresis. Immunoprecipitated proteins were then transferred onto nitrocellulose membranes, and immunoblotted using a rabbit polyclonal anti-human NPC1 antibody (Novus Biologicals) [dilution 1:1000 in Tween tris-buffered saline (TTBS) + 1% milk] and a horseradish peroxidase (HRP)-conjugated goat anti-rabbit IgG (dilution 1:2500 in TTBS + 5% milk) as a secondary antibody. Proteins were also immunoblotted using a rabbit polyclonal anti-GFP antibody (Molecular Probes) (dilution 1:2500 in TTBS + 1% milk) and an HRP-conjugated goat-anti rabbit IgG (dilution 1:2500 in TTBS + 5% milk) as a secondary antibody. Immunoreactivity was detected with ECL reagent (Supersignal West Dura/Femto, Pierce).

2.8 Reverse-transcription polymerase chain reaction (RT-PCR) to detect mRNA levels of NPC1-GFP

Forward and reverse specific primers (5'-GTACATCATGGCCGACAAGCA-3'; 5'-AACTCCAGCAGGACCATGTG-3') were designed in the eGFP area of the NPC1-eGFP coding region which was also compatible with the eGFP sequence in eGFP-N1. PC-12 cells, which were transfected with the various NPC1-eGFP containing plasmids (Maue, pAdenovator NPC1-eGFP, eGFP-N1 NPC1-eGFP, and I1061T), were harvested in Trizol, and the RNA from each of these samples was isolated. The RNA from each sample was then treated with DNAse I, in order to degrade any parental DNA that may have been present in the samples. The cDNA from each RNA sample was produced by the SuperScript II reverse transcriptase (Invitrogen) via a PCR reaction. The PCR products were then resolved on a 1.4% agarose gel, and the bands were visualized for the detection of mRNA levels in the transfected cells. This was a qualitative assay, and the strength of each band was compared to the band produced by transfection with a control eGFP-N1 plasmid. The house-keeping gene cyclophilin was used as a loading control.

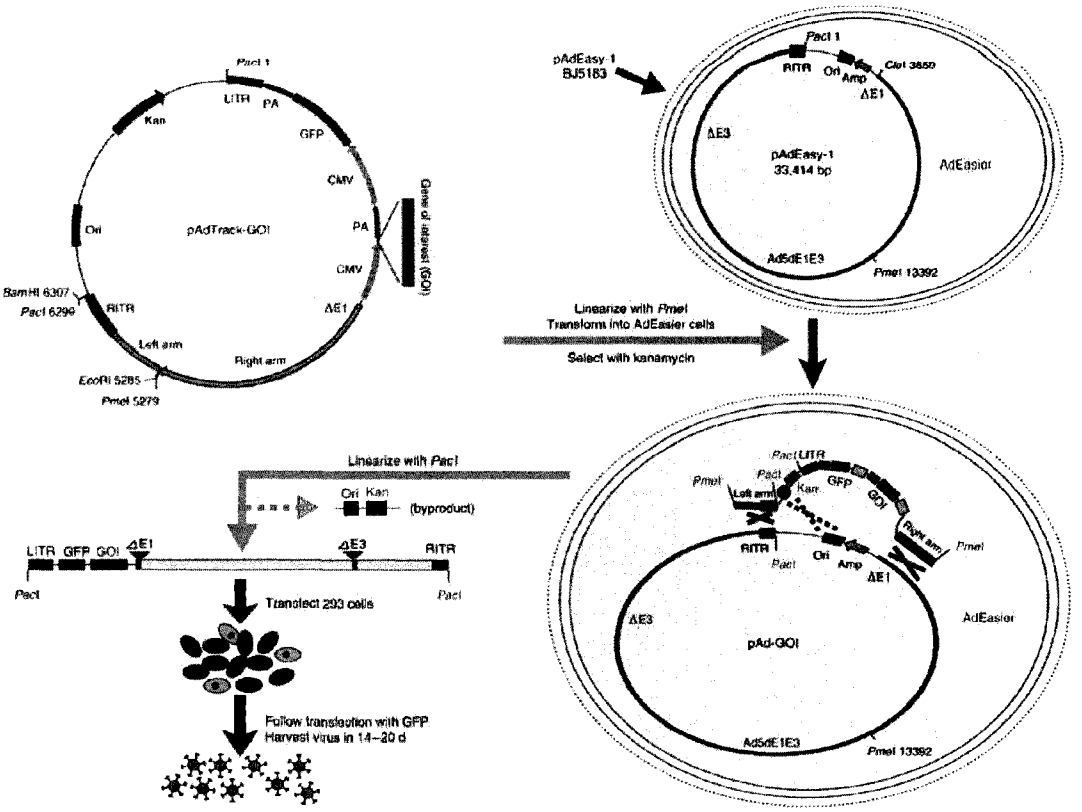

Figure 2.1 Schematic of the technology used to produce Adenovirus NPC1-GFP. The gene of interest (GOI), in our case, NPC1-eGFP, is first cloned into an appropriate shuttle vector (pAdenovator in our case). This plasmid is then linearized by digestion with the restriction enzyme PmeI or FseI, and is subsequently transformed into competent BJ5183 cells, which contain the adenoviral backbone plasmid pAdEasy-1. Once recombinants are selected for kanamycin resistance, they are confirmed by restriction endonuclease analysis, linearized with the restriction enzyme PacI, then transfected into HEK 293 cells. Recombinant adenoviruses containing the GOI are then generated within 14-20 days. Fig. taken from Luo *et al.*, 2007.

CHAPTER 3 – RESULTS

3.1 Filipin staining reveals that unesterified cholesterol accumulates in cell bodies of *Npc1*$^{-/-}$ mouse sympathetic neurons

To confirm that cholesterol accumulation occurs in cell bodies of Npc1-deficient sympathetic neurons as reported previously (8, 9, 55), *Npc1*$^{+/+}$ and *Npc1*$^{-/-}$ mouse sympathetic neurons were cultured in collagen-coated 6-well plates for 6 days, and then labeled with filipin (a dye which stains for unesterified cholesterol) and visualized under fluorescence microscopy. As shown in **Figure 3.1**, unesterified cholesterol is present in both cell bodies as well as axons in both genotypes. However, as observed previously (9, 55), there is a marked cholesterol redistribution/accumulation within the cell bodies of the *Npc1*$^{-/-}$ neurons, while the *Npc1*$^{+/+}$ genotype showed cholesterol staining around the plasma membrane but little intracellular staining. Previous studies have demonstrated that the punctuate intracellular distribution of cholesterol in Npc1-deficient neurons co-localizes with the late endosomal/lysosomal marker protein, LAMP-1 (80).

3.2 Adenoviral NPC1-eGFP infection of non-neuronal cells is much more efficient than that of neurons

Since primary neurons have been shown to be readily infected by adenovirus, and in order to study the localization and transport of the NPC1 protein, we used an

adenovirus NPC1-eGFP (Ad NPC1-eGFP), which was obtained as a generous gift from Dr. Robert Maue (Dartmouth Medical School), to infect murine sympathetic neurons. Initial experiments infecting 7-day wild-type murine sympathetic neurons in primary culture (cultured in a 24-well plate) showed that non-neuronal cells are infected at a much higher efficiency than neurons (**Figure 3.2**). Therefore, it is important to produce as pure a neuron culture as possible, which is accomplished by addition of cytosine arabinoside (ARAC) to the culture medium. ARAC kills any dividing (non-neuronal) cells. However, even in the presence of ARAC, there was still some contamination by non-neuronal cells (**Figure 3.2**).

Of the neurons that *were* infected, staining in the cell body was evident; however, no staining was visible in the axons of these neurons, as shown in **Figure 3.3**. Important to note is the fact that the infected neurons seemed to be unhealthy, possibly due to the toxicity of the adenoviral infection. The toxic effect of adenovirus infection on sympathetic neurons has been reported previously (109), although the exact mechanism of the toxicity remains elusive. Therefore, we were unable to achieve a sufficient amount of infection for our study, and were curious as to why the infection efficiency was so low and faint. Previous use of this same Ad NPC1-eGFP in our lab showed strong infection of the neurons, with fluorescence in the cell bodies as well as axons, and the health of the infected neurons did not appear to be compromised (9).

3.3 Adenovirus NPC1-eGFP viral stock has lost titer and infection efficiency

We decided to determine the infective viability of our viral stock obtained from Dr. R. Maue by performing an experiment in which wild-type mouse hepatocytes were cultured in 35mm culture dishes, and infected 4h after plating with our Ad NPC1-eGFP alongside a control adenovirus-eGFP (Ad-eGFP), containing the same CMV promoter (obtained from Dr. Rene Jacobs, University of Alberta). Both treatments were subjected to a multiplicity of infection (M.O.I.) of 25, which is the effective dose for primary cultured mouse hepatocytes. Each viral stock was diluted in regular culture medium and hepatocytes were treated with the infection medium for 2h, after which the medium was replaced with regular culture medium. Cells were visualized at 24h and 48h post-infection, and fluorescence microscopy revealed that the infection by Ad NPC1-eGFP was much less efficient (~10% of cells infected) than that of the control Ad-eGFP [~90% of cells infected (data not shown)]. Furthermore, fluorescence of the Ad NPC1-eGFP-infected cells was much dimmer compared to that of Ad-eGFP-infected cells. Control hepatocytes which were untreated did not show any fluorescence. These observations indicated that the Ad NPC1-eGFP viral stock had lost a majority of its titer and was ineffective. This could be due to the fact that we had been storing the viral stock at a temperature of -80°C instead of at 4°C (the ideal temperature at which to store adenovirus stocks). The Maue lab from which our virus was obtained had been storing the virus at 4°C, and as well, in conversing with another lab specializing in use of adenoviruses (Dr. Jason Dyck, University of Alberta), we were informed that long-term storage at improper temperatures and multiple freeze-thaw

cycles of adenoviral stocks results in a loss of infection efficiency and viral titer. This loss of titer of our Ad NPC1-eGFP was further confirmed by experiments in wild-type mouse sympathetic neurons, which were infected with effective doses (M.O.I. 100) of Ad NPC1-eGFP (**Figure 3.4A**) alongside with the control Ad-eGFP (**Figure 3.4B**). There was almost no infection with Ad NPC1-eGFP, as determined by fluorescence microscopy, whereas about 30% of cells showed strong infection with Ad-eGFP.

3.4 Newly re-constructed Adenovirus NPC1-eGFP infection of *Npc1*$^{+/+}$ and *Npc1*$^{-/-}$ mouse hepatocytes and COS-7 cells indicates that the NPC1-eGFP fusion protein is either not expressed and/or was degraded within the cell

After determining that the original Ad NPC1-eGFP has lost its titer and infectivity, we constructed a new Ad NPC1-eGFP as described in Section 2.3. Before purification of this newly-constructed adenovirus, we performed a functional assay to test for the viability and functionality of the crude adenoviral NPC1-eGFP lysate. *Npc1*$^{+/+}$ and *Npc1*$^{-/-}$ mouse hepatocytes from 7-week old mice were plated at a density of 1 X 10^6 cells/dish on 60mm collagen-coated dishes, and infected overnight with 800μL of the crude adenoviral NPC1-eGFP lysate 4h after plating. Although the titer of the viral stock was unknown at this point, previous optimization experiments in COS-7 cells showed 800μL to be the optimal amount of lysate for infection. As a comparative positive infection control, the *Npc1*$^{+/+}$ and *Npc1*$^{-/-}$ hepatocytes were also infected with Ad-eGFP at an M.O.I. of 25. The cells were then visualized by fluorescence microscopy at 24h and 48h post-infection. At 24h post-infection, there was no visible

fluorescence in the cells (data not shown). Previous experiments in which we transfected COS-7 cells with NPC1-eGFP-containing plasmids determined that the protein is not expressed until 36h post-transfection. **Figure 3.5A** shows that there was no visible difference in the localization of fluorescent protein between *Npc1*$^{+/+}$ and *Npc1*$^{-/-}$ cells at 48h post-infection. In addition, when compared to the Ad-eGFP infection (**Figure 3.5B**), Ad NPC1-eGFP-infected cells showed a much weaker fluorescence intensity as well as a much lower amount of infection (~1% of cells were infected) compared to Ad-eGFP-infected cells. Approximately 90% of the hepatocytes of both genotypes were infected efficiently. Uninfected control hepatocytes showed no fluorescence (**Figure 3.5C**).

In addition, the cells were scraped and harvested at both 24h and 48h, and immunoblotting for NPC1 as well as for eGFP was performed in order to detect expression of the NPC1-eGFP fusion protein. Although there was a small amount of fluorescence at 48h post-infection in Npc1-deficient cells infected with Ad NPC1-eGFP (**Figure 3.5A**), immunoblotting for NPC1 did not show any NPC1-eGFP fusion protein expression in these cells (**Figure 3.6A**). The immunoreactive band for NPC1-eGFP is expected at a size of ~200-220 kDa. Furthermore, immunoblotting for eGFP confirmed that NPC1-eGFP was not expressed in these cells (**Figure 3.6B,C**).

Before concluding that the fusion protein was not expressed, even though some fluorescence was visible, we investigated the idea that the level of protein expression may have been too low, and there were not enough infected cells to enable detection of the fusion protein by immunoblotting. Therefore, to further examine the expression of the NPC1-eGFP protein, we performed the same experiment in COS-7 cells, which we

previously showed were both transfected by NPC1-eGFP-containing plasmids and infected by the Ad NPC1-eGFP crude lysate at high efficiency (~70% of cells infected). COS-7 cells are known to be easily and efficiently transfected. COS-7 cells were plated at density of 200,000 cells/well in a 6-well plate, grown for 24h, and then infected with 600μL of crude Ad NPC1-eGFP lysate. Cells were also transfected with three plasmids containing NPC1-eGFP: the original Maue plasmid, the pAdenovator NPC1-eGFP plasmid, and the AdEasy 1 Adenoviral NPC1-eGFP plasmid which was used for production of the adenovirus. Transfections were performed using the HD FuGENE transfection reagent with 5μg of DNA in the optimal FuGENE:DNA ratio of 2:1. When viewed by fluorescence microscopy at 48h post-infection, all treatments except the uninfected control showed fluorescence in the majority of cells (~70%) (data not shown). The uninfected control showed no fluorescence. However, to our surprise, immunoblotting for eGFP at 48h post-infection showed only free eGFP (at a size of ~30 kDa), but not NPC1-eGFP, in all of the cells transfected with NPC1-containing plasmids (**Figure 3.7**). This finding indicated that either the NPC1-eGFP fusion protein was not expressed or had been degraded within the cell after transfection had occurred. Cellular localization of fluorescence, which was punctuate and extra-nuclear, indicated that the protein visualized was not free eGFP, as eGFP localizes ubiquitously throughout the cell, including the nucleus. Additionally, there was no detection of either free eGFP or NPC1-eGFP in cells infected with the Ad NPC1-eGFP lysate. Thus, I concluded that this adenoviral lysate was defective. Another possibility was that the viral titer was extremely low and would be increased upon virus purification; however, even after purification of the virus, infection of HEK 293 cells (to determine

the viral titer) showed that the adenovirus was defective. Neither a fluorescence nor a plaque titer could be calculated because the cells did not show any fluorescence or formation of plaques. Taken together, these results indicated that our newly-constructed Ad NPC1-eGFP was defective, and that the NPC1-eGFP fusion protein is likely being degraded to free eGFP within the cell after transfection has been achieved.

3.5 Boiling a protein sample before immunoblotting decreases detection of the NPC1 protein

It is normal standard operating procedure when performing immunoblotting to boil a sample mixture at 95-100°C for approximately 5 minutes before resolving it on the gel, in order to denature (unfold) the protein of interest (117). This boiling is necessary because antibodies typically recognize a small portion of the protein (the epitope) and this domain may reside hidden within the three-dimensional conformation of the protein, so it is necessary to unfold the protein to enable access of the antibody to the portion (117). In the case of NPC1, however, boiling the protein sample resulted in a dramatic decrease of the detection of NPC1 protein after immunoblotting with the NPC1 antibody (**Figure 3.8**). This effect was seen with homogenized liver tissue, cerebellum, and whole brain lysate. Samples are usually left without denaturing under circumstances in which the antibody recognizes an epitope as it exists only on the three-dimensional folded protein, such as when the antibody recognizes an epitope made up of non-contiguous amino acids (117). The NPC1 antibody we used, however, was raised against the C-terminus of human NPC1 (aa 1261-1278), which is a

contiguous sequence of amino acids. On the other hand, NPC1 is a multi-pass membrane protein with 13 transmembrane domains, and such proteins tend to aggregate when boiled (117), resulting in the aggregates not entering the gel efficiently, which may be applicable in the present situation. Nonetheless, upon discovering the drastic effect of boiling, all immunoblots in these studies were performed without boiling the lysates before gel electrophoresis.

3.6 Transfection of PC-12 cells with pAdenovator NPC1-eGFP and I1061T using a variety of different cell transfection reagents is inefficient

After discovering that the Ad NPC1-eGFP which we produced was defective, and that NPC1-eGFP seemed to be degraded in COS-7 cells transfected with our constructed plasmids as well as with the Maue plasmid, we sought to find out whether this degradation occurred in neurons transfected with these plasmids. Since it is known that primary cultures of sympathetic neurons are difficult to transfect with plasmids, we used PC-12 cells as a primary neuronal model. Our goal was to obtain a high efficiency of transfection in these cells with our current NPC1-eGFP-containing plasmids, so that we could gather enough cellular material for performing immunoblotting for the fusion protein. Both undifferentiated and 6-day differentiated PC-12 cells were plated at densities of 200,000 cells/well in collagen-coated 6-well plates, and transfected with pAdenovator NPC1-eGFP and I1061T plasmids. Differentiation was immediately induced in undifferentiated cells following transfection, by addition of NGF to the culture medium. All cells were visualized at 72h post-infection by fluorescence

microscopy for evaluation of protein expression and transfection efficiency. We used a variety of commercially-available transfection reagents, for all of which the manufacturers had claimed efficient transfection of neuronal cells. We performed extensive experiments under various different conditions (using manufacturer protocols) with each of these reagents in order to obtain the most efficient transfections. Transfection of cells with the eGFP-N1 vector was also performed as a positive comparative control. Transfection either in the presence or absence of serum did not show differences in transfection efficiency for both differentiated and undifferentiated PC-12 cells. Generally, transfection was significantly lower in differentiated cells compared to undifferentiated cells, which is a known phenomenon, because differentiated PC-12 cells adopt a phenotype closely resembling that of primary neurons which makes them more difficult to transfect. **Figure 3.9** shows the optimal transfection efficiencies of undifferentiated PC-12 cells using the four different transfection reagents, Superfect, Lipofectamine 2000, HD FuGENE, and Targefect-F2 plus Virofect. Our results showed that the Targefect-F2 transfection reagent was ineffective in achieving transfection. Only an estimated 1% of cells were transfected with eGFP with this reagent, and no transfection was obtained with our NPC1-eGFP constructs. Interesting to note is that the Virofect enhancer used in conjunction with Targefect-F2 is an inactivated adenovirus-derived formulation which is supposed to dramatically enhance transfection of neurons by having adenoviral binding and uptake properties; however, this was not the case in our experiments. Transfection with Superfect resulted in an estimated 20% of PC-12 cells transfected with eGFP, but no eGFP fluorescence was seen with our constructs. HD FuGENE and Lipofectamine

2000 were the most effective in achieving transfection, especially with eGFP (~40% transfection efficiency); however, only ~1% of cells were transfected with our constructs using these two reagents, and the fluorescence of the transfected cells was less intense when compared to the luminosity of eGFP fluorescence. The large discrepancy in transfection efficiency between eGFP-transfected cells and cells transfected with our constructs suggested that perhaps our specific constructs were not efficiently transfected or expressed. One possible explanation for the low transfection was the large size of these plasmids, which were approximately 13 kb in size. Generally, the larger the plasmid, the less efficient it is in cell transfection and in its ability to enter the cell. This efficiency is thought to drop exponentially at plasmid sizes above 4 or 5 kb. Therefore, it was possible that the large size of our constructs (~13 kb) compared to eGFP-N1 (which is only 4.7 kb in size), resulted in a significantly reduced ability of these constructs to enter the cells during transfection.

We also performed transfections in 6-day differentiated PC-12 cells using HD FuGENE, as this reagent seemed to be less toxic to the transfected cells than was Lipofectamine 2000, and therefore was likely to be the most suitable transfection reagent of the four. Although transfection efficiencies in the differentiated cells were extremely low with all plasmids (**Figure 3.10**), a few cells were transfected, as shown in **Figure 3.11**. The most drastic effect of this decrease in transfection efficiency in differentiated compared to undifferentiated cells was seen with eGFP transfection, which decreased from approximately 40% for undifferentiated cells to approximately 2% for differentiated cells (**Figures 3.9 and 3.10**). Therefore, we were unable to

achieve a desirable amount of transfection with our constructs in both undifferentiated and differentiated PC-12 cells.

In summary, differentiated PC-12 cells were transfected at a much lower efficiency than undifferentiated cells, and the NPC1-eGFP-containing constructs were highly inefficient in transfecting both types of PC-12 cells. This was evident by both an extremely low number of transfected cells, as well as much dimmer fluorescence of cells which were transfected, as compared to eGFP transfection. Furthermore, of the four transfection reagents tested, HD FuGENE seemed to be the best for transfection of PC-12 cells. Noteworthy of mentioning is that we had also transfected *Npc1*$^{+/+}$ and *Npc1*$^{-/-}$ mouse sympathetic neurons with our constructs using Targefect-F2 plus Virofect, the manufacturer of which claimed efficient transfection of neurons; however, we observed no transfection with this reagent under a variety of different conditions as specified by the manufacturer.

3.7 Transfection of COS-7 and PC-12 cells with a newly-constructed NPC1-eGFP cDNA in the pEGFP-N1 vector is still inefficient

In further attempting to increase the transfection efficiency of our NPC1-eGFP fusion gene, and in recognizing that a large size was potentially a problem, the cDNA of this gene was re-cloned into the smaller vector pEGFP-N1, making the total size of the new plasmid (pEGFP-N1 NPC1-eGFP) approximately 8.4 kb, as opposed to 12.5 kb (pAdenovator NPC1-eGFP) previously. The rationale we had was that this smaller plasmid, although still on the larger side for cell transfection, would be more effective

in transfecting cells, resulting in an increased transfection efficiency. However, as shown in **Figure 3.12**, transfection of COS-7 cells with pEGFP-N1 NPC1-eGFP (**Figure 3.12A**) is still much less efficient than transfection with pEGFP-N1 alone (**Figure 3.12C**), and is in fact no more efficient than transfection with our previous construct, pAdenovator NPC1-eGFP (**Figure 3.12B**). Control untransfected cells (**Figure 3.12D**) showed no fluorescence. Therefore, the smaller plasmid size did not seem to increase the amount of transfection with NPC1-eGFP cDNA. Further transfections of PC-12 cells with pEGFP-N1 NPC1-eGFP also confirmed this conclusion, as these transfections were extremely inefficient and no different from those with any of our previous constructs.

3.8 Analysis of the eGFP sequence in the NPC1-eGFP fusion gene reveals that it did not contain eGFP, but rather, a variant intermediate between GFP and eGFP

Since the size of our NPC1-eGFP-containing plasmids did not seem to be responsible for the lack of transfection (Section 3.7), there appeared to be a defect in our fusion gene itself. Also, in addition to producing a significantly lower amount of transfection, our constructs produced much dimmer fluorescence compared to that of eGFP. We therefore questioned whether our fusion protein did in fact contain eGFP. Sequence analyses had shown that we were working with the full-length and correct NPC1 gene coding sequence. We also verified the presence of the expected 6-alanine linker sequence between the NPC1 and eGFP coding sequences, and further verified the correct first few starting bases and last few ending bases of the eGFP coding sequence

in the Maue plasmid, which matched the bases in eGFP coding sequences. We had also assumed that we were working with eGFP because the lab from which we had obtained our original fusion construct (the Maue plasmid) had claimed to have cloned the NPC1 cDNA specifically into the pEGFP vector (Clontech) (9), which encodes eGFP. Therefore, we had not previously thought it necessary, nor had it crossed our mind, to perform sequence analysis over the entire GFP sequence of our construct.

Upon analyzing the GFP sequence of the originally-obtained Maue plasmid, we surprisingly discovered that this coding sequence did not, in fact, encode eGFP (**Figure 3.13**). Interestingly, the cDNA sequence did not encode plain GFP either, but rather, a variant intermediate form of GFP between GFP and eGFP. We observed over 90 silent mutations in the Maue plasmid GFP coding sequence when compared to eGFP; however, none of these produced resulting amino acid changes and were generally not of concern. What was interesting to us, however, was the lack of the F64L mutation (the presence of which distiguishes eGFP from GFP, and results in improved 37°C folding efficiency of the protein) in the Maue plasmid GFP coding sequence. The difference between GFP and eGFP is that eGFP is a doubly-mutated form of GFP, containing the mutations S65T (118) and F64L (119). However, in the case of the GFP variant in the Maue plasmid, only the S65T, but not the F64L, mutation was present. As a result, only one, but not the other, amino acid change was present in the Maue plasmid. Therefore, perhaps the reason we observed dimmer fluorescence, less transfection, and also the apparent degradation of our fusion protein, could be attributed to the fact that the fusion gene in the original Maue plasmid we received (and

subsequently, the pAdenovator NPC1-eGFP plasmid we had constructed) contained this unfamiliar GFP gene variant which was, in fact, not eGFP.

3.9 RT-PCR analysis shows that NPC1-GFP mRNA is expressed in PC-12 cells transfected with our NPC1-GFP-containing plasmids

To confirm that our NPC1-GFP-containing plasmids entered the transfected PC-12 cells, that the full NPC1-GFP cDNA was transcribed efficiently, and that the presumed protein degradation observed was occurring post-transcriptionally, we performed RT-PCR experiments to confirm the mRNA expression of the NPC1-GFP in our various constructs at 72h post-transfection. Undifferentiated PC-12 cells were transfected with the following plasmids: Maue, pAdenovator NPC1-GFP, I1061T, and eGFP-N1 NPC1-GFP. As a qualitative comparison, cells were also transfected with eGFP-N1. Cellular differentiation was induced at the time of transfection. The cells were scraped and harvested at 72h post-transfection, their mRNA was isolated, and RT-PCR was performed on all these samples using specific primers spanning a GFP region which was common to both the NPC1-GFP fusion gene and the eGFP gene in pEGFP-N1. The house-keeping gene cyclophilin was used as a loading control. The results showed that the full NPC1-GFP mRNA was expressed (**Figure 3.14**) from all the constructs tested, and that the mRNA levels were approximately the same among all NPC1-GFP-containing plasmids. [Compared to eGFP-N1 mRNA expression however, mRNA expression of NPC1-GFP-containing plasmids seemed slightly lower, but this was as expected because the level of transfection was lower]. Therefore, these data

indicate that NPC1-GFP mRNA was expressed, and that the most likely reason for the lack of expression of NPC1-GFP protein is that the protein is degraded via a post-transcriptional mechanism.

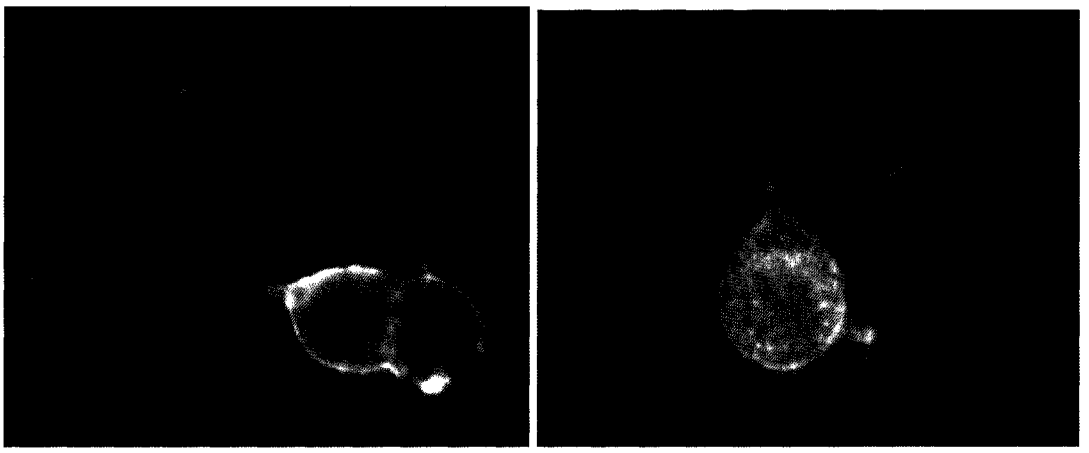

Npc1$^{+/+}$ *Npc1*$^{-/-}$

Figure 3.1 Unesterified cholesterol accumulates and is redistributed in cell bodies of Npc1-deficient mouse sympathetic neurons. Filipin staining of 6-day old wild-type (left panel) and Npc1-deficient (right panel) NPC1 mouse sympathetic neurons in primary culture shows that unesterified cholesterol accumulates in the cell bodies of Npc1-deficient neurons, whereas in neurons containing functional NPC1, the majority of unesterified cholesterol is distributed around the plasma membrane.

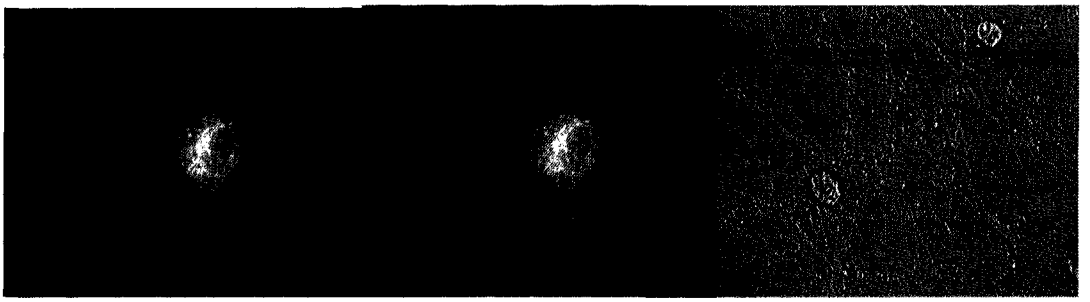

Figure 3.2 Non-neuronal cells are infected at a much higher efficiency than neuronal cells in primary culture. 7-day old cultured wild-type mouse sympathetic neurons were infected with Ad NPC1-eGFP for 24h, and visualized by fluorescent microscopy 3 days after infection. Although ARAC was present in the medium, there were still a few non-neuronal cells present, and, as shown by the bright fluorescence (left and middle panels, with increased contrast of the same image shown in the middle panel), these were infected at a much higher efficiency than neurons. The right panel is a phase-contrast image of the same cells. Data are from one experiment representative of 3 experiments with similar results.

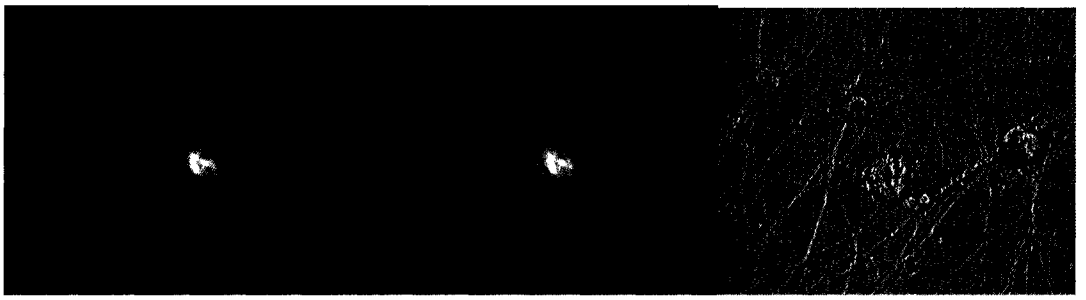

Figure 3.3 Infection of mouse sympathetic neurons with Ad NPC1-eGFP was highly inefficient, and showed expression only in cell bodies, but not axons. 7-day old wild-type mouse sympathetic neurons were infected with Ad NPC1-eGFP for 24h. Cells were visualized by fluorescence microscopy at 3 days post-infection (left and middle panels, with increased contrast of the same image shown in the middle panel). Shown in the right panel is a phase-contrast images of the same cells. The cell bodies that were infected appeared severely unhealthy, possibly due to the toxic effects of adenovirus. Data are from one experiment representative of 3 experiments with similar results.

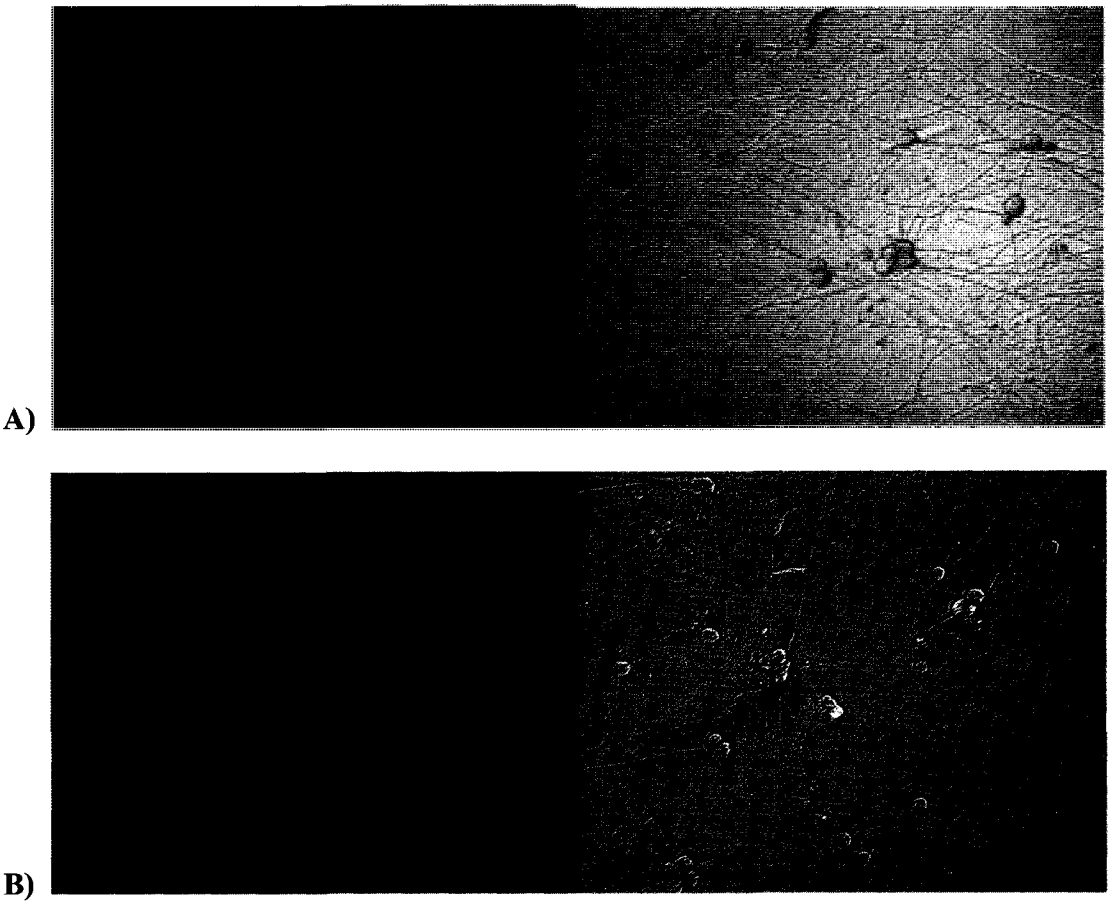

Figure 3.4 Adenoviral NPC1-eGFP stock lost titer and infection efficiency. 7-day-old wild-type mouse sympathetic neurons were infected with Ad NPC1-eGFP (A) alongside Ad-eGFP (B) for 24h, and visualized by fluorescence microscopy at 72h post-infection. The lack of infection with Ad NPC1-eGFP (A) compared to ~30% infection with Ad-GFP (B) confirmed that our adenoviral NPC1-eGFP stock had lost significant titer and infective capabilities. The left panels show fluorescence images, and the right panels are phase-contrast images of the same cells. Data are from one experiment representative of 3 experiments with similar results.

Figure 3.5

A)

Figure 3.5 Ad NPC1-eGFP-infected *Npc1*$^{+/+}$ and *Npc1*$^{-/-}$ mouse hepatocytes show extremely low infection efficiency. *Npc1*$^{+/+}$ and *Npc1*$^{-/-}$ mouse hepatocytes were infected 4h after plating and visualized at 48h post-infection. Both wild-type and knockout hepatocytes infected with Ad NPC1-eGFP crude lysate (A) showed much lower fluorescence compared to cells infected with Ad-eGFP (B). Infection with Ad NPC1-eGFP showed that the fusion protein localization was extra-nuclear, as expected, and that there was no visible difference between *Npc1*$^{+/+}$ and *Npc1*$^{-/-}$ cells. Ad-eGFP localized throughout the cells, with a higher abundance of expression in the nucleus, and no visible difference in fluorescence localization between *Npc1*$^{+/+}$ and *Npc1*$^{-/-}$ cells. Uninfected control cells (C) showed no fluorescence. The top two panels in (A), (B), and (C) show *Npc1*$^{+/+}$ cells, and the bottom two panels show *Npc1*$^{-/-}$ cells. The right panels are phase-contrast images of the fluorescence images seen in the left panels. Data are from one experiment representative of 2 experiments with similar results.

Figure 3.5

B)

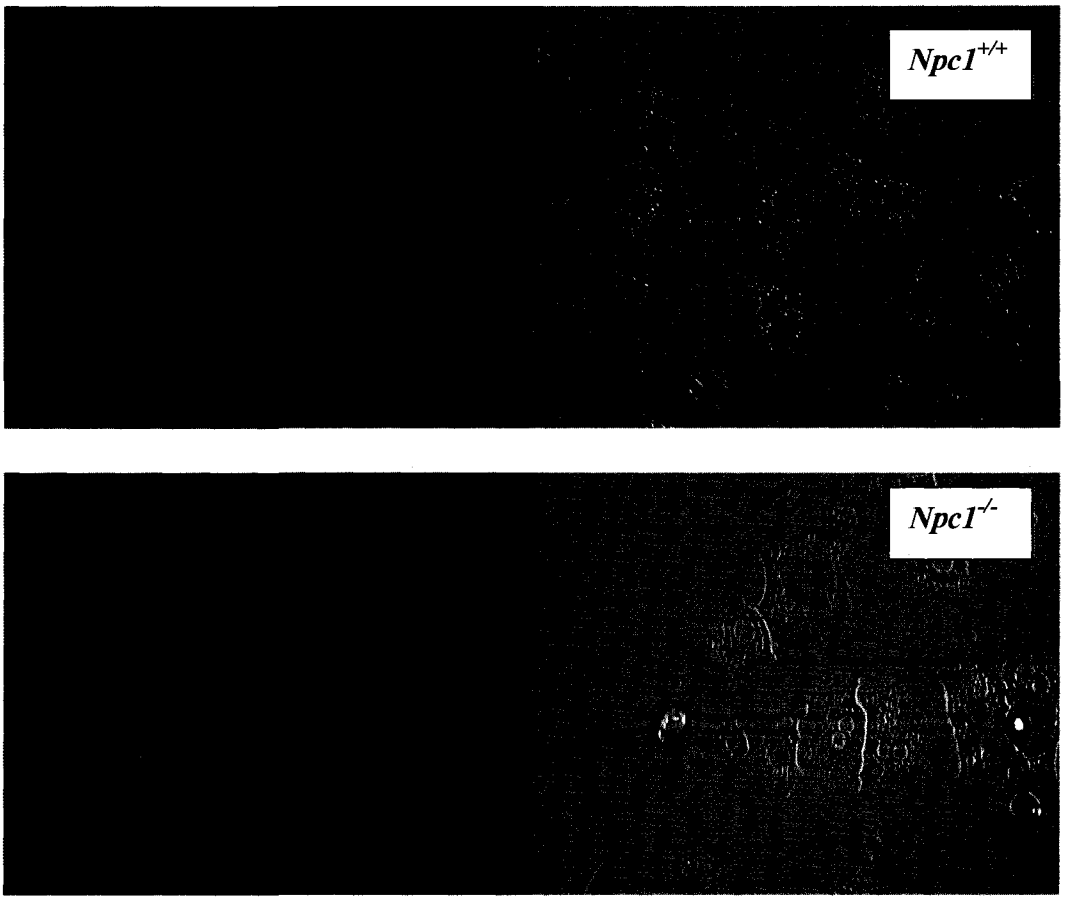

Figure 3.5

C)

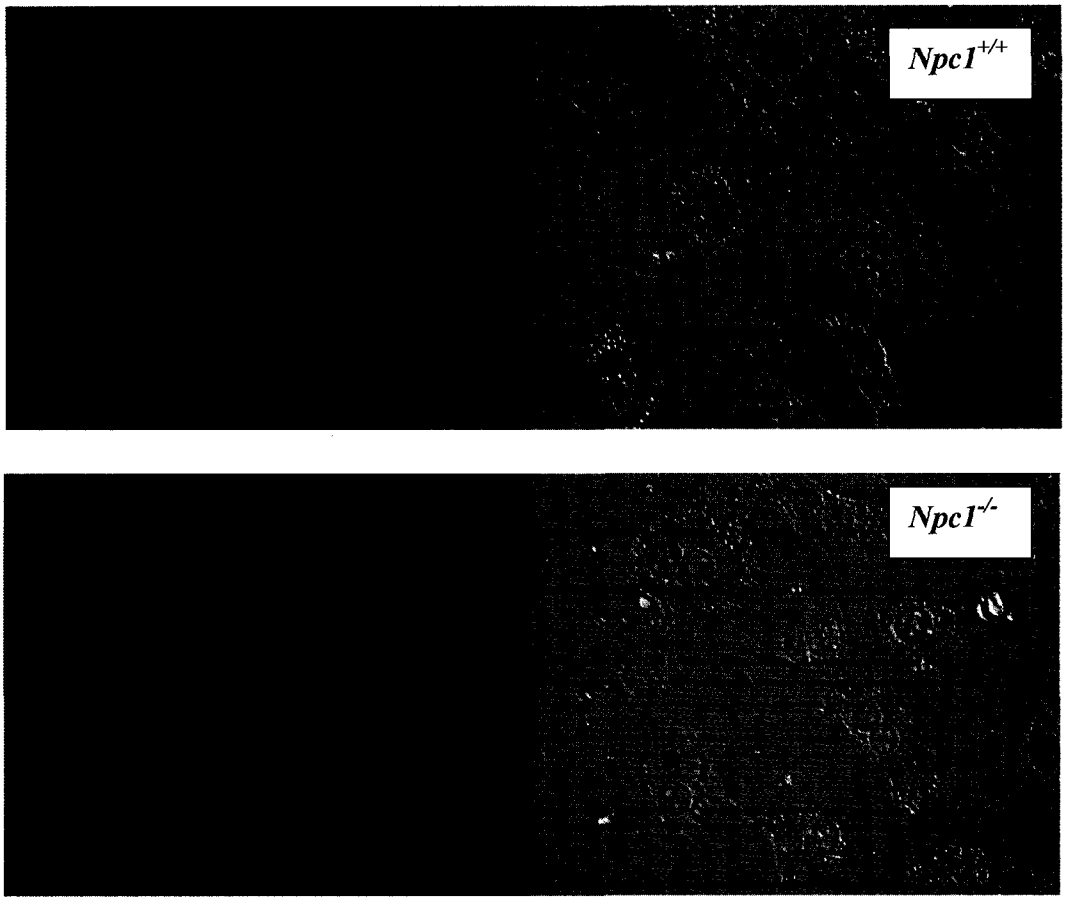

Figure 3.6

A)

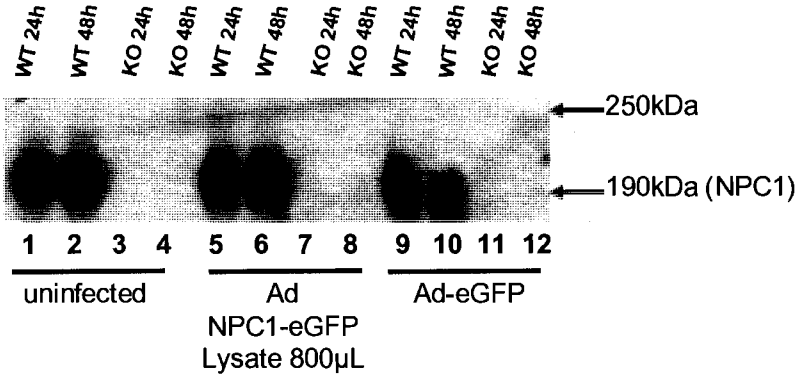
WT 24h
WT 48h
KO 24h
KO 48h
WT 24h
WT 48h
KO 24h
KO 48h
WT 24h
WT 48h
KO 24h
KO 48h
250kDa
190kDa (NPC1)
1 2 3 4 5 6 7 8 9 10 11 12
uninfected
Ad
NPC1-eGFP
Lysate 800µL
Ad-eGFP

B)

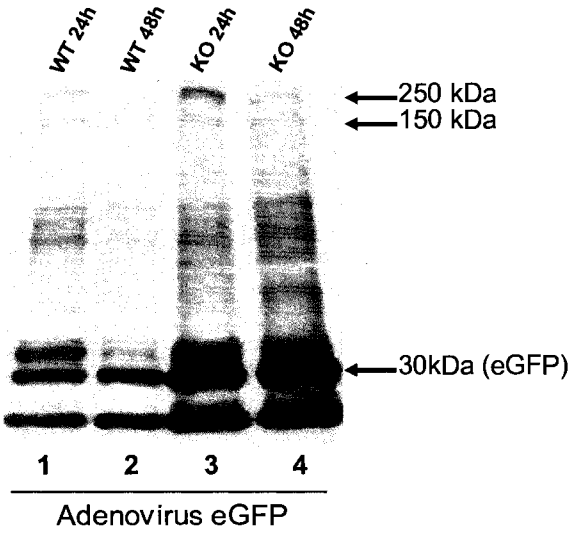
WT 24h
WT 48h
KO 24h
KO 48h
250 kDa
150 kDa
30kDa (eGFP)
1 2 3 4
Adenovirus eGFP

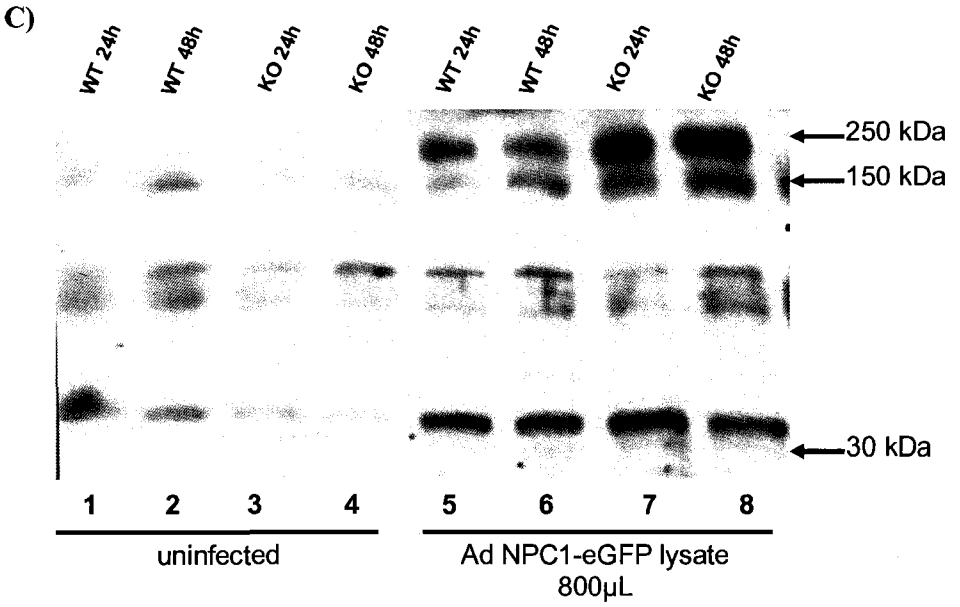

Figure 3.6 Immunoblots for NPC1 and GFP show no NPC1-eGFP fusion protein in mouse hepatocytes infected with Ad NPC1-eGFP lysate. Wild-type (WT) and *Npc1*$^{-/-}$ (KO) hepatocytes infected with Ad NPC1-eGFP lysate and Ad-eGFP were scraped and harvested at 24h- and 48h post-infection, and immunoblotting was performed for both these time points. Immunoblotting for NPC1 (A) showed no NPC1-eGFP in *Npc1*$^{-/-}$ cells infected with Ad NPC1-eGFP lysate (lanes 7 and 8), at ~200 kDa. Lanes 1-2 and 3-4 represent uninfected WT and KO cells, respectively, at 24h- and 48h post-infection. Lanes 9-10 and 11-12 represent Ad-eGFP-infected WT and KO cells, respectively, at 24h- and 48h post-infection. Immunoblotting for GFP (B,C) also did not show the fusion protein in *Npc1*$^{-/-}$ cells infected with Ad NPC1-eGFP lysate (lanes 7 and 8 in C). Lanes 1-2 and 3-4 in (C) represent uninfected WT and KO cells, respectively, at 24h- and 48h post-infection. The control Ad-eGFP-infected WT and KO cells both showed free eGFP at ~30 kDa (lanes 1-4 in B). Uninfected control WT and KO cells (lanes 1-4 in C) did not show detection of free eGFP.

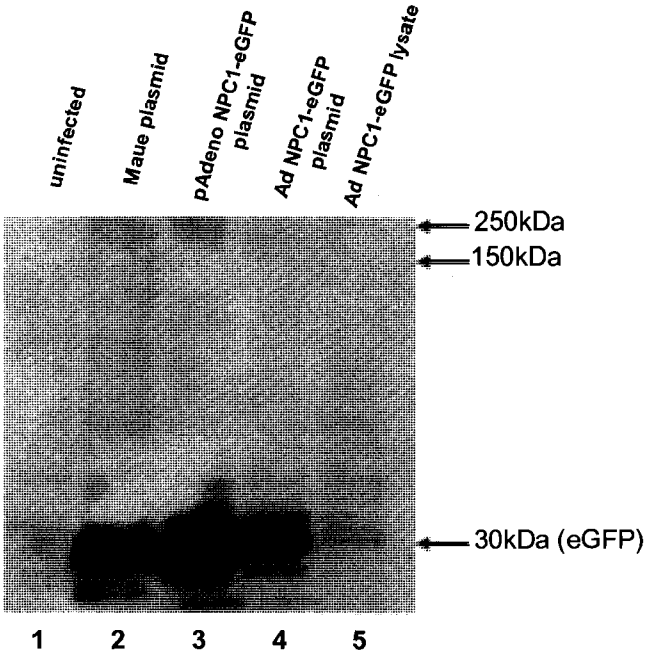

Figure 3.7 NPC1-eGFP fusion protein might be degraded to free eGFP. COS-7 cells were transfected with various NPC1-eGFP-containing plasmids, as well as with the Ad NPC1-eGFP lysate. Cells were scraped and harvested after 48h. Immunoblotting for GFP shows detection of free eGFP (at 30 kDa), but not NPC1-eGFP (expected at ~200 kDa), in cells transfected with all plasmids (lanes 2-4). Neither free eGFP nor NPC1-eGFP was detected in cells infected with Ad NPC1-eGFP lysate (lane 5), indicating that the virus may not be functional. Uninfected negative control cells also showed no eGFP or NPC1-eGFP (lane 1).

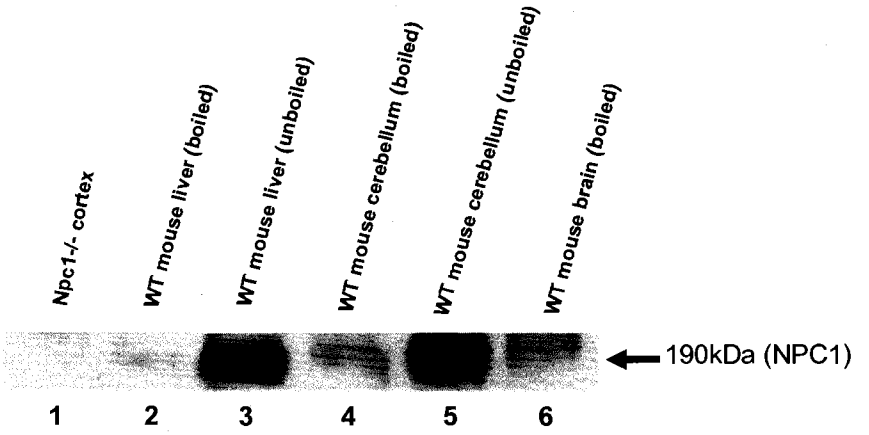

Figure 3.8 Boiling a protein sample before immunoblotting decreases detection of the NPC1 protein. Mouse tissue samples (cortex, liver, cerebellum, brain) were used. Some samples were boiled for 5 minutes at ~95°C, whereas other samples were directly resolved on the gel without boiling. Immunoblotting for NPC1 showed a drastic reduction in detection of NPC1 in boiled samples (lanes 2,4,6) compared to non-boiled samples (lanes 3 and 5). The negative control sample in lane 1 was unboiled.

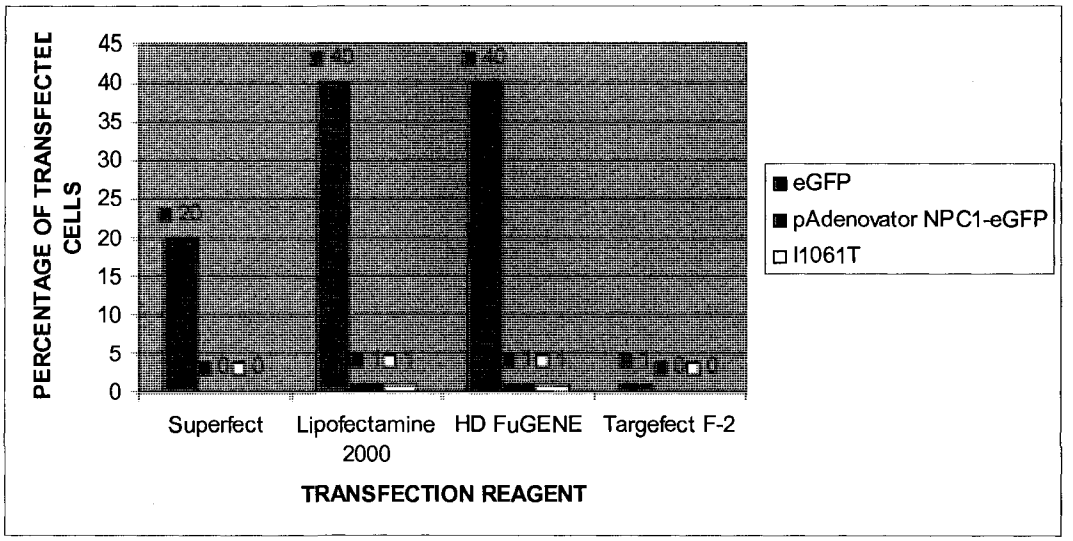

Figure 3.9 Transfection of undifferentiated PC-12 cells with pAdenovator NPC1-eGFP and I1061T using different cell transfection reagents. The most effective reagents were HD FuGENE and Lipofectamine 2000; however, transfection with pAdenovator NPC1-eGFP and I1061T was highly inefficient using all the reagents. eGFP transfection efficiency was much higher than NPC1-eGFP-containing plasmids. Targefect-F2 was ineffective. Numbers above bars represent percentage of transfected cells. The values shown are estimates from one experiment, repeated twice with similar results.

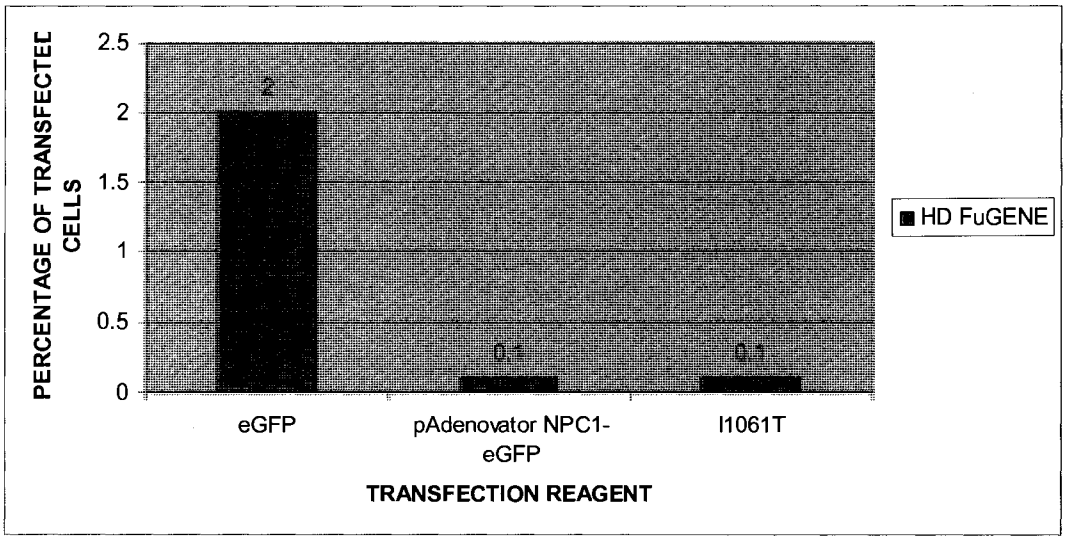

Figure 3.10 Transfection of differentiated PC-12 cells with pAdenovator NPC1-eGFP and I1061T using different cell transfection reagents is more inefficient than transfection of undifferentiated PC-12 cells. 6-day differentiated PC-12 cells were transfected with pAdenovator NPC1-eGFP, I1061T, and EGFP-N1 using HD FuGENE, which was the most effective transfection reagent for undifferentiated cells. Numbers above bars represent percentage of transfected cells. The values shown are estimates from one experiment, repeated twice with similar results.

Figure 3.11

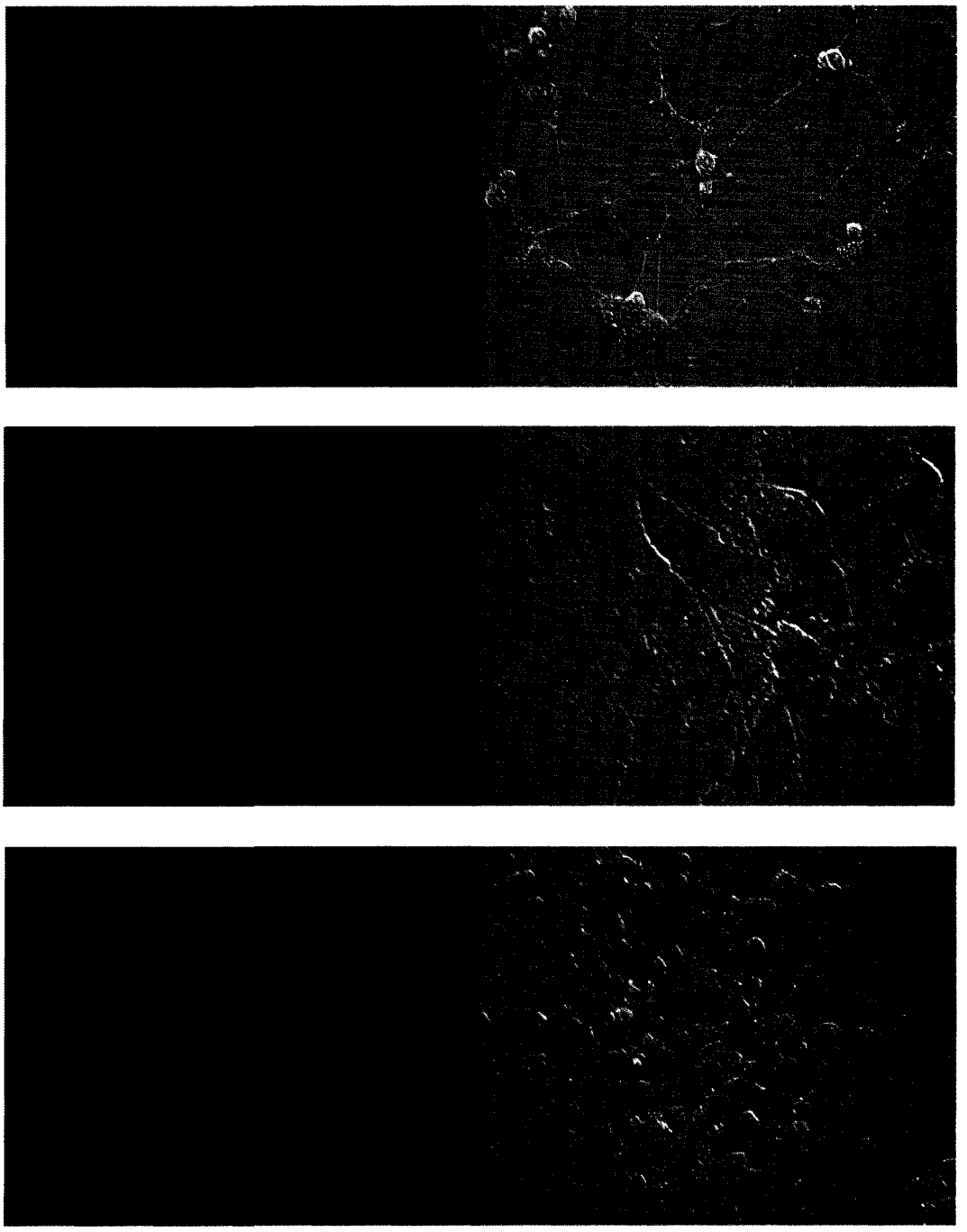

D) 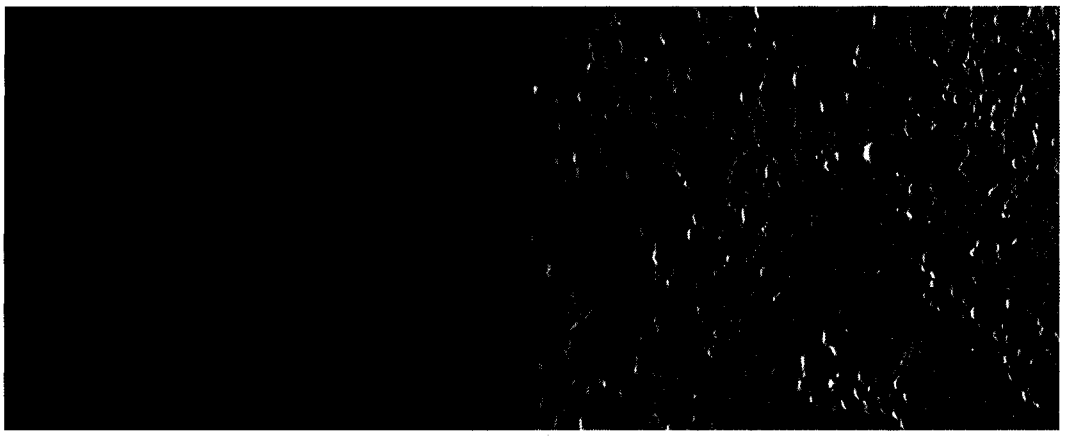

Figure 3.11 Transfection of differentiated PC-12 cells with pAdenovator NPC1-eGFP and I1061T. PC-12 cells were differentiated for 6 days, transfected, and then visualized by fluorescence microscopy at 72h post-transfection. (A) Cells transfected with eGFP. (B) Transfection with pAdenovator NPC1-eGFP. (C) Transfection with I1061T. (D) Untransfected cells. Shown side by side are phase-contrast images of the same cells. The right panels are phase-contrast images of the fluorescence images in the left panels. Data are from one experiment representative of 3 experiments with similar results.

Figure 3.12

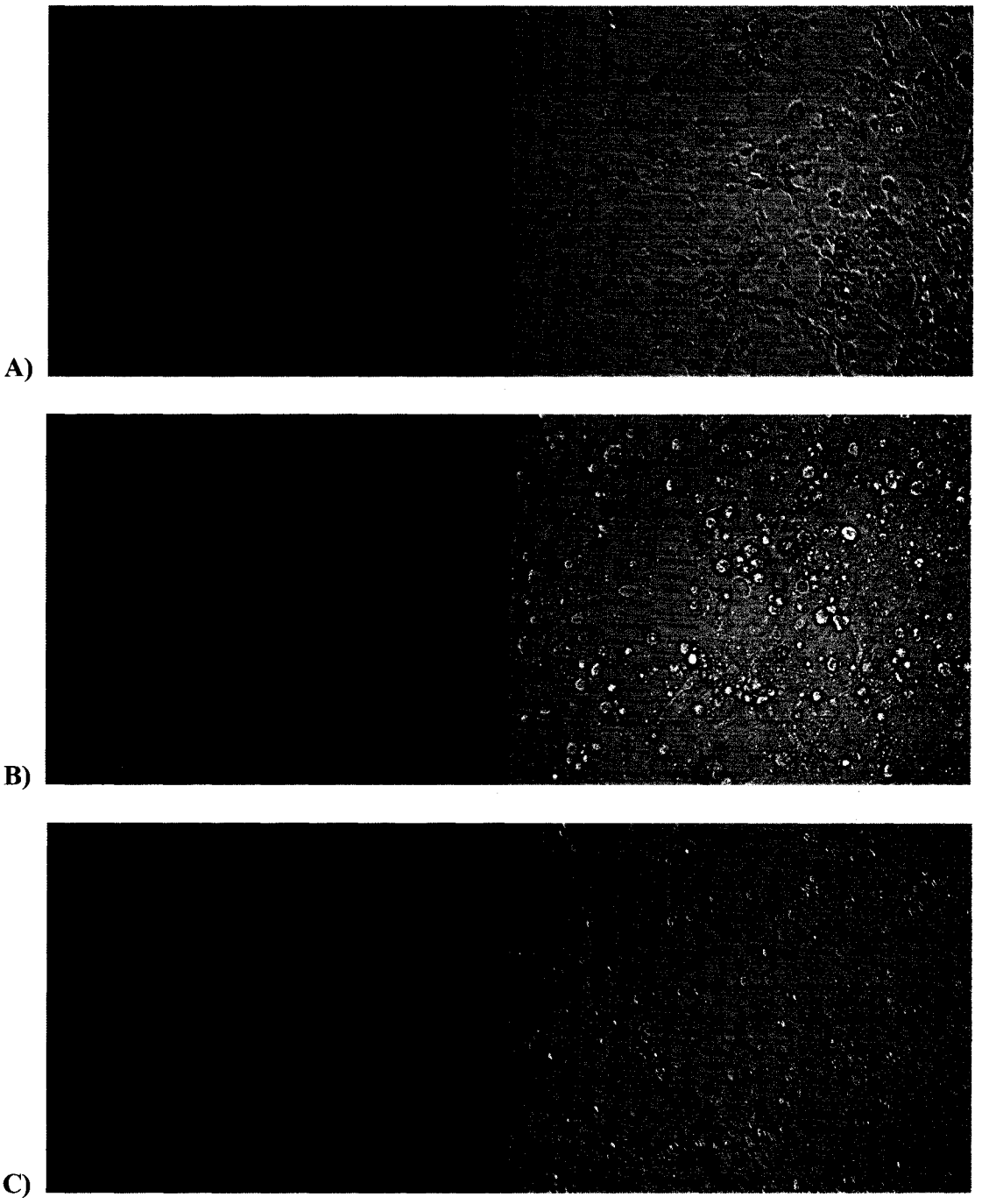

D) 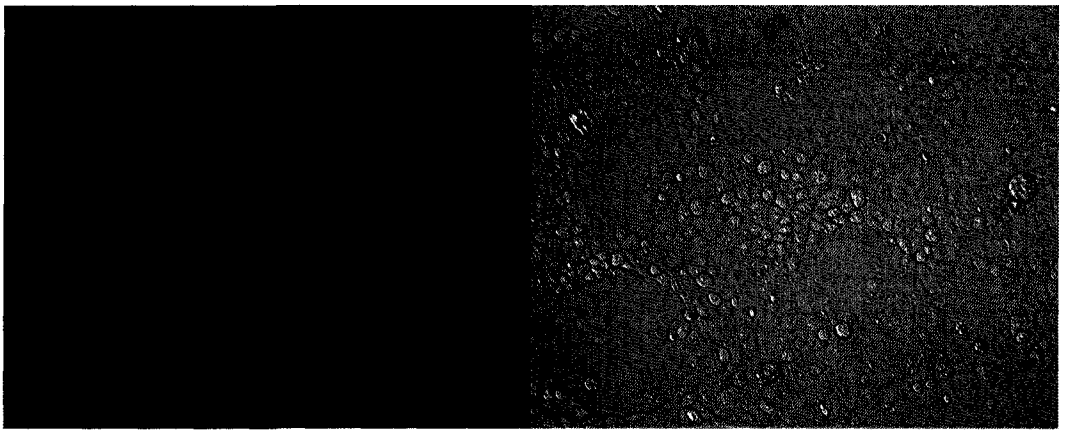

Figure 3.12 Transfection of COS-7 cells with a newly-constructed smaller vector, pEGFP-N1 NPC1-eGFP, is no more efficient than transfection with the larger NPC1-eGFP-containing plasmids. COS-7 cells were transfected, then visualized by fluorescence at 72h post-transfection. Transfection with pEGFP-N1 NPC1-eGFP (A) was no more efficient than transfection with pAdenovator NPC1-eGFP (B), and was markedly less efficient than transfection with eGFP-N1 (C). Untransfected cells (D) showed no fluorescence. The right panels are phase-contrast images of the fluorescence images in the left panels. Data are from one experiment representative of 2 experiments with similar results.

```
eGFP  181
CTCGTGACCACCCTGACCTACGGCGTGCAGTGCTTCAGCCGCTACCCCGACCACATGAAG  240
Maue  655
..G..C..T...T.C.....T.............TTC.A.A.....A.....T......  714
```

Figure 3.13 Analysis of the eGFP sequence in the NPC1-eGFP fusion gene in the Maue plasmid reveals that it did not contain eGFP, but rather, a variant intermediate between GFP and eGFP. eGFP contains two mutations, F64L and S65T, of plain GFP. The top strand shows part of the coding sequence for eGFP, whereas the bottom strand shows the corresponding GFP sequence in the Maue plasmid. The yellow-highlighted codon, coding for aa 64, codes for leucine in eGFP, and phenylalanine in the Maue plasmid GFP. This indicated that the F64L mutation was not present in the Maue plasmid GFP. This mutation distinguishes eGFP from GFP, and leads to improved (enhanced) 37°C folding efficiency of the protein. The red-highlighted bases represent points of mutation. Sequence analysis was performed using the BLAST2 sequence analysis program on the NCBI website.

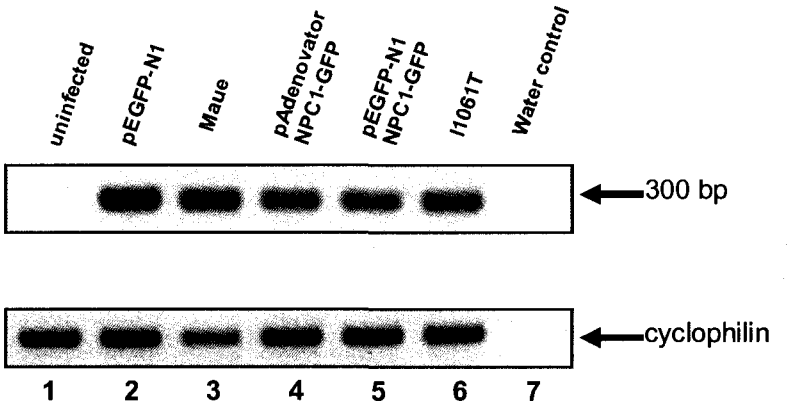

Figure 3.14 NPC1-GFP mRNA is expressed in PC-12 cells transfected with NPC1-GFP-containing plasmids. PC-12 cells were transfected with our various NPC1-GFP-containing plasmids, as well as with eGFP-N1 as a comparative control. Cells were scraped and harvested after 72h, their mRNA was isolated, and was subjected to RT-PCR analysis. The expected PCR product occurred at ~300 bp, and showed that the NPC1-GFP fusion gene entered the cells during transfection, and the full-length NPC1-GFP cDNA was transcribed into mRNA (lanes 3-6, top panel). Compared to eGFP-N1 mRNA expression, expression of NPC1-GFP mRNA was slightly lower. The negative untransfected control (lane 1) showed no mRNA expression. The water control (lane 7) contained everything required for the PCR reaction, except water was used instead of mRNA. No mRNA expression was seen for this control, as expected. The bottom panel shows cyclophilin loading controls for each sample.

CHAPTER 4 – DISCUSSION

4.1 Initial purpose of studies in trafficking of NPC1 protein in neurons

The initial purpose of our studies was to examine the trafficking of wild-type and mutant NPC1 proteins in Npc1-deficient mouse sympathetic neurons to further determine the neuron-specific function of NPC1 in distal axons, as previous findings from our lab suggested that NPC1 is involved in the synaptic vesicle recycling pathway (80), and possibly affects synaptic transmission. Previously in our lab, we had used an adenoviral vector expressing cDNA encoding an NPC1-eGFP fusion protein to infect Npc1-deficient mouse sympathetic neurons *in vitro*, and were able to observe bi-directional movement of this fluorescent chimeric protein between axons and cell bodies of these neurons (9). Furthermore, expression of this protein seemed to abolish the abnormal cholesterol accumulation in the cell bodies of these neurons (9). Therefore, we were interested in infecting *Npc1*$^{-/-}$ mouse sympathetic neurons with adenoviral vectors containing mutant NPC1 cDNAs tagged to GFP, and observing which, if any, of the NPC1 mutants were transported into distal axons of sympathetic neurons, and whether those that were transported localized normally to recycling endosomes. To date, there have been very few studies performed on assessing the transport of the NPC1 protein and its various mutant forms in neurons. Thus, investigating this aspect of NPC1 could potentially provide new insights into the neuron-specific function of NPC1 in distal axons and synaptic vesicle recycling. In

attempting to carry out these studies, however, we encountered many technical challenges that hindered us from achieving this goal.

4.2 Summary of present findings

In the present studies, we confirmed that unesterified cholesterol redistributes to/accumulates in cell bodies of Npc1-deficient mouse sympathetic neurons, as shown previously (8, 55). Then, in attempting to infect sympathetic neurons with Ad NPC1-eGFP, we discovered that adenoviral infection of non-neuronal cells was significantly more efficient than that of neurons. After achieving constantly low infection efficiencies, we eventually showed that the Ad NPC1-eGFP viral stock had lost titer and infective capability. Consequently, we constructed a new Ad NPC1-eGFP; however, infection of *Npc1*$^{+/+}$ and *Npc1*$^{-/-}$ mouse hepatocytes and COS-7 cells with the crude lysate of this Ad showed that the NPC1-eGFP fusion protein was not expressed. After purification of the virus, and upon calculation of its titer, we confirmed that the virus was not functional and indeed did not express the fusion protein. When we transfected COS-7 cells with plasmids containing the wild-type and a mutant (I1061T) NPC1-eGFP fusion gene and performed immunoblotting for NPC1 and eGFP, we saw expression of only free eGFP, but not NPC1-eGFP, indicating that the fusion protein is likely degraded within the cell. We further showed that boiling a protein sample before immunoblotting, which is standard operating procedure for most proteins, decreases detection of the NPC1 protein. In attempting to achieve high transfection efficiencies of our fusion constructs in neurons, we showed that transfection of PC-12 cells with our

NPC1-eGFP-containing plasmids using different transfection reagents was actually very inefficient, and that transfection efficiency in differentiated cells was significantly lower than in undifferentiated cells. We further showed that primary sympathetic neurons cannot be transfected with our fusion constructs. We constructed a smaller plasmid containing the NPC1-eGFP fusion gene (pEGFP-N1 NPC1-eGFP) to determine if the large size of our plasmids was a problem in achieving efficient transfection of PC-12 cells, and concluded that the size of our plasmids was not responsible for the inefficient transfection efficiencies, as the smaller plasmid was no more effective in achieving high transfection than were the larger plasmids. Upon analysis of the eGFP sequence in the NPC1-eGFP fusion gene in our constructs, results revealed that the fusion gene did not contain eGFP, but a variant intermediate between GFP and eGFP. Finally, RT-PCR analysis showed that the NPC1-GFP mRNA is expressed in PC-12 cells, indicating that the apparent degradation of NPC1-GFP to free GFP occurs via a post-transcriptional or post-translational mechanism.

4.3 Adenoviral infection of primary neurons with NPC1-eGFP

We initially wanted to confirm previous findings from our lab which showed bi-directional transport of the NPC1-eGFP fusion protein in axons of *Npc1*$^{-/-}$ mouse sympathetic neurons infected with Ad NPC1-eGFP (9). Adenoviral expression of cDNAs encoding GFP-tagged proteins is an excellent method for studying protein localization and movement in neurons because the protein can easily be visualized and followed using confocal and fluorescence microscopy. Although neurons are difficult

to transfect, they are usually infected by adenoviral vectors fairly easily because they express the CAR receptor on their cell surface, which is responsible for binding and uptake of adenovirus (110). Other cell-types which lack CAR cannot be infected with adenovirus (113). However, we encountered two problems in transfecting cells with Ad NPC1-eGFP: non-neuronal cells were transfected at a much higher efficiency than were neuronal cells, and our adenoviral stock had lost titer and a large amount of infectivity. Although ARAC was used to obtain a pure neuron culture, there were some non-neuronal cells still present underneath the monolayer of sympathetic neurons. However, the presence of these non-neuronal cells allowed us to determine that Ad NPC1-eGFP was very inefficient in infecting mouse sympathetic neurons in primary culture. Why non-neuronal cells are infected more readily and with a higher efficiency than neurons has not been determined. One possible explanation could be that these non-neuronal cells contain more CAR receptors on their surface than do neurons, and therefore are able to uptake Ads more efficiently; however, this is a speculation which must be tested experimentally.

Important to note was the unhealthy appearance of the few neurons that were infected with Ad NPC1-eGFP. The toxic effect of adenovirus infection on sympathetic neurons has been reported previously (109). The authors, in their report, claim that a similar toxicity was seen with multiple adenoviral preparations produced by different laboratories (109); therefore, it was not surprising to see these toxic effects with our cultures. One mechanism by which this toxicity can occur is by expression of viral genes by recombinant adenoviral constructs (109), but this has not yet been examined in neurons. For this reason, most functional adenoviral vectors are made E1-deficient,

since the E1 gene is responsible for viral replication (109). A good way to reduce toxicity of adenoviral vectors is to remove or inactivate more viral genes (E2, E3, E4), in addition to removal of E1 (120). However, it is important to assess the effects of these additional gene deletions on the desired expression of the recombinant protein. In our case, we were working with an E1- and E3-deficient adenoviral vector; therefore toxicity due to viral gene replication may not be a likely mechanism for the observed toxicity. Nonetheless, even though we were using an E1- and E3-deficient adenoviral vector, toxic effects of this vector were still evident (the infected neurons appeared to be unhealthy and dying), but the mechanism by which this toxicity occurs remains elusive.

Although we initially observed a small amount of infection of primary neurons with the Ad NPC1-eGFP, later infections of mouse hepatocytes and primary sympathetic neurons showed that the viral stock had lost titer and infection efficiency. We originally did not have any thoughts about the reason for the loss of titer; however, we soon discovered that we had been storing the Ad over a long term (~one year) at an inappropriate storage temperature. Our viral stock had been stored at -80°C, instead of at the optimal temperature of 4°C. The Maue lab from which we obtained the adenovirus had been storing the virus at the recommended temperature of 4°C, and in conversing with Dr. Jason Dyck (University of Alberta), whose lab specializes in production and use of adenoviruses, we were informed that long-term storage at improper temperatures and multiple freeze-thaw cycles of adenoviral stocks results in a loss of efficiency and viral titer. Another lab has also acknowledged the deleterious effects of numerous freeze/thaw cycles on loss in viral titer (109). Therefore, it is highly likely that the loss of titer of our Ad NPC1-eGFP was due to its improper long-

term storage at -80°C and the multiple freeze/thaw cycles the stock was subjected to as a result of repeated use in experiments.

After determining that our original viral stock was ineffective, we re-constructed a new Ad NPC1-eGFP. However, infection of *Npc1*$^{+/+}$ and *Npc1*$^{-/-}$ mouse hepatocytes and COS-7 cells with the crude lysate of this Ad showed that it did not express the fusion protein, and was therefore not functional. Although immunoblotting for NPC1 and eGFP in these infected cells did not show expression of the expected fusion protein, we took into account that there were not a sufficient amount of infected hepatocytes present to produce detection of the protein by immunoblotting. Therefore, we used the new Ad to infect COS-7 cells, which are easily transfected/infected at high efficiencies, to further confirm the lack of function of this Ad. Although a high amount of infection was obtained (as seen by fluorescence microscopy) in COS-7 cells, immunoblotting for NPC1 and eGFP still showed no expression of the fusion protein. However, we did not exclude the possibility that perhaps the titer of the virus was very low at that point (because it was not yet purified) and that the reason for the observed lack of protein expression was due to the low titer of the viral lysate. However, even upon purification of the virus, which we thought would result in increased viral titer, we saw no fluorescence or viral plaque formation in HEK 293 cells during calculation of the viral titer. We therefore concluded that our newly-constructed Ad NPC1-eGFP was ineffective.

The production of adenovirus, since it consists of numerous different steps and adenoviruses are extremely large constructs, is not always guaranteed to be a successful process. There are many points along the production pathway at which an error in

carrying out the protocol can result in a non-functional adenovirus. We were especially meticulous in carrying out the necessary checkpoints at each step in this pathway, and we did not see any technical problems in our Ad NPC1-eGFP until we performed the functional assay for this Ad in the mouse hepatocytes and COS-7 cells. Also, instead of observing an increase in HEK 293 cell infection after purification of the virus, we actually saw no infection by the purified virus in these cells. This indicated that there was an additional failure in our adenovirus during the purification process, although it was not determined at what stage this occurred.

4.4 The NPC1-GFP fusion protein is likely degraded to free GFP post-transcriptionally

In attempting to perform immunoblotting for the fusion protein, we transfected COS-7 cells with our fusion protein-containing plasmids in order to obtain sufficient transfected cellular material for detection of the protein by immunoblotting. To our surprise, however, immunoblotting for GFP in COS-7 cells transfected with our NPC1-GFP-containing plasmids, as well as with the Maue plasmid, indicated that the NPC1-GFP is likely degraded to free GFP. There was no evidence of fusion protein expression with any of NPC1-GFP-containing constructs, but all showed strong expression of free GFP. We were puzzled by this observation, because fluorescence localization in cells transfected with NPC1-GFP constructs showed a different localization pattern than that with eGFP. This difference in localization between our constructs and the eGFP construct was also observed in PC-12 cells and hepatocytes. In

all these cell types, eGFP fluorescence was seen throughout the cell, including the nucleus, where staining was more prominent; NPC1-GFP fluorescence, however, was extra-nuclear and appeared in a punctuate pattern. It is unlikely that the fusion gene was transcribing only the GFP portion of the NPC1-GFP cDNA, because there was no promoter in front of the GFP sequence. Additionally, RT-PCR analysis confirmed that the full NPC1-GFP mRNA was transcribed. Therefore, the degradation was occurring post-transcriptionally. Puzzled by our results, we decided to perform sequence analysis across the GFP gene sequence in the Maue plasmid, and surprisingly discovered that it did not contain eGFP, but a variant form of GFP lying between GFP and eGFP. This discovery could potentially provide the major reason for our observed results.

The difference between GFP and eGFP is that eGFP is a doubly-mutated form of GFP, containing the mutations S65T (118) and F64L (119). There were several reasons for making these mutations in GFP to yield eGFP: GFP had a poor photostability, a dim fluorescence, and a poor folding efficiency at 37°C (121). The first mutation, S65T, reported in 1995, resulted in a significantly increased fluorescence and photostability of GFP (118). The second mutation, F64L, resulted in an enhanced 37°C protein folding efficiency and even brighter fluorescence, and yielded eGFP (119). Thus, it is this second mutation which distinguishes eGFP from GFP. The GFP in the Maue fusion protein, and as a result, in the fusion protein in our other plasmids, contained the S65T mutation, but not the F64L mutation. Therefore, one possible explanation for the degradation of the fusion protein could be attributed to this lack of the F64L mutation.

Since the F64L mutation leads to an increased folding efficiency of the GFP protein, perhaps the lack of this mutation in the fusion protein leads to improper or inefficient folding of the protein. It is known that proteins which are misfolded are often targeted for degradation in the ER via the ubiquitin-proteasome pathway (122). If, indeed, the fusion protein is somehow misfolded due to the decreased folding efficiency of GFP, then this could offer a possible explanation for the degradation of NPC1-GFP to GFP by a post-transcriptional mechanism. Alternatively, a decrease in the folding efficiency of GFP could result in the fusion protein being slow to achieve its appropriate conformation. Since NPC1 undergoes extensive post-translational modifications after achieving proper folding conformation, such as glycosylation, a slowing of this process may also result in the protein being targeted for degradation (123). It has been reported that other large heavily-glycosylated polytopic proteins, such as CFTR, undergo ER-mediated degradation due to failure of these protein to fold properly prior to their arrival in the ER for post-translational modifications (124). However, these speculations must be tested, and it is uncertain whether the degradation is occurring after transcription and before the full fusion protein is translated, or whether it is occurring after translation of the protein.

4.5 Transfection of neurons with wild-type and I1061T mutant NPC1-GFP cDNAs is highly inefficient

The extremely low transfection efficiency seen in PC-12 cells transfected with our wild-type and I1061T mutant NPC1-GFP cDNAs was surprising, considering that

transfection with eGFP was much more efficient in these same cells. In addition, fluorescence seen with the NPC1-eGFP constructs was markedly dimmer than fluorescence seen with eGFP. We initially thought that the dimmer fluorescence was due to the large size of our constructs and the Maue plasmid (>8 kb), and that the large sizes resulted in decreased transfection efficiency and a subsequent lower amount of protein expression; however, transfection of COS-7 cells with a smaller NPC1-GFP-containing plasmid showed no increased fluorescence and no increase in transfection. We were therefore able to conclude that the size of our plasmids was not the reason for the decreased fluorescence and transfection efficiency observed. We also speculated that there was a problem in the fusion protein itself, and that it must have stemmed from the original fusion construct that we received from the Maue lab, because the Maue plasmid showed the same results as did all our re-constructed NPC1-GFP plasmids thereafter. Because the GFP in the Maue plasmid fusion protein is not eGFP, but another variant form of GFP, perhaps this variant form has a dimmer fluorescence. Thus, there may be more cells transfected with our plasmids as previously thought, but the fluorescence in these cells is so low that may not be easily detected by fluorescence microscopy.

We also observed that the more cells resemble neurons in primary culture, the more difficult they are to transfect with plasmids. In fact, we were unable to achieve any transfection of primary sympathetic neurons in culture using a variety of transfection reagents, for which the manufacturers' claimed produced high transfection efficiencies in these particular cells. Neuronally-differentiated PC-12 cells also were transfected at much lower efficiencies than were undifferentiated PC-12 cells. Why

neurons are more difficult to transfect than other types of cells is yet to be investigated. We do conclude, however, that the most effective transfection reagent for transfecting undifferentiated and differentiated PC-12 cells, of the four that we tested, was HD FuGENE. Although transfection efficiency values were similar for this reagent and Lipofectamine 2000, the latter reagent showed more signs of producing cell toxicity, rendering the former reagent most effective for transfection.

4.6 Future directions of studies in trafficking of the NPC1 protein

To date, as mentioned before, there have been very few studies performed on assessing the transport of the NPC1 protein and its various mutant forms in neurons. Based on the results we have gathered over the course of the present studies, perhaps it is not so surprising why so few studies have been carried out on this topic. Neurons, in general, are very difficult and time-consuming to work with compared to other cell types. In addition, they are extremely difficult to transfect with plasmids. Additionally, the toxicity of adenoviral vectors to neurons slightly limits the applicability of adenoviral vectors with neurons. It is important to investigate the role of NPC1 in neurons however, because it is in these cells that some of the most devastating effects of NPC occur. The idea of using GFP-tagged NPC1 to visualize the transport of NPC1 protein in neurons is theoretically an ideal one, and if performed successfully, can prove to be very rewarding, as seen previously (9). Thus, further investigating this aspect of NPC1 could potentially provide new insights into the neuron-specific function of NPC1 in distal axons and synaptic vesicle recycling. It will be important to improve current

gene-delivery methods in order to effectively study the transport of NPC1 and its various mutants in neurons. If adenoviruses which produce no toxicity can be developed, adenoviral-mediated gene delivery would be an especially ideal method to use in studying NPC1 transport in neurons. It will be interesting to see whether, or which, if any, NPC1 mutants are transported bi-directionally and play a role in distal axons in the synaptic vesicle recycling pathway and synaptic transmission. One thing to take into account however, is that these *in vitro* studies may not simulate the same situation occurring *in vivo*, and they would have to be performed separately in an *in vivo* model if any conclusions are to be drawn for therapeutic purposes. Although there is a vast unknown in the area of NPC1 trafficking in neurons, this subject, if explored further, may provide much needed insight on the neuron-specific role of NPC1, which may further contribute to development of effective therapeutic strategies to combat the neurological devastations of NPC disease.

References

1. Pentchev, P.G., M. T. Vanier, et al. 1995. Niemann-Pick Disease type C: cellular cholesterol lipidosis. In *The Metabolic and Molecular Bases of Inherited Diseases*. C.R. Scriver, et al., editor. New York: McGraw-Hill. 2625-2639.

2. Crocker, A.C., and Farber, S. 1958. Niemann-Pick disease: a review of eighteen patients. *Medicine* 37:1-95.

3. Brady, R.O., Kanfer, J.N., Mock, M.B., and Fredrickson, D.S. 1966. The metabolism of sphingomyelin. II. Evidence of an enzymatic deficiency in Niemann-Pick diseae. *Proc Natl Acad Sci U S A* 55:366-369.

4. Chang, T.Y., Reid, P.C., Sugii, S., Ohgami, N., Cruz, J.C., and Chang, C.C. 2005. Niemann-Pick type C disease and intracellular cholesterol trafficking. *J Biol Chem* 280:20917-20920.

5. Winsor, E.J., and Welch, J.P. 1978. Genetic and demographic aspects of Nova Scotia Niemann-Pick disease (type D). *Am J Hum Genet* 30:530-538.

6. Carstea, E.D., Polymeropoulos, M.H., Parker, C.C., Detera-Wadleigh, S.D., O'Neill, R.R., Patterson, M.C., Goldin, E., Xiao, H., Straub, R.E., Vanier, M.T., et al. 1993. Linkage of Niemann-Pick disease type C to human chromosome 18. *Proc Natl Acad Sci U S A* 90:2002-2004.

7. Carstea, E.D., Morris, J.A., Coleman, K.G., Loftus, S.K., Zhang, D., Cummings, C., Gu, J., Rosenfeld, M.A., Pavan, W.J., Krizman, D.B., et al. 1997. Niemann-Pick C1 disease gene: homology to mediators of cholesterol homeostasis. *Science* 277:228-231.

8. Karten, B., Vance, D.E., Campenot, R.B., and Vance, J.E. 2002. Cholesterol accumulates in cell bodies, but is decreased in distal axons, of Niemann-Pick C1-deficient neurons. *J Neurochem* 83:1154-1163.

9. Paul, C.A., Reid, P.C., Boegle, A.K., Karten, B., Zhang, M., Jiang, Z.G., Franz, D., Lin, L., Chang, T.Y., Vance, J.E., et al. 2005. Adenovirus expressing an NPC1-GFP fusion gene corrects neuronal and nonneuronal defects associated with Niemann pick type C disease. *J Neurosci Res* 81:706-719.

10. Vance, J.E., Hayashi, H., and Karten, B. 2005. Cholesterol homeostasis in neurons and glial cells. *Semin Cell Dev Biol* 16:193-212.

11. Vance, J.E., Karten, B., and Hayashi, H. 2006. Lipid dynamics in neurons. *Biochem Soc Trans* 34:399-403.

12. Yang, C.C., Su, Y.N., Chiou, P.C., Fietz, M.J., Yu, C.L., Hwu, W.L., and Lee, M.J. 2005. Six novel NPC1 mutations in Chinese patients with Niemann-Pick disease type C. *J Neurol Neurosurg Psychiatry* 76:592-595.

13. Scott, C., and Ioannou, Y.A. 2004. The NPC1 protein: structure implies function. *Biochim Biophys Acta* 1685:8-13.

14. Runz, H., Dolle, D., Schlitter, A.M., and Zschocke, J. 2008. NPC-db, a Niemann-Pick type C disease gene variation database. *Hum Mutat* 29:345-350.

15. Garver, W.S., Xie, C., Repa, J.J., Turley, S.D., and Dietschy, J.M. 2005. Niemann-Pick C1 expression is not regulated by the amount of cholesterol flowing through cells in the mouse. *J Lipid Res* 46:1745-1754.

16. Vance, J.E. 2006. Lipid imbalance in the neurological disorder, Niemann-Pick C disease. *FEBS Lett* 580:5518-5524.

17. Infante, R.E., Radhakrishnan, A., Abi-Mosleh, L., Kinch, L.N., Wang, M.L., Grishin, N.V., Goldstein, J.L., and Brown, M.S. 2008. Purified NPC1 protein: II. Localization of sterol binding to a 240-amino acid soluble luminal loop. *J Biol Chem* 283:1064-1075.

18. Ory, D.S. 2004. The niemann-pick disease genes; regulators of cellular cholesterol homeostasis. *Trends Cardiovasc Med* 14:66-72.

19. Infante, R.E., Abi-Mosleh, L., Radhakrishnan, A., Dale, J.D., Brown, M.S., and Goldstein, J.L. 2008. Purified NPC1 protein. I. Binding of cholesterol and oxysterols to a 1278-amino acid membrane protein. *J Biol Chem* 283:1052-1063.

20. Tseng, T.T., Gratwick, K.S., Kollman, J., Park, D., Nies, D.H., Goffeau, A., and Saier, M.H., Jr. 1999. The RND permease superfamily: an ancient, ubiquitous and diverse family that includes human disease and development proteins. *J Mol Microbiol Biotechnol* 1:107-125.

21. Davies, J.P., Chen, F.W., and Ioannou, Y.A. 2000. Transmembrane molecular pump activity of Niemann-Pick C1 protein. *Science* 290:2295-2298.

22. Cruz, J.C., Sugii, S., Yu, C., and Chang, T.Y. 2000. Role of Niemann-Pick type C1 protein in intracellular trafficking of low density lipoprotein-derived cholesterol. *J Biol Chem* 275:4013-4021.

23. Ikonen, E., and Holtta-Vuori, M. 2004. Cellular pathology of Niemann-Pick type C disease. *Semin Cell Dev Biol* 15:445-454.

24. Mukherjee, S., and Maxfield, F.R. 2004. Lipid and cholesterol trafficking in NPC. *Biochim Biophys Acta* 1685:28-37.

25. Cheruku, S.R., Xu, Z., Dutia, R., Lobel, P., and Storch, J. 2006. Mechanism of cholesterol transfer from the Niemann-Pick type C2 protein to model membranes supports a role in lysosomal cholesterol transport. *J Biol Chem* 281:31594-31604.

26. Liscum, L. 2000. Niemann-Pick type C mutations cause lipid traffic jam. *Traffic* 1:218-225.

27. Blanchette-Mackie, E.J. 2000. Intracellular cholesterol trafficking: role of the NPC1 protein. *Biochim Biophys Acta* 1486:171-183.

28. Wattenberg, B.W., and Silbert, D.F. 1983. Sterol partitioning among intracellular membranes. Testing a model for cellular sterol distribution. *J Biol Chem* 258:2284-2289.

29. DeGrella, R.F., and Simoni, R.D. 1982. Intracellular transport of cholesterol to the plasma membrane. *J Biol Chem* 257:14256-14262.

30. Kaplan, M.R., and Simoni, R.D. 1985. Transport of cholesterol from the endoplasmic reticulum to the plasma membrane. *J Cell Biol* 101:446-453.

31. Urbani, L., and Simoni, R.D. 1990. Cholesterol and vesicular stomatitis virus G protein take separate routes from the endoplasmic reticulum to the plasma membrane. *J Biol Chem* 265:1919-1923.

32. Liscum, L., and Dahl, N.K. 1992. Intracellular cholesterol transport. *J Lipid Res* 33:1239-1254.

33. Neufeld, E.B., Cooney, A.M., Pitha, J., Dawidowicz, E.A., Dwyer, N.K., Pentchev, P.G., and Blanchette-Mackie, E.J. 1996. Intracellular trafficking of cholesterol monitored with a cyclodextrin. *J Biol Chem* 271:21604-21613.

34. Liscum, L., and Sturley, S.L. 2004. Intracellular trafficking of Niemann-Pick C proteins 1 and 2: obligate components of subcellular lipid transport. *Biochim Biophys Acta* 1685:22-27.

35. Pfrieger, F.W. 2003. Cholesterol homeostasis and function in neurons of the central nervous system. *Cell Mol Life Sci* 60:1158-1171.

36. Edmond, J., Korsak, R.A., Morrow, J.W., Torok-Both, G., and Catlin, D.H. 1991. Dietary cholesterol and the origin of cholesterol in the brain of developing rats. *J Nutr* 121:1323-1330.

37. Jurevics, H., and Morell, P. 1995. Cholesterol for synthesis of myelin is made locally, not imported into brain. *J Neurochem* 64:895-901.

38. Turley, S.D., Burns, D.K., and Dietschy, J.M. 1998. Preferential utilization of newly synthesized cholesterol for brain growth in neonatal lambs. *Am J Physiol* 274:E1099-1105.

39. Spady, D.K., and Dietschy, J.M. 1983. Sterol synthesis in vivo in 18 tissues of the squirrel monkey, guinea pig, rabbit, hamster, and rat. *J Lipid Res* 24:303-315.

40. Dietschy, J.M., and Turley, S.D. 2004. Thematic review series: brain Lipids. Cholesterol metabolism in the central nervous system during early development and in the mature animal. *J Lipid Res* 45:1375-1397.

41. Bjorkhem, I., Lutjohann, D., Breuer, O., Sakinis, A., and Wennmalm, A. 1997. Importance of a novel oxidative mechanism for elimination of brain cholesterol. Turnover of cholesterol and 24(S)-hydroxycholesterol in rat brain as measured with 18O2 techniques in vivo and in vitro. *J Biol Chem* 272:30178-30184.

42. Lund, E.G., Xie, C., Kotti, T., Turley, S.D., Dietschy, J.M., and Russell, D.W. 2003. Knockout of the cholesterol 24-hydroxylase gene in mice reveals a brain-specific mechanism of cholesterol turnover. *J Biol Chem* 278:22980-22988.

43. Xie, C., Turley, S.D., and Dietschy, J.M. 1999. Cholesterol accumulation in tissues of the Niemann-pick type C mouse is determined by the rate of lipoprotein-cholesterol uptake through the coated-pit pathway in each organ. *Proc Natl Acad Sci U S A* 96:11992-11997.

44. Xie, C., Burns, D.K., Turley, S.D., and Dietschy, J.M. 2000. Cholesterol is sequestered in the brains of mice with Niemann-Pick type C disease but turnover is increased. *J Neuropathol Exp Neurol* 59:1106-1117.

45. German, D.C., Liang, C.L., Song, T., Yazdani, U., Xie, C., and Dietschy, J.M. 2002. Neurodegeneration in the Niemann-Pick C mouse: glial involvement. *Neuroscience* 109:437-450.

46. Baudry, M., Yao, Y., Simmons, D., Liu, J., and Bi, X. 2003. Postnatal development of inflammation in a murine model of Niemann-Pick type C disease: immunohistochemical observations of microglia and astroglia. *Exp Neurol* 184:887-903.

47. Pfrieger, F.W. 2003. Outsourcing in the brain: do neurons depend on cholesterol delivery by astrocytes? *Bioessays* 25:72-78.

48. Brecht, W.J., Harris, F.M., Chang, S., Tesseur, I., Yu, G.Q., Xu, Q., Dee Fish, J., Wyss-Coray, T., Buttini, M., Mucke, L., et al. 2004. Neuron-specific apolipoprotein e4 proteolysis is associated with increased tau phosphorylation in brains of transgenic mice. *J Neurosci* 24:2527-2534.

49. Mahley, R.W., Weisgraber, K.H., and Huang, Y. 2006. Apolipoprotein E4: a causative factor and therapeutic target in neuropathology, including Alzheimer's disease. *Proc Natl Acad Sci U S A* 103:5644-5651.

50. Rothe, T., and Muller, H.W. 1991. Uptake of endoneurial lipoprotein into Schwann cells and sensory neurons is mediated by low density lipoprotein receptors and stimulated after axonal injury. *J Neurochem* 57:2016-2025.

51. Karten, B., Hayashi, H., Francis, G.A., Campenot, R.B., Vance, D.E., and Vance, J.E. 2005. Generation and function of astroglial lipoproteins from Niemann-Pick type C1-deficient mice. *Biochem J* 387:779-788.

52. Ko, D.C., Milenkovic, L., Beier, S.M., Manuel, H., Buchanan, J., and Scott, M.P. 2005. Cell-autonomous death of cerebellar purkinje neurons with autophagy in Niemann-Pick type C disease. *PLoS Genet* 1:81-95.

53. Patel, S.C., Suresh, S., Kumar, U., Hu, C.Y., Cooney, A., Blanchette-Mackie, E.J., Neufeld, E.B., Patel, R.C., Brady, R.O., Patel, Y.C., et al. 1999. Localization of Niemann-Pick C1 protein in astrocytes: implications for neuronal degeneration in Niemann- Pick type C disease. *Proc Natl Acad Sci U S A* 96:1657-1662.

54. Ong, W.Y., Kumar, U., Switzer, R.C., Sidhu, A., Suresh, G., Hu, C.Y., and Patel, S.C. 2001. Neurodegeneration in Niemann-Pick type C disease mice. *Exp Brain Res* 141:218-231.

55. Karten, B., Vance, D.E., Campenot, R.B., and Vance, J.E. 2003. Trafficking of cholesterol from cell bodies to distal axons in Niemann Pick C1-deficient neurons. *J Biol Chem* 278:4168-4175.

56. Treiber-Held, S., Distl, R., Meske, V., Albert, F., and Ohm, T.G. 2003. Spatial and temporal distribution of intracellular free cholesterol in brains of a Niemann-Pick type C mouse model showing hyperphosphorylated tau protein. Implications for Alzheimer's disease. *J Pathol* 200:95-103.

57. Liscum, L., Ruggiero, R.M., and Faust, J.R. 1989. The intracellular transport of low density lipoprotein-derived cholesterol is defective in Niemann-Pick type C fibroblasts. *J Cell Biol* 108:1625-1636.

58. Tashiro, Y., Yamazaki, T., Shimada, Y., Ohno-Iwashita, Y., and Okamoto, K. 2004. Axon-dominant localization of cell-surface cholesterol in cultured hippocampal neurons and its disappearance in Niemann-Pick type C model cells. *Eur J Neurosci* 20:2015-2021.

59. Fassbender, K., Simons, M., Bergmann, C., Stroick, M., Lutjohann, D., Keller, P., Runz, H., Kuhl, S., Bertsch, T., von Bergmann, K., et al. 2001. Simvastatin strongly reduces levels of Alzheimer's disease beta -amyloid peptides Abeta 42 and Abeta 40 in vitro and in vivo. *Proc Natl Acad Sci U S A* 98:5856-5861.

60. Kobayashi, T., Beuchat, M.H., Lindsay, M., Frias, S., Palmiter, R.D., Sakuraba, H., Parton, R.G., and Gruenberg, J. 1999. Late endosomal membranes rich in lysobisphosphatidic acid regulate cholesterol transport. *Nat Cell Biol* 1:113-118.

61. Feng, Y., Press, B., and Wandinger-Ness, A. 1995. Rab 7: an important regulator of late endocytic membrane traffic. *J Cell Biol* 131:1435-1452.

62. Novick, P., and Zerial, M. 1997. The diversity of Rab proteins in vesicle transport. *Curr Opin Cell Biol* 9:496-504.

63. Meresse, S., Gorvel, J.P., and Chavrier, P. 1995. The rab7 GTPase resides on a vesicular compartment connected to lysosomes. *J Cell Sci* 108 (Pt 11):3349-3358.

64. Lombardi, D., Soldati, T., Riederer, M.A., Goda, Y., Zerial, M., and Pfeffer, S.R. 1993. Rab9 functions in transport between late endosomes and the trans Golgi network. *Embo J* 12:677-682.

65. Zhang, M., Dwyer, N.K., Love, D.C., Cooney, A., Comly, M., Neufeld, E., Pentchev, P.G., Blanchette-Mackie, E.J., and Hanover, J.A. 2001. Cessation of rapid late endosomal tubulovesicular trafficking in Niemann-Pick type C1 disease. *Proc Natl Acad Sci U S A* 98:4466-4471.

66. Millat, G., Bailo, N., Molinero, S., Rodriguez, C., Chikh, K., and Vanier, M.T. 2005. Niemann-Pick C disease: use of denaturing high performance liquid chromatography for the detection of NPC1 and NPC2 genetic variations and impact on management of patients and families. *Mol Genet Metab* 86:220-232.

67. Imrie, J., Dasgupta, S., Besley, G.T., Harris, C., Heptinstall, L., Knight, S., Vanier, M.T., Fensom, A.H., Ward, C., Jacklin, E., et al. 2007. The natural history of Niemann-Pick disease type C in the UK. *J Inherit Metab Dis* 30:51-59.

68. Ganley, I.G., and Pfeffer, S.R. 2006. Cholesterol accumulation sequesters Rab9 and disrupts late endosome function in NPC1-deficient cells. *J Biol Chem* 281:17890-17899.

69. Neufeld, E.B., Wastney, M., Patel, S., Suresh, S., Cooney, A.M., Dwyer, N.K., Roff, C.F., Ohno, K., Morris, J.A., Carstea, E.D., et al. 1999. The Niemann-Pick C1 protein resides in a vesicular compartment linked to retrograde transport of multiple lysosomal cargo. *J Biol Chem* 274:9627-9635.

70. Lusa, S., Blom, T.S., Eskelinen, E.L., Kuismanen, E., Mansson, J.E., Simons, K., and Ikonen, E. 2001. Depletion of rafts in late endocytic membranes is controlled by NPC1-dependent recycling of cholesterol to the plasma membrane. *J Cell Sci* 114:1893-1900.

71. Underwood, K.W., Jacobs, N.L., Howley, A., and Liscum, L. 1998. Evidence for a cholesterol transport pathway from lysosomes to endoplasmic reticulum that is independent of the plasma membrane. *J Biol Chem* 273:4266-4274.

72. Ko, D.C., Gordon, M.D., Jin, J.Y., and Scott, M.P. 2001. Dynamic movements of organelles containing Niemann-Pick C1 protein: NPC1 involvement in late endocytic events. *Mol Biol Cell* 12:601-614.

73. Hirokawa, N. 1997. The mechanisms of fast and slow transport in neurons: identification and characterization of the new kinesin superfamily motors. *Curr Opin Neurobiol* 7:605-614.

74. Chen, J., Kanai, Y., Cowan, N.J., and Hirokawa, N. 1992. Projection domains of MAP2 and tau determine spacings between microtubules in dendrites and axons. *Nature* 360:674-677.

75. Nixon, R.A. 1998. The slow axonal transport of cytoskeletal proteins. *Curr Opin Cell Biol* 10:87-92.

76. Gunawardena, S., and Goldstein, L.S. 2004. Cargo-carrying motor vehicles on the neuronal highway: transport pathways and neurodegenerative disease. *J Neurobiol* 58:258-271.

77. Vance, J.E., Campenot, R.B., and Vance, D.E. 2000. The synthesis and transport of lipids for axonal growth and nerve regeneration. *Biochim Biophys Acta* 1486:84-96.

78. Parton, R.G., Simons, K., and Dotti, C.G. 1992. Axonal and dendritic endocytic pathways in cultured neurons. *J Cell Biol* 119:123-137.

79. Parton, R.G., and Dotti, C.G. 1993. Cell biology of neuronal endocytosis. *J Neurosci Res* 36:1-9.

80. Karten, B., Campenot, R.B., Vance, D.E., and Vance, J.E. 2006. The Niemann-Pick C1 protein in recycling endosomes of presynaptic nerve terminals. *J Lipid Res* 47:504-514.

81. Breckenridge, W.C., Morgan, I.G., Zanetta, J.P., and Vincendon, G. 1973. Adult rat brain synaptic vesicles. II. Lipid composition. *Biochim Biophys Acta* 320:681-686.

82. Nagy, A., Baker, R.R., Morris, S.J., and Whittaker, V.P. 1976. The preparation and characterization of synaptic vesicles of high purity. *Brain Res* 109:285-309.

83. Wagner, J.A., Carlson, S.S., and Kelly, R.B. 1978. Chemical and physical characterization of cholinergic synaptic vesicles. *Biochemistry* 17:1199-1206.

84. Deutsch, J.W., and Kelly, R.B. 1981. Lipids of synaptic vesicles: relevance to the mechanism of membrane fusion. *Biochemistry* 20:378-385.

85. DeVries, G.H., Zetusky, W.J., Zmachinski, C., and Calabrese, V.P. 1981. Lipid composition of axolemma-enriched fractions from human brains. *J Lipid Res* 22:208-216.

86. Mitter, D., Reisinger, C., Hinz, B., Hollmann, S., Yelamanchili, S.V., Treiber-Held, S., Ohm, T.G., Herrmann, A., and Ahnert-Hilger, G. 2003. The synaptophysin/synaptobrevin interaction critically depends on the cholesterol content. *J Neurochem* 84:35-42.

87. Lang, T., Bruns, D., Wenzel, D., Riedel, D., Holroyd, P., Thiele, C., and Jahn, R. 2001. SNAREs are concentrated in cholesterol-dependent clusters that define docking and fusion sites for exocytosis. *Embo J* 20:2202-2213.

88. Chamberlain, L.H., Burgoyne, R.D., and Gould, G.W. 2001. SNARE proteins are highly enriched in lipid rafts in PC12 cells: implications for the spatial control of exocytosis. *Proc Natl Acad Sci U S A* 98:5619-5624.

89. Thiele, C., Hannah, M.J., Fahrenholz, F., and Huttner, W.B. 2000. Cholesterol binds to synaptophysin and is required for biogenesis of synaptic vesicles. *Nat Cell Biol* 2:42-49.

90. Sudhof, T.C. 2004. The synaptic vesicle cycle. *Annu Rev Neurosci* 27:509-547.

91. Munkacsi, A.B., A. F. Porto, et al. 2007. Niemann-Pick type C disease proteins: orphan transporters or membrane rheostats? *Future Lipidology* 2:357-367.

92. Vanier, M.T., and Millat, G. 2003. Niemann-Pick disease type C. *Clin Genet* 64:269-281.

93. Mauch, D.H., Nagler, K., Schumacher, S., Goritz, C., Muller, E.C., Otto, A., and Pfrieger, F.W. 2001. CNS synaptogenesis promoted by glia-derived cholesterol. *Science* 294:1354-1357.

94. Bauer, P., Knoblich, R., Bauer, C., Finckh, U., Hufen, A., Kropp, J., Braun, S., Kustermann-Kuhn, B., Schmidt, D., Harzer, K., et al. 2002. NPC1: Complete genomic sequence, mutation analysis, and characterization of haplotypes. *Hum Mutat* 19:30-38.

95. Millat, G., Marcais, C., Rafi, M.A., Yamamoto, T., Morris, J.A., Pentchev, P.G., Ohno, K., Wenger, D.A., and Vanier, M.T. 1999. Niemann-Pick C1 disease: the I1061T substitution is a frequent mutant allele in patients of Western European descent and correlates with a classic juvenile phenotype. *Am J Hum Genet* 65:1321-1329.

96. Greer, W.L., Riddell, D.C., Gillan, T.L., Girouard, G.S., Sparrow, S.M., Byers, D.M., Dobson, M.J., and Neumann, P.E. 1998. The Nova Scotia (type D) form of Niemann-Pick disease is caused by a G3097-->T transversion in NPC1. *Am J Hum Genet* 63:52-54.

97. German, D.C., Quintero, E.M., Liang, C., Xie, C., and Dietschy, J.M. 2001. Degeneration of neurons and glia in the Niemann-Pick C mouse is unrelated to the low-density lipoprotein receptor. *Neuroscience* 105:999-1005.

98. Watari, H., Blanchette-Mackie, E.J., Dwyer, N.K., Glick, J.M., Patel, S., Neufeld, E.B., Brady, R.O., Pentchev, P.G., and Strauss, J.F., 3rd. 1999. Niemann-Pick C1 protein: obligatory roles for N-terminal domains and lysosomal targeting in cholesterol mobilization. *Proc Natl Acad Sci U S A* 96:805-810.

99. Bolognani, F., and Perrone-Bizzozero, N.I. 2008. RNA-protein interactions and control of mRNA stability in neurons. *J Neurosci Res* 86:481-489.

100. Karten, B., Hayashi, H., Campenot, R.B., Vance, D.E., and Vance, J.E. 2005. Neuronal models for studying lipid metabolism and transport. *Methods* 36:117-128.

101. Hayashi, H., Karten, B., Vance, D.E., Campenot, R.B., Maue, R.A., and Vance, J.E. 2004. Methods for the study of lipid metabolism in neurons. *Anal Biochem* 331:1-16.

102. Campenot, R.B. 1977. Local control of neurite development by nerve growth factor. *Proc Natl Acad Sci U S A* 74:4516-4519.

103. Campenot, R.B. 1982. Development of sympathetic neurons in compartmentalized cultures. II Local control of neurite growth by nerve growth factor. *Dev Biol* 93:1-12.

104. Karten, B., H. Eng, et al. 2002. In *Apoptosis Methods and Techniques*. A.C. LeBlanc, editor. Totowa: Humana Press. 163-175.

105. Greene, L.A., and Tischler, A.S. 1976. Establishment of a noradrenergic clonal line of rat adrenal pheochromocytoma cells which respond to nerve growth factor. *Proc Natl Acad Sci U S A* 73:2424-2428.

106. Shea, T.B., Fischer, I., and Sapirstein, V.S. 1985. Effect of retinoic acid on growth and morphological differentiation of mouse NB2a neuroblastoma cells in culture. *Brain Res* 353:307-314.

107. Vaudry, D., Stork, P.J., Lazarovici, P., and Eiden, L.E. 2002. Signaling pathways for PC12 cell differentiation: making the right connections. *Science* 296:1648-1649.

108. Kelly-Spratt, K. 1998. Transfection of PC-12 cells: a model system for primary neuronal cells. In *Qiagen News*. 3-4.

109. Easton, R.M., Johnson, E.M., and Creedon, D.J. 1998. Analysis of events leading to neuronal death after infection with E1-deficient adenoviral vectors. *Mol Cell Neurosci* 11:334-347.

110. Arsenault, H., E. De Luca, at al. Adenovator Vector System Applications manual Version 1.1.

111. Le Gal La Salle, G., Robert, J.J., Berrard, S., Ridoux, V., Stratford-Perricaudet, L.D., Perricaudet, M., and Mallet, J. 1993. An adenovirus vector for gene transfer into neurons and glia in the brain. *Science* 259:988-990.

112. Luo, J., Deng, Z.L., Luo, X., Tang, N., Song, W.X., Chen, J., Sharff, K.A., Luu, H.H., Haydon, R.C., Kinzler, K.W., et al. 2007. A protocol for rapid generation of recombinant adenoviruses using the AdEasy system. *Nat Protoc* 2:1236-1247.

113. Worgall, S., Worgall, T.S., Kostarelos, K., Singh, R., Leopold, P.L., Hackett, N.R., and Crystal, R.G. 2000. Free cholesterol enhances adenoviral vector gene transfer and expression in CAR-deficient cells. *Mol Ther* 1:39-48.

114. Hidaka, C., Milano, E., Leopold, P.L., Bergelson, J.M., Hackett, N.R., Finberg, R.W., Wickham, T.J., Kovesdi, I., Roelvink, P., and Crystal, R.G. 1999. CAR-dependent and CAR-independent pathways of adenovirus vector-mediated gene transfer and expression in human fibroblasts. *J Clin Invest* 103:579-587.

115. Loftus, S.K., Morris, J.A., Carstea, E.D., Gu, J.Z., Cummings, C., Brown, A., Ellison, J., Ohno, K., Rosenfeld, M.A., Tagle, D.A., et al. 1997. Murine model of Niemann-Pick C disease: mutation in a cholesterol homeostasis gene. *Science* 277:232-235.

116. Hawrot, E., and Patterson, P.H. 1979. Long-term culture of dissociated sympathetic neurons. *Methods Enzymol* 58:574-584.

117. www.abcam.com/technical. Western Blotting - A Beginner's guide.

118. Heim, R., Cubitt, A.B., and Tsien, R.Y. 1995. Improved green fluorescence. *Nature* 373:663-664.

119. McRae, S.R., Brown, C.L., and Bushell, G.R. 2005. Rapid purification of EGFP, EYFP, and ECFP with high yield and purity. *Protein Expr Purif* 41:121-127.

120. Wang, Q., and Finer, M.H. 1996. Second-generation adenovirus vectors. *Nat Med* 2:714-716.

121. Inouye, S., and Tsuji, F.I. 1994. Aequorea green fluorescent protein. Expression of the gene and fluorescence characteristics of the recombinant protein. *FEBS Lett* 341:277-280.

122. Gelsthorpe, M.E., Baumann, N., Millard, E., Gale, S.E., Langmade, S.J., Schaffer, J.E., and Ory, D.S. 2008. Niemann-Pick type C1 I1061T mutant encodes a functional protein that is selected for endoplasmic reticulum-associated degradation due to protein misfolding. *J Biol Chem* 283:8229-8236.

123. Sitia, R., and Braakman, I. 2003. Quality control in the endoplasmic reticulum protein factory. *Nature* 426:891-894.

124. Ward, C.L., and Kopito, R.R. 1994. Intracellular turnover of cystic fibrosis transmembrane conductance regulator. Inefficient processing and rapid degradation of wild-type and mutant proteins. *J Biol Chem* 269:25710-25718.

125. Wilusz, C.J., Wormington, M., and Peltz, S.W. 2001. The cap-to-tail guide to mRNA turnover. *Nat Rev Mol Cell Biol* 2:237-246.

126. Garneau, N.L., Wilusz, J., and Wilusz, C.J. 2007. The highways and byways of mRNA decay. *Nat Rev Mol Cell Biol* 8:113-126.

127. Shaw, G., and Kamen, R. 1986. A conserved AU sequence from the 3' untranslated region of GM-CSF mRNA mediates selective mRNA degradation. *Cell* 46:659-667.

128. Chen, C.Y., and Shyu, A.B. 1995. AU-rich elements: characterization and importance in mRNA degradation. *Trends Biochem Sci* 20:465-470.

129. Watari, H., Blanchette-Mackie, E.J., Dwyer, N.K., Watari, M., Burd, C.G., Patel, S., Pentchev, P.G., and Strauss, J.F., 3rd. 2000. Determinants of NPC1 expression and action: key promoter regions, posttranscriptional control, and the importance of a "cysteine-rich" loop. *Exp Cell Res* 259:247-256.

130. Loftus, S.K., Morris, J.A., Carstea, E.D., Gu, J.Z., Cummings, C., Brown, A. 1997. Murine model of Niemann-Pick C disease: mutation in a cholesterol homeostasis gene. *Science* 277:232-235.

131. Cadigan, K.M., Spillane, D.M., and Chang, T.Y. 1990. Isolation and characterization of Chinese hamster ovary cell mutants defective in intracellular low density lipoprotein-cholesterol trafficking. *J. Cell Biol.* 110:295-308.

132. Higashi, Y., Murayama, S., Pentchev, P.G., Suzuki, K. 1993. Cerebellar degeneration in the Niemann-Pick type C mouse. *Acta Neuropathol.* 85:175-184.

133. Zervas, M., Somers, K.L., Thrall, M.A., Walkley, S.U. 2001. Critical role for glycosphingolipids in Niemann-Pick disease type C. *Curr Biol.* 20:95-97.

134. Suzuki, K., Parker, C.C., Pentchev, P.G., Katz, D. Ghetti, B., D'Agostino, A.N. 1995. Neurofibrillary tangles in Niemann-Pick disease type C. *Acta Neuropathol.* 89:227-238.

135. Elleder, M., Jirasek, A., Smid, F., Ledvivona, J., Beslet, G.T. 1985. Niemann-Pick disease type C. Study on the nature of the cerebral storage process. *Acta Neuropathol.* 66:325-336.

136. P.G. Pentchev, et al. 1985. A defect in cholesterol esterification in Niemann–Pick disease (type C) patients. *Proc. Natl. Acad. Sci. U.S.A.* 82:8247– 8251.

137. E.B. Neufeld, et al. 1999. The Niemann–Pick C1 protein resides in a vesicular compartment linked to retrograde transport of multiple lysosomal cargo. *J. Biol. Chem.* 274:9627– 9635.

138. L. Liscum, J.R. Faust. 1989. The intracellular transport of low density lipoprotein-derived cholesterol is inhibited in Chinese hamster ovary cells cultured with 3-h-[2 (diethylamino)ethoxy]androst-5-en-17-one. *J. Biol. Chem.* 264:11796– 11806.

139. Mitter, D.C, Reisinger, B., Hinz, S., Hollmann, S.V., Yelamanchili, S., Treiber-Held, T.G., Ohm, A., Herrmann, Ahnert-Hilger, G. 2003. The synaptophysin/synaptobrevin interaction critically depends on the cholesterol content. *J. Neurochem.* 84:35-42.